ISSN (PRINT)
2322-0031

INTERNATIONAL JOURNAL OF INTELLIGENT COMPUTING AND APPLIED SCIENCES

Bi - ANNUAL JOURNAL | VOLUME-6 | ISSUE-1 | NOVEMBER-2021

DRIEMS Publication House
Tangi, Odisha, India
www.ijicas.com

About the Journal

The International Journal of Intelligent Computing and Applied Sciences (IJICAS) publishes research papers in the fields of Computer Technology Engineering and Applied Sciences. Original, previously unpublished research articles written in perfect English are sought for inclusion in the biannual journal, which will be published in the month of January and July each year. The articles for the International Bibliography M. L. A. Handbook must be created to meet its international standard (7th Edition).

The IJICAS is an English-language International Journal published twice a year. IJICAS goal is to publish peer-reviewed research and review articles in the growing disciplines of Computer Science Technology and Applied Sciences as soon as possible. The IJICAS publishes publications in the domains of computer technology, engineering, and applied sciences that focus on research, development, and application. All manuscripts are peer reviewed by the editors, and if appropriate, sent for blind peer-review. Contributor papers must be original, have not been published elsewhere previously or concurrently, and are critically reviewed before being published. Research articles must be written in English and must contain suitable grammar and terminology.

Aim and Scope

The aim of IJICAS is to inspire the researchers to identify problems and find out solution there to, for greater good and mankind. Keeping pace with the rapid changes in the field of science and technology the journal will take up issues as fast possible and its readers will be able to keep abreast of the technological advancement at home and abroad. The “IJICAS” is an International journal in English to be published. The objective of this journal is to identify, recognize and globalize the individual innovative ideas to glorify and strengthen the global knowledge level of the universe. It also aims at publishing peer reviewed research and review articles in rapidly developing fields of Engineering, Computer Technology and Applied Sciences. This journal is having full access to the research and review papers. The journal will cover up the latest outstanding developments in the field of computer technology, engineering and applied sciences but not limited to the branches, mentioned below:

- Computational Mathematics
- Data Structure, Algorithms
- Artificial Intelligence
- Automated software Engineering

- Bioinformatics and scientific computing
- Cloud Computing
- Compilers and Interpreters
- Computational intelligence, database
- Computer architecture
- Computer architecture and embedded systems
- Computer games, data communication
- Computer graphics and virtual reality
- Computer modeling
- Computer security, digital electronics
- Computer simulation
- Computing ethics
- Computer-aided design/manufacturing
- Data communications
- Data mining
- Digital signal processing
- Distributed systems
- Expert systems
- High performance computing
- Image processing watermarking
- Information systems
- Mobile computing
- Multimedia applications
- Parallel and distributed computing
- Programming languages
- Reconfigurable computing systems
- Security and cryptography
- Software engineering and CASE
- Applications of computer science and engineering
- Intelligent systems and approach
- Information technology application
- Knowledge management
- Embedded system
- Analog and digital devices and services

Author Instruction

Research papers and reviews related to topic, listed above will be accepted for perusal for publication. The contributors are requested to send the manuscripts online (submit button). MS. No. will be mailed within a week. The article must not exceed 15 pages.

IJICAS accepts research and review articles in engineering, computer technology and applied sciences. The manuscript would be considered on specific branches of engineering, science and technology but not limited. The braches are mentioned earlier in the aim and scope.

Therefore, the corresponding author is requested to mention the branches which come under the title of the journal. All manuscripts are subject to RAPID peer review process and those of high quality (which are not previously published under consideration for publication by another journal) would be published without any delay in subsequent issue. Online submission of the manuscript is strongly recommended. Submit manuscript in the ‘Submit Manuscript’ button.

Subscription Order

IJICAS is published two issues per volume.
For subscription payment with order should be made to:
DRIEMS
Tangi, Cuttack -754022, India
TeleFax: (0671)2595755
For electronic PDF files
IJICAS papers are available to download from website www.ijicas.com

Editorial

It is my proud privilege to announce that the inaugural issue of volume 6 of the International Journal of Intelligent Computing and Applied Sciences (IJICAS) will be published in 2021, based on chosen received papers from across the world. This issue has articles from a variety of fields in Intelligent Computing and Applied Sciences. Original research submissions of high quality will be published in IJICAS.

This journal aims to provide a forum for academics, educators, and professionals in the field of applied sciences and engineering to share their findings, innovative practice, and explore future trends and applications. However, this journal, on the other hand, will serve as a venue for the transmission of information on both theoretical and applied research in the aforementioned domain, with the ultimate goal of b ridging the gap between these related fields of study. As a result, the forum accelerates the advancement of technology for the future generation. This publication offers a comprehensive view on contemporary engineering subjects of relevance. A review article's scope and manuscript review method are identical to contemporary scientific submissions to IJICAS, which use a double-blind review process. I'd like to express my gratitude to the eminent personalities for reviewing articles for the journal during the last year.

I am pleased to notice that IJICAS will gain widespread acclaim among educators, academics, and professionals in a short period of time. Nine shortlisted articles addressing diverse elements of intelligent computing and applied sciences have been published in the inaugural issue of Volume 6.

Dr. Rajendra Kumar Das

Editors – in- Chief

Contents

Study on Geotechnical Properties of Expansive Soil Using Mineral Admixtures

[1]Sourya Snigdha Mohapatra, [2] Biswajit Jena
[1,2]Asst. Professor, Dept. of Civil Engineering, DRIEMS Autonomous Engineering College, Cuttack, Odisha
[1]smohapatra@driems.ac.in#, [2]biswajit.jena@driems.ac.in

ABSTRACT

Due to the presence of water in clayey soil, it is prone to volume changes showing significant swelling and shrinkage. This type of soil is recognised as expansive soil or black cotton soil with high moisture content variations. Due to this variation, hydraulic pressure is generated in soil resulting in the heaving or lifting of the structures as well as differential settlement in the soil. This expansive nature of the soil creates damage to the structure hampering the mechanical properties of the soil making it liquefiable. Various ground improvement techniques have been adopted for enhancing the properties of soil to avoid the mentioned risk. In the present work, investigations are carried out to stabilise the black cotton soil using different mineral admixtures and glass fibres at various percentage. The experiments are done in the laboratory by blending the ideal amount of ground granulated blast furnace slag, ordinary Portland cement (0.3%, 0.6%, 0.9% and 1.2%) and the glass fibre (0.25%, 0.5%, 0.75% and 1%) with black cotton soil to study the mechanical aspects and their behaviour. Optimum moisture content and maximum dry density for the variations of the admixtures have been found out through Standard proctor test whereas UCS and CBR were checked at 3,7 and 14 days of curing period for the mix proportions with corresponding MDD values.

Keywords: *Black cotton soil, GGBFS, Glass Fibre, OPC, OMC, MDD, UCS, CBR*

1. INTRODUCTION

Most of the civil engineers face challenges at different times due to the problematic soils like black cotton soil as they cover around 20% of the land area in India, Which can be accessible on an average found up to a depth of 3.7m [3]. These kind of soils make the construction of any structure risky and rampageous. So these soils should be treated within time to overcome such fatal disasters. Most often variations have been observed in these soils due to the change in season which can cause decrease in shear strength and stiffness and remarkable volume change and also which are considered to be obstaclein the field of construction. Stabilization is highly necessary to improve the mechanical properties of such soil to overcome the damages caused due to soil instability. Admixtures like cement, and lime are most commonly used for the soil stabilization purpose. Ground granulated blast furnace slag (GGBFS) is a kind of mineral admixture that can be originated from the un-used by product of the iron manufacturing plants and can be used as a partial replacement to soil in order to improve the soil properties in corporation with ordinary Portland cement in small quantity and silicate glass fibres as a soil strengthening material. Normally glass fibres are not being used as a common stabilizing agent still it has a considerable strength enhancement quality [10].

The soil being stabilised results in flexible increase in performance than the virgin soil. The swelling and shrinkage properties also get reduced due to the effect of GGBFS in expansive soil. From various laboratory tests and their outcomes, it has been proved that GGBFS plays a vital role in increasing the strength of the soil from 0% to 25% by arid weight. With the percentage increase of GGBFS OMC reduces with an increase in MDD, making the soil dense and stiff. Hardness of the soil increases with an increase in specific gravity [13,14].

The experimental investigation here represents the qualitative use of GGBFS, OPC and glass fibre together as a favourable admixture for he collected expansive soil in improvising its geotechnical properties up to the mark.

2 OBJECTIVE OF THE STUDY

Objectives of the study are

a) To study the variation in properties of black cotton soil in corporation with GGBFS.

b) To study effect of 12mm glass fibres with varying percentage on black cotton soil.

c) To investigate the effect of optimum percentage of GGBFS when combined with varying percentage of OPC and glass fibres on black cotton soil.

3 MATERIALS USED

3.1 Black cotton soil:

Expansive soil is commonly known for its shrinkage and swelling properties with the variation of water content. The soil used in the present investigation has been collected from Tangi area of Cuttack, Odisha. Tests have been carried out on the soil to determine the properties of the soil which are given in the table below:

Table-1: Mechanical properties of the BC soil

Sr. no	Soil properties	values
1	Specific gravity	2.62
2	Liquid limit	63.73%
3	Plastic limit	26.08%
4	Plasticity index	37.65
5	Free swell index	38
6	MDD	1.45
7	OMC	33.5
8	CBR(unsoaked)	1.345
9	UCS	1.06
10	Soil classification	CH

3.2 Ground granulate blast furnace slag(GGBFS):

GGBFS is the maximum used mineral admixture in the present experiment which is a partial replacement of the additives. The admixture has been collected from RAMCO cement pt. ltd Jajpur,Odisha. The properties of GGBFS observed from various tests conducted are given in table below:

Table-2: Chemical composition of GGBFS

Chemicals present	percentage
Magnesia	8.366
Sulphur	0.51
Sulphide	0.62
Chloride	0.006
Silicate	91
Moisture	0.9

Table-3: physical properties of GGBFS

Properties	Values
Specific gravity	2.78
Fineness(M^2/Kg)	367
Residue (%)	8.6

3.3 Ordinary Portland cement:

The OPC used for the mentioned work has been procured from a local dealer of cement in Tangi area, Cuttack, Odisha.

3.4 Silicate glass fibre:

Silicate Glass fibres vary in their sizes like 6mm and 12mm. here in the mentioned work 6mm thickness of the glass fibre has been used which was procured from Reliance Infra pvt. Limited. through online procedure.

The properties of the fibre provided by the manufacturer are given in the table below.

Table-4: properties of the GF given by Manufacturer

Mechanical properties	values
Specific gravity	2.7-2.74
Tensile strength, MPa	1700
Effect of temperature Softening point	860^0C

4 PREPARATION OF THE SAMPLE:

As per the IS code, the properties of the BC soil were found out without mixing with any admixture. To determine the optimum value of the GGBFS best suited for the soil,the various basic properties of chosen soil were found out with GGBFS.

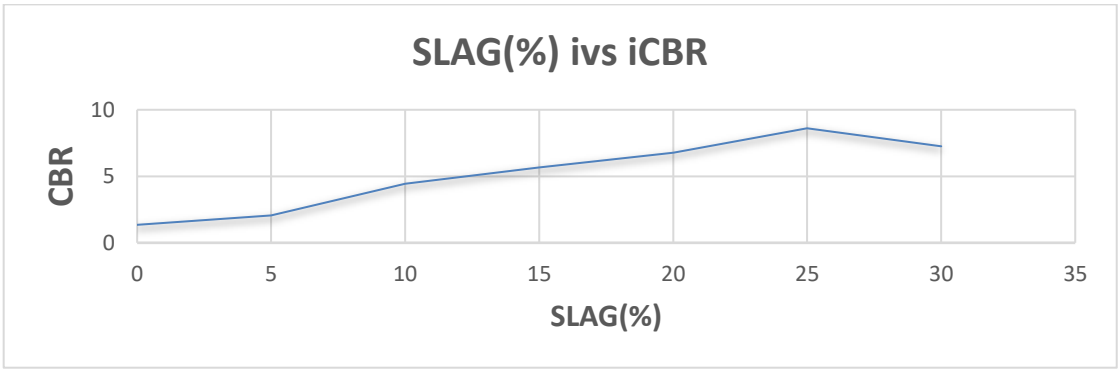

Graph-1: plot on variation of CBR with % of slag

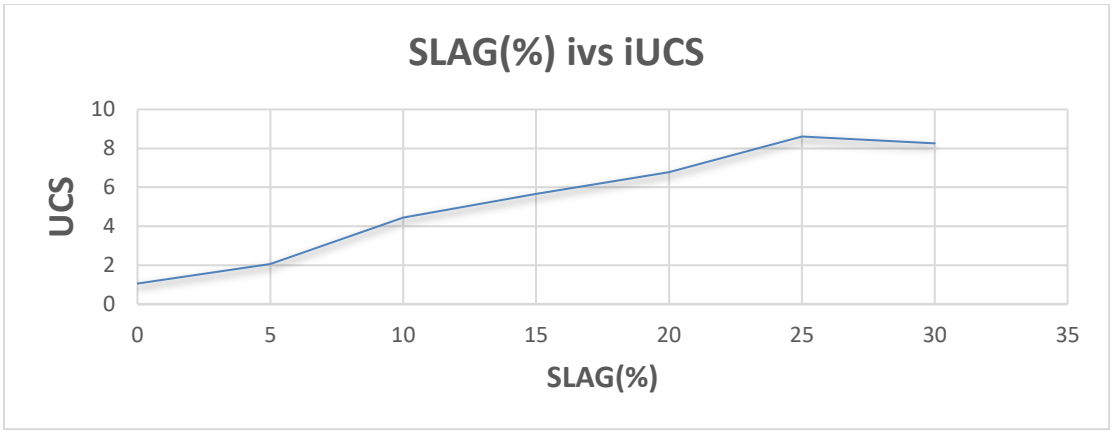

Graph-2: plot on variation of UCS with % of slag

From the above graphs presented, it was observed that as the slag percentage increases,CBR and UCS values also increase. 25% of GGBFS gives the best result when treated with the soil. So the optimum value of GGBFS was found to be 25%.

After finding the optimum percentage of GGBFS, the partially replaced soil with 25% of GGBFS was treated with Ordinary Portland cement 0.2%, 0.5%, 0.8% & 1.1% and 0.25%, 0.5%, 0.75% and 1% of glass fibres. The mechanical propertieswere carried out in the laboratory by conducting the standard proctor test, unconfined compressive strength test and California bearing ratio test. Themaximum dry density and optimum moisture content values were found out from the compaction curves as per IS codes. OnceOMC & MDD values for different prepared samples of B.C.SOIL+GGBS with varying percentage of cement & GF were foundout, the mix proportions for which the best results of MDD were found out, the UCS and CBR samples were prepared for the same and keptfor curing. These prepared samples of UCS and CBRwere tested in the UCS machine at 3, 7 & 14 days of curing.

5 RESULT AND DISCUSSION:

The OMC and MDD results of soil with 25% GGBS and varying proportions of OPC and glass fibres have been represented in the table given below:

Table-5: OMC and MDD results for different mix proportions of soil with GGBFS, GF and OPC

Sr.no	Soil proportions	OMC(%)	MDD(gm/cm^3)
1	**B.CSOIL+25%GGBS+0.2%OPC+0.25%GF**	26.7	1.727
2	**B.CSOIL+25%GGBS+0.5%OPC+0.25%GF**	26.4	1.736
3	**B.C.SOIL+25%GGBS+0.8%OPC+0.25%GF**	25.6	1.754
4	**B.CSOIL+25%GGBS+1.1%OPC+0.25%GF**	25.0	1.776
5	**B.C.SOIL+25%GGBS+0.2%OPC+0.5%GF**	24.8	1.821
6	**B.CSOIL+25%GGBS+0.5%OPC+0.5%GF**	23.3	1.843
7	**B.CSOIL+25%GGBS+0.8%OPC+0.5%GF**	22.4	1.875
8	**B.CSOIL+25%GGBS+1.1%OPC+0.5%GF**	22.8	1.813
9	**B.CSOIL+25%GGBS+0.2%OPC+0.75%GF**	20.6	1.924
10	**B.CSOIL+25%GGBS+0.5%OPC+0.75%GF**	20.2	1.945
11	**B.CSOIL+25%GGBS+0.8%OPC+0.75%GF**	19.8	1.927
12	**B.CSOIL+25%GGBS+1.1%OPC+0.75%GF**	20.1	1.825
13	**B.CSOIL+25%GGBS+1.1%OPC+1.0%GF**	20.3	1.937
14	**B.CSOIL+25%GGBS+1.1%OPC+1.0%GF**	20.9	1.742
15	**B.CSOIL+25%GGBS+1.1%OPC+1.0%GF**	21.5	1.542
16	**B.CSOIL+25%GGBS+1.1%OPC+1.0%GF**	22.4	1.038

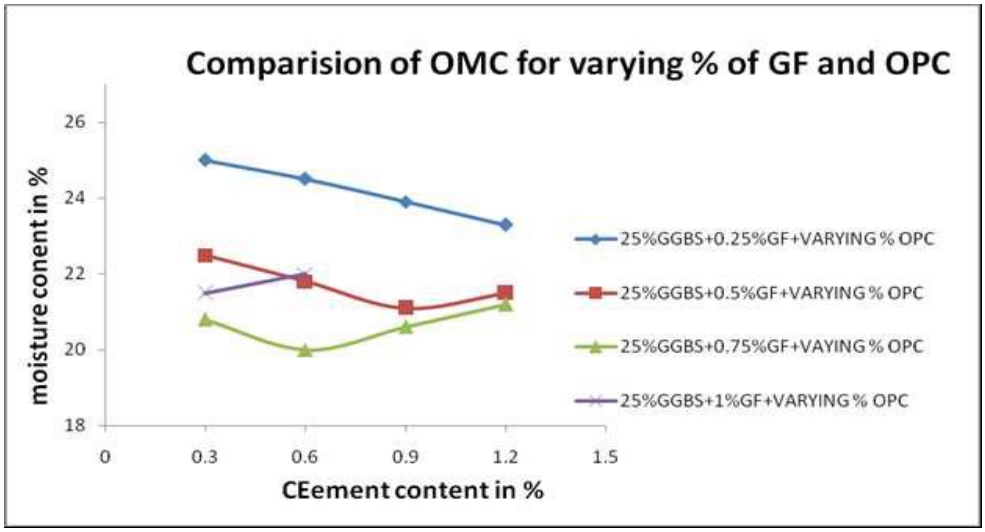

Graph-3:Comparative OMC results for varying percentage of GF and OPC with optimum GGBS

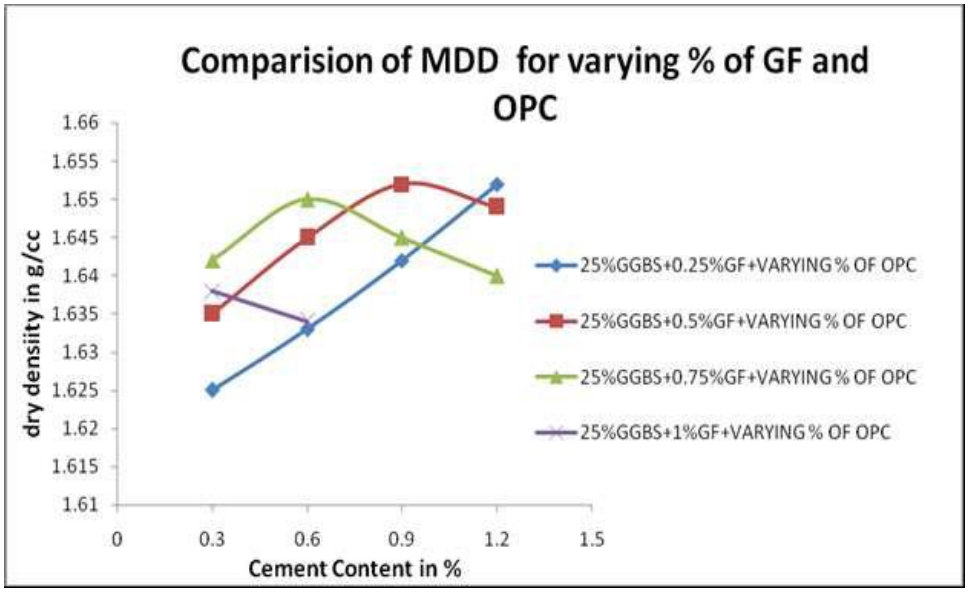

Graph-4: Comparative MDD results for varying percentage of GF and OPC with optimum GGBFS

From the above compaction curves, it is observed that with a small percentage increase in cement from 0.2%-1.1%, themaximum dry density also increases from 1.727g/cc to 1.776g/cc and there is gradual reduction in OMD value from 26.7% to 25%. By the addition of 25% GGBS with 0.5% GF and cement 0.2-1.1%, the MDD increases from 1.821g/cc to 1.875g/cc up to 0.8% of cement and it is being reduced when 1.2% cement is used.Further increase in GF up to 0.75% with 25% GGBS and varying percentage of cement, it is seen up to 0.5% of cement theMDD increases but further increase in dosage of cement lowers the value of MDD because of its workability. When the percentageof GF increase from 0.75% to 1% there is reduction in the value of MDD. The glass fibre is workable up to 0.75% only when used with 0.5% of cement. The glass fibre with 0.75% gives maximum value of compaction when compare to other blending proportions.

The unconfined compressive strength of the soil treated with 25% of GGBFS and varying proportions of OPC and GF are tested and the results of the mixed proportions with optimum MDD are given in the table below

Table-6: UCS values at optimised MDD results

Sr. no	Soil proportions	UCS(kg/cm^2)		
		3days	7days	14days
1	25%GGBS+0.25%GF+1.1%OPC	1.67	3.26	4.11
2	25%GGBS+1.0%GF+0.2%OPC	1.73	3.75	5.22
3	25%GGBS+0.5%GF+0.5%OPC	1.81	4.62	5.45
4	25%GGBS+0.75%GF+0.8%OPC	1.87	4.89	5.76

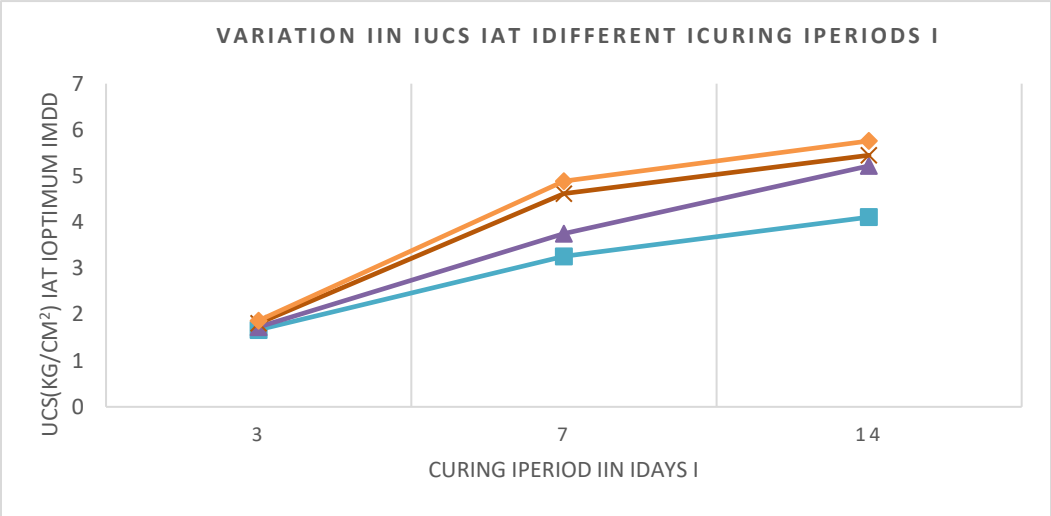

Graph-5: comparative plot of UCS with curing period

The above graph shows the comparative unconfined compressive strength for the different mix proportions with curing time.Four different mix proportions were used for finding the values of unconfined compressive strength by keeping the optimumdosage of GGBS i.e. 25%. The UCS values were observed for 3, 7 and 14 days of curing period.

The UCS value of the virgin soil for zero day of curing was 1.06kg/cm^2. For 3 days of curing period, the optimum UCSvalue achieved for mix proportion 0.75%GF+0.8%OPC. The value reached to 1.87kg/cm^2 which is 1.7 times the strength ofunreinforced soil achieved at zero days of curing.

When we observe the specimen cured for 7 days, the maximum value achieved is 4.89kg/cm^2 which is 4.6 times the strengthof unreinforced soil when the soil is blended with 0.75%GF and 0.5%OPC in case of 14 days of curing period, 4.11kg/cm^{2}achieved for the mix proportion 0.25%GF+1.1%OPC with 25%GGBS. Whereas highest value achieved is 5.76 kg/cm^2 which is5.4 times the value of unreinforced soil tested at zero day.

From the above graph it has been observed that the UCS value increases with the curing period. From the study it is also seen thatthe strength increase up to 0.75% of glass fibre. Further increase of glass fibre results in the reduction of UCS value. The glassfibre is workable up to 0.75% when used with 0.5% of ordinary Portland cement.

Table-7: CBR values at optimised MDD results

Sr. no	Soil proportions	CBR		
		3days	7days	14days
1	25%GGBS+0.25 %GF+1.1%OPC	1.73	4.55	5.67
2	25%GGBS+1.0 %GF+0.2%OPC	1.85	4.76	5.78
3	25%GGBS+0.5 %GF+0.5%OPC	1.88	4.89	6.21
4	25%GGBS+0.75 %GF+0.8%OPC	1.92	5.68	6.57

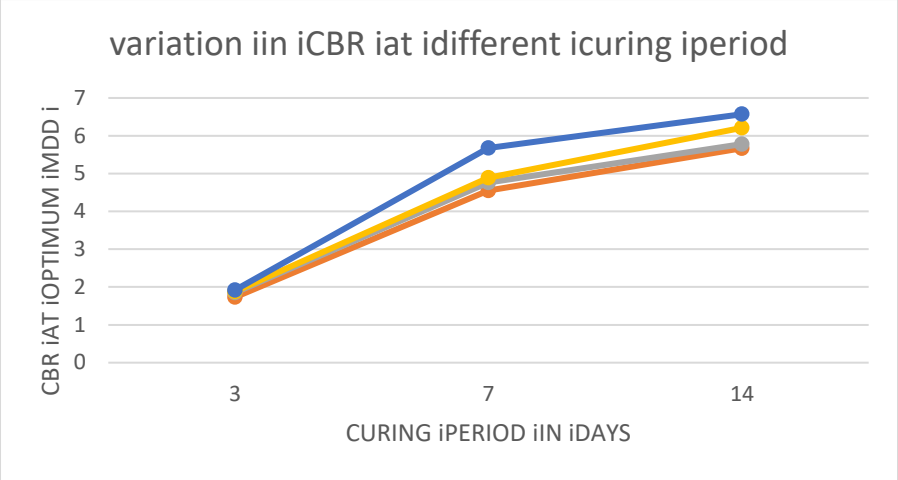

Graph-6: comparative plot of CBR with curing period

The above graph shows the comparative California bearing ratio value for the different mix proportions with curing time. Four different mix proportions were used for finding the values of CBR by keeping the optimum dosage of GGBS i.e. 25%. The CBR values were observed for 3, 7 and 14 days of curing period.

The CBR value of the virgin soil for zero day of curing was 1.345. For 3 days of curing period, the optimum CBR value achieved for mix proportion 0.75%GF+0.8%OPC. The value reached to 1.92 which is 1.4 times the CBR of the untreated soil achieved at zero days of curing.

When we observe the specimen cured for 7 days, the maximum value achieved is 5.68 which is 4.2 times the strength of untreated soil when the soil is blended with 0.75%GF and 0.5%OPC.In case of 14 days of curing period, 6.57CBR value is achieved which is around 5times the CBR value of the untreated soil.

From the above graph it has been observed that the CBR value increases with the curing period. CBR value also responses as UCS. O.75% of glass fibre in the mix proportion gives the best results for CBR with 0.5% of OPC.

CONCLUSION

So many research works have been conducted on soil in corporation with GGBFS,GF and OPC as mineral admixture to improve the soil properties. From the above experimental investigation it can be concluded that:

- Black cotton soil when treated with optimum dosage of GGBFS in corporation with a small quantity of other strengthening admixtures gives significant results for the geotechnical parameters.
- 25% of GGBFS was found to be the optimum dosage for the soil to be stabilised.
- A small portion of the GF that is .75% and 0.5% of OPC was also the favourable quantity for the soil improvement.at this proportion of GF and OPC, with 25% of GGBFS the soil reached its optimum MDD value.
- UCS and CBR for the black cotton soil also reached their maximum values at the optimum dosage of GGBFS, 0.75% of GF and .5% of OPC.

- The Unconfined compressive strength was found to be increased around 5.4 times of the untreated soil whereas the un soaked CBR was found to be increased around 5 times of the untreated soil. Overall there was an significant improvement in the soil properties due to the use of GGBFS with glass fibre and OPC.

REFERENCES

1. *Ashutosh rawat, Rajesh jain,(2017)"effects of blast furnace slag on index properties of black cotton soil" International Research Journal of Engineering and Technology (IRJET) Volume: 04 Issue: 01.*
2. *Abhijith S and Aruna T,(2015), "Effect of Sisal Fibers and GGBS on Strength Properties of Black Cotton Soil", International Journal of Innovative Research in Science, Engineering and Technology ,Vol. 4, Issue 7, pp.5409-5417.*
3. *Ashish Kumar Pathak, Dr. V. Pandey, Krishna Murari . J.P.Singh (2014), "Soil Stabilization Using Ground Granulated Blast Furnace Slag", Int. Journal of Engineering Research and Applications www.ijera.com ISSN: 2248-9622, Vol. 4, Issue 5, May 2014, pp.164-171.*
4. *Baki Bagriacik "Experimental Study about Soil Improvement with Glass Fibers" International Journal of Engineering Research Volume No.6, Issue No.8, pp : 392-396*
5. *Chandra, S., Viladkar M. N. and Nagrale P. (2008) "Performance evaluation of fiber reinforced soil - fly ash mixtures", Journal of Transportation Engineering, Vol. 134, No.1, pp. 1-14.*
6. *Consoli, N. C., Prietto, P. D. M. and Ulbrich, L. A. (1999). ''The behaviour of a fibre-reinforced cemented soil.' Ground Improvement, London, 3(1), 21–30.*
7. *Chen, F.H. (1988). "Foundations on Expansive Soils", Elsevier Scientific Publishing Co., Amsterdam.*
8. *Dimpa Moni Kalita, indrani mili, Himadri Baruah, Injamamul Islam (2014)"comparative study of soil reinforced with natural fiber, synthetic fiber and waste material" international journal of latest trends in engineering and technology(IJLTET) VOL. 6 Issue 4.*
9. *Dhananjay Kumar Tiwari , Dr. R.K.Dixit , Dr. Subrat Roy,(2016)" Study on Stabilization of Black Cotton Soil by Using Stone Dust & Polypropylene Fibers", International Journal of Innovative Research in Science, Engineering and Technology, Vol. 5, Issue 9, pp.16872-16876.*
10. *Freitag, D. R., (1986) "Soil randomly reinforced with fibers", Journal of Geotechnical Engineering, ASCE Vol. 112 (8), pp. 823–826.*
11. *Gupta P., Saran S. and Mittal R., (2008) "Behaviour of fiber reinforced sand in different test conditions", Indian Geotechnical Journal, 2008, pp. 272-282*
12. *Ground Improvement Techniques, December 18, (2008) [online] at http://www.engineeringcivil.com.*
13. *Gyanen Takhelmayum1, savitha.A.L2, Krishna Gudi (2013)"Experimental Studies on Soil Stabilization Using Fine and Coarse GGBS ISSN 2250-2459.*
14. *Henry Vidal, (1968), "The Principles of Reinforced Earth", Highway Research Record, Vol. 282, pp. 1-16.*
15. *Hausmann, M.R., (1990) "Engineering Principles of Ground Modification", Mc Graw-Hill Book Co., New Delhi.*
16. *K. Suresh, V. Padmavathi, Apsar Sultana(2009) " Experimental Study of Stabilization of black cotton soil by using stone dust and fibres.*
17. *Katti, R.K. (1979)," Search for Solutions to Problems in Black Cotton Soils". First IGS annual lecture. I G J. 9: pp 1- 80.*
18. *Kumar, B.S.C. and Ramesh, K., 2017. Durability Studies of GGBS and Metakaolin Based Geopolymer Concrete. Technology, 8(1), pp.17-28.*
19. *Lunkad, S.K. (1977)," The Effect of Soil Genesis and Expanding Layered Lattice Mineral on the Engineering Index properties of Residual Trappe an Soils of Malwa Plateau",. Proceedings of the First National Symposium on Expansive Soils, HBTI, Kanpur, India. pp. 10-1 to 10-7.*

20. *Likhitha.H, Raghavendra.H.N, Rakesh.K.P (2018)"Stabilization of Sub grade Black Cotton Soil using Cement and M- Sand" International Journal of Engineering Technology Science and Research Volume 5, Issue 1.*
21. *Mostafa Deep Hashem , Afaf Abdel Haleem Mahmoud , Ahmed Moussa Abu Bakr , Ahmed Awad Hag(2016) " Stabilization of expansive sub grade soil by using additives" Journal of Engineering Sciences Assiut University Faculty of Engineering Vol. 44 No. 2 PP. 122 – 131.*
22. *Reddy, M.M., Reddy, K.R.S., Asadi, S.S., 2018. An experimental study on combination of geosynthetic material with sand for evaluation of shear strength parameters. International Journal of Pure and Applied Mathematics, 119 (14), pp.1779-1786.*
23. *Roy, S. and Char, A.N.R. (1969)," Engineering Characteristics of Black Cotton Soils as Related to Their Mineralogical Composition". Proceedings of Symposium on Characteristics of and Construction Techniques in Black Cotton Soil. The College of Military Engineering, Poona, India. Pp. 19-23.*
24. *Soganc, A.S (2015)," The Effect of Polypropylene Fiber in the Stabilization of Expansive Soils", World Academy of Science, Engineering and Technology International Journal of Geological and Environmental Engineering Vol. 9, No: 8, pp.994-997.*
25. *Vikas Rameshrao Kulkarni, Ganesh Keshavrao Patil (2014), "Expermental Study of Stabilization of B.C. Soil by Using Slag and Glass Fibers" Journal of Civil Engineering and Environmental Technology Volume 1, Number 2; pp. 107-112*
26. *V Sathiya priya, Dr.P.D.Arumairaj (2016) "Experimental and analytical investigation of artificial fiber reinforced sub grade soil for flexible pavement" international journal of engineering trends and technology (IJETT)- VOUME 35..*

BIOGRAPHICAL NOTES

Sourya Snigdha Mohapatra is Assistant Professor, Department Of Civil Engineering, DRIEMS, Cuttack. She did her M.TECH in Geotechnical Engineering from VSSUT Burla and member of different reputed professional bodies like Institution of Engineers(India)IEI, ISTE etc.. She has more than 5 years of teaching & industrial experience. She has published journal papers & attended many conferences on geotechinal engineering. Recently awarded a research project under collaborative research & innovation scheme (CRIS), TEQIP-III, BPUT, Rourkela

Biswajit Jena holds a bachelor's degree in Civil Engineering from KIIT University Bhubaneswar and M-Tech in Structural Engineering from NIT Rourkela and member of different reputed professional bodies like Institution of Engineers(India)IEI, ISTE and also awarded as chartered engineer. He has worked with different construction industries in the past several years. Biswajit Jena is passionate about engineering education and research in India and has transitioned into the education & research sector for last 10 years. Recently awarded a research project under collaborative research & innovation scheme (CRIS), TEQIP-III, BPUT, Rourkela

Routing Protocols in Delay Tolerant Networks: A Survey

[1]Pradosh Kumar Gantayat, [2]Sachikanta Dash

Associate Professor, Department of Computer Science and Engineering
DRIEMS Autonomous Engineering College, Odisha,India
[1]kumarpradosh13@gmail.com, [2]dr.sachikanta@driems.ac.in

ABSTRACT

The Delay Tolerant Network architecture envisions a protocol suite that handles numerous specialised difficulties in heterogeneous networks and goes well beyond the regular Internet Suite's capabilities (DTN). It is a highly successful design that uses the store and forward technique to achieve end-to-end reliability. We present an overview of DTN in this work, including its properties, types of routing protocols, comparisons across protocols, and advanced DTN topologies. It can also be used in a variety of domains like as the military, social networking sites, and providing network services to remote locations. The study also discusses the security of a network employing DTN as well as cyber-attacks. The purpose of this study is to provide a brief overview of how the DTN is strengthening wireless networks.

Keywords: *Delay Tolerant Network, Replica Bundles, Cyber Attack*

1. INTRODUCTION

Delay Tolerant Networks are new networks in the realm of wireless networks that focus on providing end-to-end connection in places where networks are unreliable. Bundle layer protocol is used by the DTN. The DTN began in 2002 with Kevin Fall's inventions in Interplanetary Internet Design, which are covered in the first section of the Literature Survey. Traditional TCP/IP protocols were unable to function in the challenged networks, necessitating the development of a new architecture. The DTN is used in critical applications such as military and satellite communication, with security being a top priority. The globe is obsessed with the internet, but only a few distant locations have access to it. The new architectures allow the DTN to supply services even to rural areas. The DTN provides tight security through encryption and other ways, which is at the heart of today's wireless communication. The DTN is also keeping a close eye on the attacks.

2. REVIEW OF THE LITERATURE

Kevin Fall et al.[1] have proposed the issues that today's networks face and developed a general oriented design as a solution for these "challenging networks." The challenged networks evolve due to node mobility or are partitioned due to RF signal interference, near-earth satellite communication and long-distance radio links which suffer from many unpredictable situations such as environmental changes and the inability to store and forward messages, and Military Wireless AdHoc networks where there are critical situations for priority basing. These issues force us to think of new approaches to design architectures that will help us overcome the situation and ensure network stability. The features of the challenged networks are divided into three categories: path and link characteristics,

network architectures, and end system characteristics, each of which is further divided into subcategories. High latency, low data rate, disconnection, and extended queue times are all features of the path and link. Interoperability concerns and security concerns are among the network characteristics. The end system has a short lifespan, operates at a low duty cycle, and has limited resources. In everyday life, people communicate via Internet protocols, but in the case of Challenged networks, the situation is different since there is no end-to-end compatibility. This resulted in the creation of Architecture that is “Delay Tolerant Message-Oriented.”

Delay Tolerant networks provide a range of options for challenging networks. It is built on message switching, with bundlers handling the bundles of messages and Bundle forwarders or Gateways handling the routers that handle them. When a node is exposed to other networks, DTN uses an overlay architecture, which forms the topmost layers over the current architectures and strengthens the network by providing a gateway. The gateways are used to store communications from neighbouring regions and to deliver data in the event of a network outage. The gateways are given names in tuples that include the area and entity names. The region-based routing methods and algorithms are heavily reliant on path selection and scheduling. The bundler is made up of several convergence layers that work along with the transport layer protocols to provide dependable delivery. Because there is no end-to-end scheduling, time synchronisation is the most difficult task. Despite the fact that the NTP protocol has solved this problem, the challenging networks still have a lot of problems. To make the architecture secure enough, we put a "postage stamp" in the messages we transmit, which includes sender identity, authorization, and service class. Cryptography keys are frequently used as well. The DTN uses standard transport layer protocols as well as DTN region-specific techniques implemented by the bundlers to govern flow. To prioritise and assure reliability, the FCFS (First Come First Serve) method is employed for congestion control. Message bundlers are responsible for implementing the application interface. The DTN-based end application must not expect on-time responses and is also responsible for generating the Tuple names.

Anh-Minh Nguyen et al.[2]wrote an article describing the importance and functionality of DTN in social networking services. For a reliable connection, social networking services have traditionally relied on Mobile Adhoc networks. However, once the link is gone, we are unable to transmit the data any further. The DTN offers the benefit of storing and forwarding communications. The hop-by-hop transfer ensures that the data is saved somewhere along the network's path. The use of DTN has expanded as the number of users and devices has grown, as it provides a dependable and secure connection. Because the data is held at some point of node in the network, this also emphasises connection even when the devices shut down. The DTN network works as a sandwiched layer between the devices and the Adhoc network in this configuration. The exact architecture of DTN in social networking services is depicted in Figure 1. In real-time scenarios, p2p is a social networking tool.

Salman Ali et al.[3]have proposed a paper on Delay Tolerant Network Routing Protocols. In the challenging networks, routing protocols play a crucial part in message transport. DTN, unlike traditional Mobile Adhoc Networks (MANET), uses unique routing techniques. They are divided into three groups: replica-based, knowledge-based, and coding-based.

The replica based routing principle states that each node makes several copies of the message and retransmits it after establishing a successful connection. Direct contact – where the sender holds the data until the message reaches the receiver, two hop relay – where the message is withheld with the first n nodes that come in contact with the source and the message is transmitted to the destination once any one of the nodes connects to the receiver, and three hop relay – where the message is withheld with the first n nodes that come in contact with the source and the message is transmitted to the destination once any one of the nodes connects to the receiver Tree based flooding- relays are made as tree nodes, epidemic routing- all nodes in the network become message carriers, maxprop Priority message sending system, probabilistic routing – data transfer depends on a node's ability to communicate with others, and spray and wait – a coherent method that sets an upper bound for data transfer to nodes.

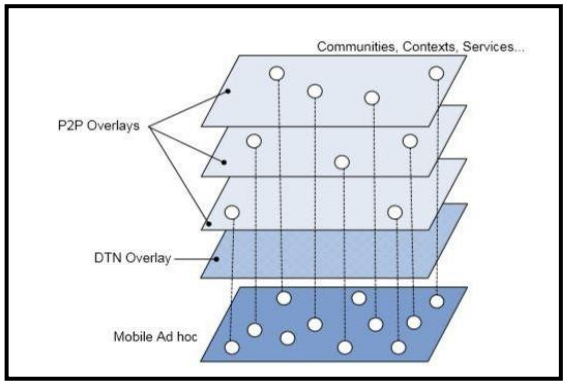

Fig 1. DTN in Social Networking Services

Knowledge-based protocols require prior knowledge about the path in order to choose the most efficient and effective way to store and convey data. Location based routing functions by assigning coordinates to nodes, source routing- source has prior knowledge of network topology, per hop routing- node acts as a judge to data transfer for other nodes, hierarchical routing- node by node data transfer, gradient routing- enacts by allowing a certain weight for each node, and link metric routing- e.g.

Coding-based protocols use encryption and decryption at the transmitter and receiver to ensure that only one node receives the data. They are further divided into Estimation based Erasure Coding, which transports a high number of messages with fixed overheads, and Hybrid Erasure Coding, which uses an aggressive forwarding technique.

A article by HideyaOchiai et al.[4]describes the use of IP over DTN with asynchronous packet delivery. DTN is typically installed in a bundle layer, which necessitates new architecture, connectivity, and maintenance, all of which are costly. In IP networking, the new architecture employs the DTN framework as a data link. Sender A sends a message that is broken down into a series of datagrams with the help of the routing table, which is then encapsulated by the DTN framework and sent over the DTN data connection. When the data link reaches the required gateway, IP packets are sent to the recipient. As a result, the transport and application layers are asynchronous. The DTN data link is built using PEAR, and the implementation is done by constructing a prototype in Linux (PHP Extension and Application Repository). There are five network segments, four of which are connected to the internet and one to PEAR. Three of the four are DTN nodes, while the fourth is connected to the

internet. The battery is the first of the three. Between the Ethernet and DTN frameworks, IP packets are stored and transmitted. This structure is unique.

A paper on the application of Delay Tolerant Network in Military Communications was given by ZiyiLu et al.[5]. Traditional protocols such as TCP/IP have a number of drawbacks, including data transfer delays, increased error rates, and erratic reliability. DTN's architecture is influenced by military applications because it employs a store-and-forward data transport method. The DTN's bundle layer architecture provides end-to-end connection. The military is confronted with three major issues. The most common type of attack is a denial-of-service attack, in which the attacker can flood the sender or receiver with massive volumes of data. DTN offers a solution to this problem by identifying bundles and restricting access to only authorised users. As a result, the other issue is information fragmentation, which is addressed by data integrity intelligence. The third issue, and the most essential in military applications, is data security. DTN uses BAH (Bundle Authentication Header) for single hop authentication, PSH (Payload Security Header) for end-to-end authentication, and CH (Confidentiality Header) to encrypt payload. DTN thus supports and addresses a number of important challenges in military applications.

A paper on DTN-based internet services for remote places was presented by Emir Husni et al.[6]. In response to a real-time challenge in Indonesia, a new service-delivery system was developed. Making the Transport service, train as a host the remote places news and mails are delivered. Trains provide services to rural areas.There is a main server that connects the worldwide internet and serves as the system's heart. The railway station server serves as a data transfer node between the main server and the train.

The train, which also includes the Customer Premise Equipment, serves as a DTN router. A village server takes on the role of village server leader. The data that is addressed to all of the remote areas is mostly downloaded by the central server. The Station server then downloads the mail and news for the region covered by the trains on that route. The information from the station server is downloaded by the trains router. The train broadcasts all of the information to the village as it passes by. Messages are kept and forwarded to the central system if there are villages that are not on the route. Various field tests are undertaken to ensure compatibility, and an average of 300 e-mails are sent per route per trip.

A paper on Three Point Encryption was given by Roy Cabaniss et al.[7]. The security of a wireless network is one of its most important criteria. With the current DTN routing technique, old systems are unreliable. It is not a matter of safety to rely on alternative security solutions that use third-party vendors. The paper discusses two main security techniques, namely the Chaining algorithm and the Fragmentation Algorithm. The basic idea behind Chaining Encryption is to force the calculation to go across k hubs, or links, without allowing any of them to see the plaintext. The first message is encoded with each connection's open key and then sent to the nearest connection. The encryption layer of that hub is ejected at each connection. The message is encrypted with it on the off access to the final connection. The message is sent to the endpoint only when each layer has been replaced with the final connection's key. Once it's there, it's decoded k times, each time removing a layer of encryption. The following is the formula for the encryption algorithm:

A bit delay is used in the chaining technique. The Fragmentation Algorithm was created to reduce this trade-off. The communication is fractured into different parts, each of which is subsequently routed across a single link at the same time. The tradeoff is reduced as a result. This technique has a flaw in that it does not guarantee that all fragments will route effectively in real-world settings.

A study on Intelligent Routing in DTN has been proposed by AzadehOmidvar et al.[8]. The DTN has a few drawbacks, such as delay and changing topology. The DTN is put in critical locations such as interplanetary operations and military communications where delay is not an option. An innovative AI-based method known as the Genetic Algorithm has been created to improve the delivery rate ratio.

In Genetic Algorithm's mechanism the number of duplicates is set to one from the start. The calculation determines the delivery proportion after the warm-up phase. The computation finds the number of duplicates to spread across related neighbours using delivery proportion as wellness work. Additional duplicates are removed as the algorithm approaches the desired delivery proportion. This is an approach for optimization that relies on standard procedures such as selection, crossover, and mutation.

A work on Anatomy on Routing in DTN has been proposed by Vandana Juyal et al.[9]. The author of this paper discusses DTN's design difficulties before comparing the performance of various routing algorithms. The DTN has a number of design flaws, including high portability, coerced assets, limited buffer space, power concerns, no consistent path, a sparse system, no connectivity, and no hidden framework. The author has conducted a comprehensive literature review on DTN's routing strategies. He simulated and carefully observed the reports to compare the various routing systems, and so provided a comparative analysis of Epidemic, Trust based Routing, and Cluster based Routing. MANET, to name a few. According to the findings, MANET connection is relatively high, mobility is low among all routing protocols, and mobility structure is heterogeneous in MANET but homogenous in all other cases. Epidemic has a lot of resources, trust-based routing has a lot of resources, cluster based routing has a lot of resources, and MANET has a lot of resources. [9]

A paper on attacks in delay tolerant networks was presented by Preeti Nagrath et al.[10]. Because DTNs are a system of heterogeneous systems, the hubs in DTNs travel throughout the system for communication, making it challenging to maintain security in a DTN domain. Malicious and selfish nodes are the two types of misbehaving nodes.

Selfish Attack: A system's several hubs can become selfish by only sending their own messages. Because correspondence is prone to uncommon pioneering contacts that are necessary to transfer messages without a start to finish related way across hubs, a hub's selfish behaviour in DTNs is damaging to the system. A black hole attack is when a malicious hub makes itself desirable in order to pull the most bundles from the hub in touch.

DTNs are asset-limited systems, hence they are vulnerable to flooding attacks. Several malicious hubs try to drain system assets by flooding the system with false/pointless messages. Several hubs then forward these messages to other hubs, wasting data transmission and the limited cushion space provided by DTN hubs. According to the analysis, the black hole assault is a serious hazard that reduces almost 20% of communications, flooding reduces nearly 8% of messages, and the selfish attack reduces nearly 6% of messages.

CONCLUSION

We surveyed DTN's varied papers in this study, starting with its origins and challenges and ending with the applications it supports. In today's world, the paper presents a basic description of DTN. We present an overview of DTN in this work, including its properties, types of routing protocols, comparisons across protocols, and advanced DTN topologies. It can also be used in a variety of domains like as the military, social networking sites, and providing network services to remote locations. The study also discusses the security of a network employing DTN as well as cyber-attacks. Unlike MANETS, DTN does not consider mobility. Typically, characteristics such as time to live, energy, transmission speed, and pause time are considered to improve the performance of various routing protocols in MANETS; however, these parameters are not included in Delay Tolerant Network Routing, which is the focus of our future work.

REFERENCES

1. *Kevin Fall, "A Delay-Tolerant Network Architecture for Challenged Internets" in SIGCOMM Conference in February 2003.*
2. *Anh-Minh Nguyen , Noël Crespi, "SOCIAL-DTN: Why Social Networking Services is more fruitful to Mobile Delay-Tolerant Networks?" in 2009 International Conference on Ultra-Modern Telecommunications & Workshops.*
3. *Salman Ali, Junaid Qadir, Adeel Baig, "Routing Protocols in Delay Tolerant Networks – A Survey" in 2010 6thInternational Conference on Emerging Technologies (ICET).*
4. *Hideya Ochiai, Kenichi Shimotada , Hiroshi Esaki, "IP over DTN: Large-Delay Asynchronous Packet Delivery in the Internet" in 2009 International Conference on Ultra Modern Telecommunications and Workshops.*
5. *ZiyiLU,Jianhua Fan, "Delay/Disruption Tolerant Network and its Application in Military Communications" in2010 International Conference On Computer Design And Appliations (ICCDA 2010).*
6. *Emir Husni, "Delay Tolerant Network Based Internet Services for Remote Areas Using Train Systems" in 201117th IEEE International Conference on Networks.*
7. *Roy Cabaniss, Vimal Kumar, and Sanjay Madria, "Three Point Encryption (3PE) - Secure Communications inDelay Tolerant Networks", in 2012 31st International Symposium on Reliable Distributed Systems.*
8. *Azadeh Omidvar, Dr. Karim Mohammadi," Intelligent Routing In Delay Tolerant Networks" in The 22nd IranianConference on Electrical Engineering (ICEE 2014), May 20-22, 2014.*
9. *Vandana Juyal , Nitin Pandey , Ravish Saggar "An Anatomy on Routing in Delay Tolerant Network" in 2016IEEE International Conference on Computational Intelligence and Computing Research (ICCIC).*
10. *Preeti Nagrath, Sandhyan Aneja, G.N.Purohit, "Attacks in Delay Tolerant Networks: Classification and Analysis"in 2019 11th International Conference on Communication Systems & Networks*

BIOGRAPHICAL NOTES

Dr. Pradosh Kumar Gantayat is presently working as Associate Professor in the Department of Computer Science and Engineering at DRIEMS Autonomous Engineering College. His Main research area are Delay Tolerant network, Wireless Network, Soft Computing. He has published many research papers in reputed Journal and Conferences.He has received "Best Paper "award at NIT Meghalaya and Research Excellence Award from InSc Bangalore in the year 2021.

Dr. Sachikanta Dash is presently working as Associate Professor in the department of Computer Science and Engineering at DRIEMS Autonomous Engineering College. He received his B.Tech degree in Information Technology from Utkal University in 2004, M.Tech. degree Gandhi Institute of Engineering and Technology, Gunupur , BPUT, Orissa in 2009 and Ph.D. degree in Computer Science Berhampur University, India in 2019. He has published more than 8 journals of national and international publications in the field of Image processing, Blockchain, Healthcare sector, machine learning. He is a member of ISTE, CSI and IAENG.

Metrics for Cloud Computing to Enhance User Satisfaction and Loyalty

[1]Surajit Mohanty*, [2]Shekharesh Barik, [3]Rojalin Dash

[1,2,3]*Department of CSE, DRIEMS, Cuttack*

{surajit.mohanty, shekharesh.barik}@driems.ac.in, rojalindash@gmail.com

ABSTRACT

In the distributed computing platform, cloud computing provides promising delivery platform. Cloud computing is a model for on demand network access in a distributed shared environment of configurable computing resources. The efficiency of cloud depends on the usability of various cloud services and also depends on performance of the task execution. For this usability aspect design of various cloud services need to be interactive, goal oriented and easy to understand. This will give a positive platform to the end user and enhance user satisfaction and loyalty. Usability aspect can be measured using various evaluation technique, metric play a vital role for this evaluation process of cloud computing environment.

Keywords: *Distributed computing, , Usability Evaluation Techniques, Usability Metrics*

1. INTRODUCTION

Utility processing with savvy acknowledgment turned into the establishment of Cloud figuring model which permits clients and suppliers to get to the assets effectively in a self-productive way, with pay-more only as costs arise style, subsequently diminishing starting foundation cost and further developing asset use by augmenting the viability of asset. As of late, the Global IT environment and new business sectors economy are extraordinarily affected by the effect of distributed computing which can able to meet the fluctuating and erratic business requests as a result of its accomplishing rationality and financial matters of scale. Subsequently thinking about the advantages of end client, ease of use is most fundamental quality for estimating client fulfillment level in distributed computing climate. Consequently, ease of use will be characterized as the most common way of expanding the viability of dispersed assets with amplifying registering power to guarantee client dependability and fulfillment. Proficiency, fulfillment and adequacy, are the three prime objectives of cloud that urges to accomplishing clients explicit objective. Subsequently it tends to be expressed "a usable cloud consistently support the Users' particular assignments in an effective way". Convenience assessment can be characterized as deliberate methodology of assortment of information that makes a superior comprehension of clients conduct to move toward the cloud administration to perform for a specific assignment. To make cloud administration, appropriate engineering, estimation and plan standards are applied. These cycles assists client with utilizing cloud administration effectively at nominal cost.

2. USABILITY EVALUATION

The excursion of usability was begun in basic climate however continue to a complicated climate. The expression "usability " was presented in the last part of the 1980s [7]. In the year 2006 an investigation on convenience testing caried out by Miller [1], [5] where he examined about ease of use testing and enhance quality confirmation property. From his distribution we able to realize that ease of use testing ought to be caried out at the underlying stage to conquer the issues and great convenience testing technique can make the assistance quicker. To gauge the presentation of a site in cloud, L.Fang [2] proposed distinctive convenience assessment strategies. Assessment strategies like heuristic assessment, center gathering intellectual walkthrough, and poll can be taken on to gauge the ease of use and in 2010, A. Lodhi, [3], [5] depicted ease of use heuristics as an evaluation boundary for ease of use testing and a few analyses was led to set up to legitimize his examination. In 2012, L.Hasan [4], [5] performed investigate ease of use assessing in nine Jordanian college sites. Some ease of use characteristic was thought about to assess the convenience like effectiveness of ease of use, engineering plan and instructive substance. 237 client were chosen to do a specific undertaking on a particular site and give input .A report was created from criticism to gauge their fulfillment level of clients. Google, Hotmail, Amazon Yahoo and IBM are ceaselessly endeavoring to work with the clients through more developments.

3. USABILITY ATTRIBUTES, BENEFITS AND CHALLENGES THAT INFLUENCE CLOUD COMPUTING WORKING ENVIRONMENT

3.1. Usability attribute

As indicated by J. Nielsen, convenience is characterized by the accompanying five quality parts [8].

- **Learnability of Client :** It characterizes that client's ability of adapting rapidly and effectively of the various functionalities of an item to accomplish objective of a specific undertakings.
- **Efficiency:** It characterizes how quick clients are refined various errands and how viably client can perform assignment to gauge the expenses.
- **Memorability factor:** it characterizes the memory capacity of end client when they do not have acclimated to worked with a similar interface for a more extended period.
- **Frequent Errors:** End users commit numerous mistakes while working and coordinating with the cloud administration. This credits centers around how frequently client can make mistake and would they be able to adapt to issue effortlessly and solace. This trait is connected with the work for mistake rectification which significantly worry of recuperation from blunder and heartiness of gadget.
- **Satisfaction:** It characterizes how client is fulfilled in the wake of working and coordinating with the Cloud based application with respective Environment and how they are worried about the hour of execution. Fulfillment is estimated by input of client's demeanor, discernments, and sentiments.

Advantages of Usability Evaluation

- **Enhancing Higher Level of Usage:** Cloud administrations will not be difficult to utilize and meeting the assumptions for their customers, and fledgling clients can ready to get to the help offered [12].

- **Lowering End User Support Cost:** Usable administrations assist the client with looking through the required substance and achieve his/her objectives with the cloud application. The interface of cloud application tasks must be straightforward by the end client rule out assistance of outer intercession, which decreases client support cost. Exactness is key parts of the substance. Exactness will diminish the likelihood of client's whine to the specialist organization about the nature of administration associated .
- **Impact on Usability factor :** Usability assessment should impact each progression of ease of use designing factor.
- **Impact of Usability geting Return from Investment:** From an efficient viewpoint, distributed computing administration permits clients and suppliers admittance to assets with self-administration way and pay-more only as costs arise design. Ease of use methods can decrease costs like turn of events, support cost, preparing cost, documentation and upkeep costs, which by implication limit the advancement time, and further develop attractiveness (Cheskin: 1999). Convenience mindful associations keep up with the thumb decides that the money saving advantage proportion for the ease of use is $1:$10-$100. In the event that they burned through one dollar for carrying out convenience methods, the association will get an advantage between$10 and $100. Growing top notch cloud applications improve the validity of the application deals with the cloud administration of different association with full fulfillment of the clients and customers [12].

3.3. CHALLENGES RELATED USABILITY

There are followings few difficulties that for which the most part the convenience region faces:

- **Scalability Factor:** Scalability factor is one of the common difficulties of Cloud ease of use. For a model if any progressions done by social site like Face book (a person to person communication site), it will immediately influence enormous number of clients. In any case, eight years back that influenced less clients. So adaptability is one of issue to ease of use of distributed computing environment.
- **Visual Design Plan:** Visual plan assumes a significant part of utilization and correspondence with client. At the point when client covers their expenses or buys an aircraft reservation ticket, need straightforward application and don't have any desire to focus on the mechanics of deciphering the application's screen. Clear and succinct visual plan should fulfill the client.
- **Interactivity:** One of the significant difficulties for cloud specialist organization is the way the cloud administration turns out to be more intelligent to client.
- **Dynamic Changing Application:** Dynamic changing Application is a most significant test in ease of use. Architect can confront genuine adverse result in case changes can be done erroneously. The issues of changes basically influence those clients who utilize it as often as possible.

4. USABILITY OF CLOUD REQUIRMENT AND DESIGN PROCESS

In cloud environment, convenience is a fundamental condition. The valuable strategy for ease of use is client trying, which are talked about here [9], [12].

From the entry level, a few clients ought to be chosen and afterward educate the clients to perform undertakings in explicit cloud stage. Finally, evaluator sees if client accomplishes the work effectively ready to do and where they deal with issue with the UI.

Convenience assumes a crucial part in every phase of the plan cycle of making cloud.

Following advances are caried out for the plan interaction:

Stage 1. Prototyping another necessity, the plan engineer need to recognize the prerequisite and fulfillment level of client.

Stage 2. To get greater quality item at low costs, engineer makes an examination with contenders' plans and grows greater quality item dependent on client necessity.

Stage 3. Then, at that point Evaluator considered as end user should direct a field evaluation study to notice client's conduct, their solace and hardships.

Stage 4. At the end evaluator deliver paper models of new plan thoughts.

Stage 5. End User Evaluator verify and refines the plan thoughts with various cycles to find the best outcome.

Stage 6. After execution of the all plan at the end; test will be led to decrease the ease of use issues.

5. METHOD FOR USABILITY ASSESSMENT

The essential strides of appraisal are

- This will anticipate if convenience will meet the objective.
- This will get criticism from client to further develop plan of item.
- This will survey the objectives that have been carried out.

5.1. Focus on Interest of Usability Assessment Method

Ease of use appraisal relies upon the condition of the assessment and the evaluation focus on how it functions admirably on various angles. We will examine some significant situations of convenience appraisal [10].

5.1.1 Application's Information Content. Ease of use appraisal is extraordinarily relying on the enlightening substance. Ease of use appraisal is carried out to assess the rightness of data, planning and various functionalities related to the frameworks.

5.1.2 User Interface Functionality. Usefulness of the UIF is a significant property answerable for the use of introducing parts of the UIF relationship. This element assists client with getting to various data content by perusing and exploring measurements. Client can ready to look, select, recover and store the data after effective route.

5.1.3 Performance of Enduser. Client execution is most fundamental ease of use evaluation and can be recognized by two angles. Initial, one is Effectiveness. (Regardless of whether the client got the data effectively to give the right yields); and second is effectiveness (the length that client can accomplish result or objective).

5.1.4 Workload Distributed To End User. This factor relies upon the attributes and characteristics of errand, which carried out by the client. The result of undertakings decides the client execution .Userstress is a major factor of intellectual burden and it relies upon self capacity to achive and to adapt to exhaustion.

5.1.5 Enduser Satisfaction. Client fulfillment is viewed as an imperative trait while considering convenience issues. However the framework is proficient, or produces yields successfully yet the client, response to the framework is generally significant. Client not really settled if the framework will be acknowledged being used.

5.1.6 Analysis of Cost/Benefit. Cost and advantage investigation centers around usefulness of the framework so client can accomplish a fulfillment level to convey his work at sensible expense.

5.2. Evaluation Process of Usability

Convenience is taken as iterative techniques that focus on genuine clients and the assignment performed by them. Assortment of strategies is associated with convenience designing and appraisal. These strategies are depicted beneath:

Behaviour of client and errand: Here the enduser evaluator goes through perception performed by clients while endeavoring any undertaking in their work environment and examination of their work measures evaluator tracks down their psychological fulfillment level [10].

Interviews and polls: A bunch of surveys are ready prior to leading a meeting with clients, and from input of client the report is produced dependent on client inclinations, encounters and their reuirments.[10], [8].

Competitive examination and Evaluation: Evaluation of ease of use centers around the comparable items that are accessible on the lookout. In this manner, serious investigation is performed between comparative item to give a helpful convenience study [10], [5].

Paper prototyping: In this interaction, clients are included to play out the undertaking in the unpleasant and hand portrayed model, prior to start of real coding. Contingent upon their presentation, the genuine execution is done [10], [5].

Design of Guidelines: This incorporates set o standard rules, which might be trailed by creators to guarantee maintaining consistency in plan of the product during the plan stage [10].

Usability testing Method: In this method, client tests an item and gives criticism to evaluator. Enduser evaluator breaks down their criticism to discover issue with the goal that restorative measure can be concidered [8].

6. METHODS FOR USABILITY EVALUATION

There are a few methodologies of convenience assessment techniques. Some of them are examined beneath:

6.1. Approaches of Assessment Methods for Usability Evaluation:

6.1.1 HEURISTIC EVALUATION. Evaluator and undertaking master assumes significant part in heuristic technique[8]. It tends to be considered as a quick interaction and financially plausible. Endusers inspect the UIF and design an examination concentrate with set up heuristic strategies to decrease the issue looked by client.

6.1.2 User Based Evaluation. This technique for the most part centers around the input of client in plan stage. The incomplete/fast models are needed in the plan period of ease of use assessments which will make total variants of the best quality item.

6.1.3 Evaluation with Respect to Design Principal.Configuration stage has an extraordinary commitment and effect on set up ease of use assessment .Collections of rules and guidelines are fundamental for plan measures of assessment of convenience.

6.1.4 Evaluation with Respect to Assessment Model. This is a hypothetical deign model that indicates man-machine interface and Cognitive human capacities in convenience.

7. METRICS FOR CLOUD USABILITY

There are a few measurements which depend on factual and countable data.Countable measurements can be developed from crude information that are gathered from different log, video recording, meeting and surveys. We will talk about 10 measurements which are utilized for ease of use assessment [5],[8], [6], [17].

Unstructured meeting: In this strategy questioner isn't worried about the particular of frameworks. They pose the inquiry to client to gather data dependent on their experience.

Completion Rates: Completion rate can be considered as an essential ease of use metric. It tends still up in the air as door metric too. It tends to be addressed as a two fold measurement (1 can be considered as Success of undertaking and 0 is treated as disappointment of assignment.)

Usability Problems: It is considered as a vital measurement for estimating ease of use movement. This centers the issue which is finished by client while utilizing the cloud administration or web administration. It additionally depicts seriousness evaluations of those issues.

Task Time: It is one of the significant key metric that can be utilized to quantify the effectiveness and efficiency of cloud and web administration. All out task time characterizes what amount of time a client requires to do a job. Assignment time is the length between a Start task times and end task time.

Task Level Satisfaction: When client finishes a job their input is fundamental to decide the fulfillment and trouble level of errands.

Test Level Satisfaction: A meeting is to be led with clients toward the finish of convenience test and from the criticism of the client, analyzer decide the simplicity of ease of use. Framework Usability Scale (SUS) is needed for testing of programming, equipment and gadgets .SUS is innovation autonomous and is extremely basic that gives worldwide perspective on abstract appraisals of convenience.

Errors: Error might be experienced by client by fouling up activity, exclusion and slip-ups while playing out a task. Depiction of mistake alongside each occasion is recorded which is useful in Usability Inspection issues.

Conversion: Conversion metric is utilized for the estimation of the adequacy of an item. It is fundamental measurement utilized in web based business. Ease of use of transformation rates is utilized in all periods of the business interaction by zeroing in on the ease of use issues, blunders and decreases with time.

Single Usability Metric (SUM): This measurement is the blend of four convenience measurements separately task fulfillment rate, normal number of blunders, normal time on undertaking and post-task fulfillment. This measurements is summation of productivity, adequacy and fulfillment.

Standard Units of Measure (SUoM) metric is especially utilized for cloud assessment based on business requirement. Specialist organization and sellers give cloud metric that applicable to it.

To deal with the cloud environment and administrations following measurements need to be followed [18].

Costing of Cloud level: It portrays the implementing of cost for cloud based on this identified with income of business.

Cloud Cost dependent on Application viewpoints: The fundamental point of this measurement to expand business benefit for minimal price. Cloud Cost identified with per Transaction of business foundation.

Average Load Time: It is the time taken for the heap time to transfer video and picture

File CRUD Times: The time needed to Read, Create, and Update or Delete a document of predefined fixed size.

Database CRUD Times: It is average time needed to execute the orders to make, read, refresh or erase document from wanted cloud data set.

Average and Peak CPU Utilization: It is a pivotal lattices which relies upon how much rate CPU is registered in cloud climate and the number of example is presently running.

Network-In: This measurements recognizes number of bytes got in all organization UI by the case.

CONCLUSION

Today the World Wide Web acquire colossal prominence due to different administrations gave to the client in the field of distributed computing and man and Machine interface. Accordingly, convenience turns into an imperative property for estimating client fulfillment level, which might additionally work on the exhibition and adequacy of programming item just as web cloud. Ease of use can be considered as a quality to quantify the insight of Cloud while playing out the assignment to accomplish the client's objective and requirements. In this paper we sum up ease of use assessment procedures, appraisal and issue identified with distributed computing administrations. The clients' presentation in the cloud climate can work on the nature of cloud administration, That prompts expansion in ROI and client fulfillment level..

REFERENCES

1. *J. Miller, "Usability Testing: A Journey, Not a Destination," Internet Computing IEEE, 10(6), pp. 80-83, 2006.*
2. *F. Liu, "Usability evaluation on websites" In 9th International Conference on Computer-Aided Industrial Design and Conceptual Design, CAID/CD, pp. 141-144, China, 2008.*
3. *A. Lodhi, "Usability Heuristics as an assessment parameter: For performing Usability Testing", In 2nd IICSTE, pp. 256-259. USA, 2010.*
4. *L. Hasan, "Evaluating the usability of nine Jordanian university websites", In 2nd ICCIT pp. 91-96, Tunisia, 2012.*
5. *S. Roy, P.K. Pattnaik, "Some Popular Usability Evaluation Techniques for Websites", Advances in Intelligent Systems and Computing 247, FICTA, pp. 535-543, 2013.*
6. *Measuring Usability [Online]. Available: http://www.measuringusability.com.*
7. *J. Nielsen, "The Usability Engineering Lifecycle. IEEE Computer, 25(3), pp. 12-22, 1992.*

8. *J. Nielsen, "Usability Engineering", Academic Press, Cambridge, MA, 1993.*
9. *L O. Bello and S. Zeadally, "Toward efficient smartification of the Internet of Things (IoT) services," Future Generation Computer Systems, vol. 92, pp. 663–673, 2017.*
10. *S. Li, L. Da Xu, and S. Zhao, "5G Internet of Things: A survey," Journal of Industrial Information Integration, vol. 10, pp. 1–9, 2018..*
11. *A. Xu, S. Gao, "Discussion on Usability and Optimization Issues in Overseas University Websites: A British University as an Example," 11th International Symposium on Distributed Computing and Applications to Business, Engineering & Science, pp-482-485, 2012.*
12. *Evidence-Based User Experience Research, Training, and Consulting [Online]. Available: http://www.useit.com*
13. *Usability Evaluation, [Online]. Available: http://www.usabilityhome.com.*
14. *R. Bias, "The Pluralistic Usability Walkthrough: Coordinated Empathies" In: Nielsen, J. and Mack, R. Usability Inspection Methods, Chapter 3, pp. 63-67. John Wiley, 1994.*
15. *Monther, A.A.; Tawalbeh, L. Security techniques for intelligent spam sensing and anomaly detection inonline social platforms. Int. J. Electr. Comput. Eng. 2020, 10, 2088–8708.*
16. *J. Nielsen, "Heuristic evaluation", In: Nielsen, J, Mack, R. L. (Eds.), Usability Inspection Methods, John Wiley & Sons, pp. 25-64, New York, 1994.*
17. *S. Ahmed, D. Mohammad, B. Rex Kline, K.P. Hrkirat, " Usability Measurement and Metrics: A consolidated model", Software Quality Journal, pp. 159-178, 2006.*
18. *Measuring the User Experience, Second Edition: Collecting, Analyzing, and Presenting Usability Metrics, [Online], Available: http://www.amazon.com*

BIOGRAPHICAL NOTES

Surajit Mohanty is working as Associate Professor, Department of CSE, DRIEMS, autonomous engineering college, Cuttack , Odisha having 15 year of experience in industry and teaching, in the following domain Data mining, IoT and software engineering having more than 20 national and international publication out of which four are Scopus indexed.

Shekharesh Barik is working as Associate Professor, Department iof CSE, DRIEMS, autonomous engineering college, Cuttack , Odisha having 17 year of experience in teaching, in the following domain Data base, data structure, Computer graphic and IoT having more than 20 national and international publication out of which five are Scopus indexed.

Rojalin Dash is working as Associate Professor, Department iof CSE, DRIEMS, autonomous engineering college, Cuttack , Odisha having 8 year of experience in industry and teaching, in the following domain Data analytics , advanced computer architecture, cloud Computing and having more than 10 national and international publication.

Interactive Machine Learning Classification Techniques for Diabetes Mellitus Prediction

[1]Sachikanta Dash, [2]Pradosh Kumar Gantayat, [3]Raghunath Rout

Department of CSE, DRIEMS, Cuttack

{dash.sachikanta,kumarpradosh13,raghunathrout78}@gmail.com

ABSTRACT

Diabetes is a chronic condition with the potential to destabilize the global health-care system. Diabetes affects 382 million people globally, according to the International Diabetes Federation. By 2035, this number will have risen to 592 million. Diabetes is a condition that causes blood glucose levels to rise. Frequent urine, increased thirst, and increased appetite are all signs of high blood glucose. Blindness, renal failure, amputations, heart failure, and stroke are just a few of the diabetic complications. Our bodies convert food into sugars, or glucose, when we eat it. Machine learning is a relatively young branch of data science that studies how computers learn from their past experiences. The goal of this project is to use a mix of machine learning approaches to build a system that can identify diabetes in a patient earlier and more accurately. Support Vector Machine, Logistic Regression, Random Forest, and K-Nearest Neighbor are four supervised machine learning algorithms used in this work to predict diabetes. The accuracy of the model is calculated using each algorithm. After that, the model with the highest accuracy for predicting diabetes is chosen. A comparison analysis is proposed in this work for properly predicting diabetes mellitus. This study also attempts to provide a more effective method for detecting diabetes illness.

Keywords: *K Nearest Neighbor, Logistic Regression, Support Vector Machine, Random Forest, ROC.*

1 INTRODUCTION

This article requires certain precise actions related to diabetes control and prevention. Previously, statistics showed that one out of every 10 people in the United States had diabetes. Regardless, it is expected that by 2045, it will be able to assist one out of every three people. This is a real problem that has to be addressed. When the blood glucose concentration rises to dangerously high levels, diabetes becomes a chronic condition. This is a major cause of various problems and illnesses, such as renal disease and heart disease. Diabetic predisposition is also caused by a variety of bad food habits and a lack of proper bodily routines. The World Health Organization (WHO) has said that the total number of people living with diabetes has skyrocketed in recent years. Managing multiple diabetic datasets is required to enhance the present rate of diabetes patients and reduce it to an absolutely inconsequential level by focusing on reducing it on a large scale. Certain approval techniques are also incorporated to operate with the diabetes forecast project's pure precision.

Diabetes is a rapidly spreading disease that affects individuals of all ages, including children. To understand diabetes and how it develops, we must first understand what happens in the body without diabetes. Carbohydrate meals are

our body's primary source of energy. Bread, cereal, pasta, rice, fruit, dairy products, and vegetables are all carbohydrate foods (especially starchy vegetables). When we ingest these nutrients, it is then converted to glucose by our body. The glucose then travel through the bloodstream in our body. Few glucose particle is also transported to our brain, that helps us and giving us the ability for operate and thinking properly. The rest of the glucose particle then sent to the body's cells for energy. The remaining are sent to liver for latter use of energy. Insulin is necessary for the body to utilize glucose for energy. Insulin is a hormone that is generated in the pancreas by beta cells. Insulin works in a similar way as a key in a lock. Insulin attaches to cell doors and opens them, allowing glucose to flow from the circulation into the cell through the cell door. When the pancreas is unable to create enough insulin or the body is unable to use the insulin it does make (insulin resistance), glucose builds up in the bloodstream, causing hyperglycemia and diabetes. The presence of excessive quantities of sugar (glucose) in the blood and urine is a symptom of diabetes mellitus.

1.1 Type of Diabetes with Symptoms

The diabetes mellitus can be categories to following three types [1]:

- Type-1 diabetes is defined by the pancreas producing less insulin than the body requires, a condition known as "insulin-subordinate diabetes mellitus" (ISDM). Type-1 diabetics require supplemental insulin to compensate for the pancreas' decreased insulin production.
- Type-2 diabetes is defined as insulin resistive body, which occurs when the body's cells react to the insulin differently than they would ordinarily. "Adult starting diabetes" or "non-insulin subordinate diabetes mellitus" (NISDM) are other terms for this condition. This kind of diabetes is more common in those with a high BMI or who have a sedentary lifestyle.
- During the time of pregnancy, the third type of diabetes called Gestational diabetes may develop.

A typical human's sugar levels may vary from range 70 to 99 milligrams per deciliter. A person is classified as diabetes when her or his fasting glucose level reached to 126 mg/dL. In medical point of view, someone having a glucose level of 100 to 125 mg/dL may be considered as pre-diabetic [2]. In such an individual, type 2 diabetes is more prone to develop. GDM (gestational diabetes mellitus) is a kind of diabetes that develops during pregnancy that is not clearly evident diabetes during 2nd and 3rd trimester of pregnancy. Diabetic may be caused by other factors, such as monogenic diabetes syndromes, exocrine pancreas diseases.

Symptoms: The symptoms for diabetes may vary depending on blood glucose level. Some people, particularly those with type-2 diabetes or prediabetes, may not show any signs at all. Symptoms of type-1 diabetes appear more quickly and are more severe. Some of the signs and symptoms of type 1 and type 2 diabetes are as follows:

- Urination on a regular basis
- An increase in thirst
- Tired/Sleepiness
- Loss of weight

- Distorted eyesight
- Emotional ups and downs
- Perplexity and inability to concentrate
- Infections are common

Diabetes has a number of causes*:* Genetic factors account for the majority of diabetes cases. At least two faulty genes on chromosome, the chromosome that controls the body's antigen response, are to blame. The development of type 1 and type 2 diabetes has been related to viral infection. Rubella, Coxsackievirus, mumps, hepatitis B virus, and CMV infection have all been related to an increased risk of diabetes.

2 LITERATURE SURVEY

This section looks at a few works that are linked in some way. Numerous scientific research have utilised the Pima Indians Dataset for Diabetes (PIDD) to predict diabetes. Weka and machine learning approaches were used in [3]. Data mining, Machine learning, neural network, and hybrid techniques are among the methodologies used by researchers.

Swapna et al. in [4] used electrocardiogram (ECG) data to detect diabetes using deep learning algorithms. They retrieved features using a convolution neural network (CNN) then support vector machine algorithm is used to extract the features. Finally, they determined that the accuracy rate was 95.7 percent. In this healthcare area, a variety of computing approaches were utilized. The application of several machine learning algorithms for predicting diabetes mellitus is the subject of this literature review. We extract information from the provided medical data in order to achieve flawless accuracy. Md. Faisal Faruque et al. [5] used the random forest method to create a predictive analytic model. Jyotismita Chaki et al. [6] utilized 10 fold cross validation as an assessment technique for three distinct algorithms: decision tree, naive bayes, and SVM, with naive bayes outperforming the other algorithms by 75 percent.

To forecast diabetes mellitus in its early stages, Choi, B.G et al.[7] utilized random forest, KNN, nave bayes, SVM, and decision tree. We are now using machine learning algorithms and statistical data in the healthcare area to comprehend the sick data that has been discovered. Because the machine learning area encompasses a wide range of approaches and studies, it's difficult to establish a comparison based on which algorithm is faster at producing prediction results. The algorithm's categorization was not tested using the cross validation approach. Different data mining approaches were utilised to predict and assess diabetic mellitus. We used real-world data sets by gathering information from the supplied datasets since we employed three data mining approaches.

K.VijiyaKumar et al. [8] presented the Random Forest method using machine learning techniques. The suggested model produces the best diabetic prediction results, demonstrating quickly predicting diabetes mellitus.

Predicting diabetes onset: an ensemble supervised learning technique was reported by Nonso Nnamoko et al. [9]. For the ensembles, five commonly used classifiers are utilised, and their outputs are aggregated using a meta-

classifier. The findings are reported and compared to other research in the literature that used the same dataset. It is demonstrated that diabetes onset prediction can be done more accurately utilising the proposed technique.

Diabetes Prediction Using Machine Learning Techniques, given by Tejas N. Joshi et al. [10], seeks to predict diabetes using three distinct supervised machine learning methods: SVM, Logistic regression, and ANN. This study provides an excellent method for detecting diabetes illness sooner. Sisodia, D et al. [11] proposed employing data mining to build an Intelligent Diabetic Disease Prediction System that provides analysis of diabetes malady using a database of diabetes patients. In this approach, they suggest using Bayesian and KNN (K-Nearest Neighbor) algorithms to a diabetes patient database and analysing it using multiple diabetes characteristics to forecast diabetes illness.

Muhammad Azeem Sarwar et al. [12] used four different machine learning algorithms indicating which algorithm is best algorithm for diabetes prediction. Researchers are interested in diabetes prediction in order to train a software to determine if a patient is diabetic or not by using a suitable classifier on a dataset. The categorization procedure, according to prior studies, has not much improved. As Diabetes Prediction is an important topic in computers, a system is necessary to tackle the difficulties highlighted based on past research.

We examined actual diagnostic medical data based on numerous risk variables in order to classify machine learning techniques and forecast diabetes mellitus in this study.

3 VARIOUS MACHINE LEARNING APPROACHES

To predict diabetes, we employ a variety of classification methods. This is a crucial characteristic that plays a big part in prediction. The methods are as follows:

Logistic Regression: In 1958, statistician DR Cox invented logistic regression, which predates the area of machine learning. It's a type of supervised machine learning approach used in classification tasks (for predictions based on training data). Logistic Regression employs the same equation as Linear Regression, however the result is a categorical variable in logistic regression, whereas it is a value in other regression models. The independent variables can be used to predict binary outcomes. The Logistic regression model is a form of machine learning classification model that has the binary valueslike 0 or 1, -1 or 1, true or false as dependent variable and the independent variable like interval, ordinal, binominal or ratio-level[13]. The logistic/sigmoid equation function is as follows

$$y = \frac{1}{1+e^{-x}} \qquad (1)$$

K nearest neighbor: Both classification and regression issues may be solved using the K-Nearest Neighbor (KNN) technique [14]. However, in the industry, it is more commonly utilised in classification issues. KNN is a straightforward computation that stores all existing examples and ranks new ones based on the votes of its k neighbours. To place the case in the class with the most people among its K nearest neighbours, a distance work is used. The Manhattan, Hamming, Euclidean, and Makowski distances are among the distance capabilities. The first 3 nos. of features are used for indefinite functions, whereas the 4th one is used for absolute variables. If K = 1, the case is essentially assigned to the class of the next-closest neighbour. Selecting K for KNN modelling might be challenging at times. Its main benefit is the ease with which it may be translated and the little amount of time it takes to compute

Support Vector Machine (SVM) Classifier: SVM is a supervised machine learning method that excels in pattern identification and is used as a training process for deducing classification and regression rules from data. When the number of characteristics and instances is large, SVM is the most exact method. The SVM algorithm creates a binary classifier. In an SVM model, each data item is represented as a point in an n-dimensional space, with n being the number of features, and each feature as the value of a coordinate in the n-dimensional space. The basic objective of SVM is to use an appropriate hyper plane to categorize data points in a multidimensional space. A hyper plane is considered as a boundary of classification for data points. The hyper plane classifies the data points with the biggest gap between the classes and the hyper plane. In this technique, each data item in n-dimensional space is represented as a point, with the value of each feature matching to the value of a certain coordinate. Because the two closest focuses are the furthest distant from the line in figure 1, the dark line divides the data into two different organized groupings. Our classifier is represented by this line. Based on falling of testing data on both side of the line, the new data be able to categorized into one of two categories.

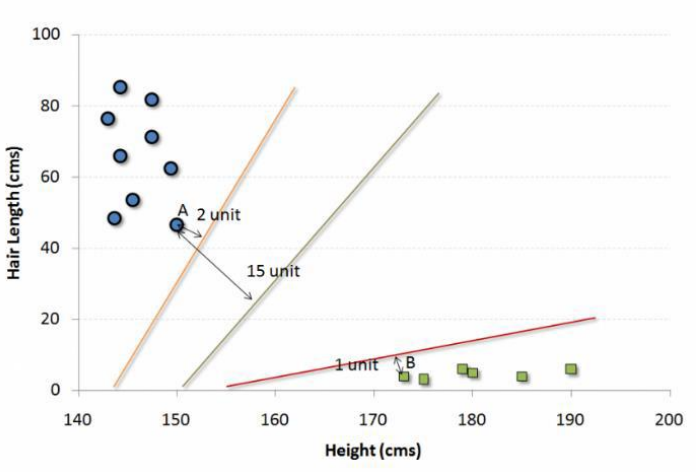

Fig. 1. Support Vector Machine

Random Forest (RF): The RF is made up of several separate decision trees that operate together as an ensemble, as the name indicates. For each tree, the RF predicts a class, and the classes with the majority of votes become our model's prediction report. Random Forest is another frequently used supervised machine learning technique. This

method works well for both regression and classification issues, although it excels at the latter. As the name indicates, the Random Forest technique analyses many decision trees before providing an output. As a consequence, it's a decision tree collection. This technique is based on the assumption that if additional trees were present, they would all reach the same conclusion. For classification, it utilizes a voting technique and then selects the class, but for regression, it takes the mean of all decision tree outputs. It works well with large datasets with several dimensions.

4 METHODOLOGY

This section will cover the various classifiers used in machine learning to predict diabetes. We'll also go through our recommended technique for increasing accuracy. In this article, five alternative techniques were employed. The many methods utilized are listed below. The accuracy measurements of the machine learning models are the output. The model may then be utilized to make predictions.

4.1 Dataset Description

The diabetes data set is downloaded from Kaggle repository[15]. A diabetes dataset of 2000 cases were used. The diabetes dataset of Pima Indians was used to test the techniques. The goal is to determine whether or not the patient is diabetic based on the measurements. Parameters used in Pima datasets are; 1) Age 2) Glucose 3) BloodPressure 4) BMI 5) Insulin 6) SkinThickness 7) DiabetesPedigreeFunction 8) Pregnancies 9) Outcome. Figure 2 depicts description matrix of Pima Indian dataset and figure 3 depics hit map of the correlation matrix of the same.

	Pregnancies	Glucose	BloodPressure	SkinThickness	Insulin	BMI	DiabetesPedigreeFunction	Age	Outcome
count	768.000000	768.000000	768.000000	768.000000	768.000000	768.000000	768.000000	768.000000	768.000000
mean	3.845052	120.894531	69.105469	20.536458	79.799479	31.992578	0.471876	33.240885	0.348958
std	3.369578	31.972618	19.355807	15.952218	115.244002	7.884160	0.331329	11.760232	0.476951
min	0.000000	0.000000	0.000000	0.000000	0.000000	0.000000	0.078000	21.000000	0.000000
25%	1.000000	99.000000	62.000000	0.000000	0.000000	27.300000	0.243750	24.000000	0.000000
50%	3.000000	117.000000	72.000000	23.000000	30.500000	32.000000	0.372500	29.000000	0.000000
75%	6.000000	140.250000	80.000000	32.000000	127.250000	36.600000	0.626250	41.000000	1.000000
max	17.000000	199.000000	122.000000	99.000000	846.000000	67.100000	2.420000	81.000000	1.000000

Fig.2. Screen shot of description of matrices of Pima dataset

Fig.3. Hit map of correlation matrix for the dataset

4.2 Implementation and Design

The study's implementation was done with Google Colab, and the coding was done with the python programming language. The Pima dataset and the gathered dataset were used to forecast availability of diabetes using various machine learning approaches such as SVM , k-nearest neighbour, RF and LR classifications. After collection of dataset, the missing values are checked as in table 1. After then, each classifier's predictions are compared to one another. The procedures to implement the machine learning algorithm are illustrated in Figure 4.

The data set used to predict diabetes is shown in Figure 2. The diabetes parameters serve as the variable which is dependent, whereas the other factors served as independent ones. For the dependent diabetes features only two values are accepted, with a “zero” indicating No diabetes and a “One” signifying availability of diabetes. The whole sample is divided into two groups, with a ratio of 70:30 for the training and testing dataset. All four methods of classification, i.e. were used for prediction. The training data was then used to predict the test set outcomes using SVM , k-nearest neighbour, RF and LR classifications, resulting in the confusion matrix given in Table 2

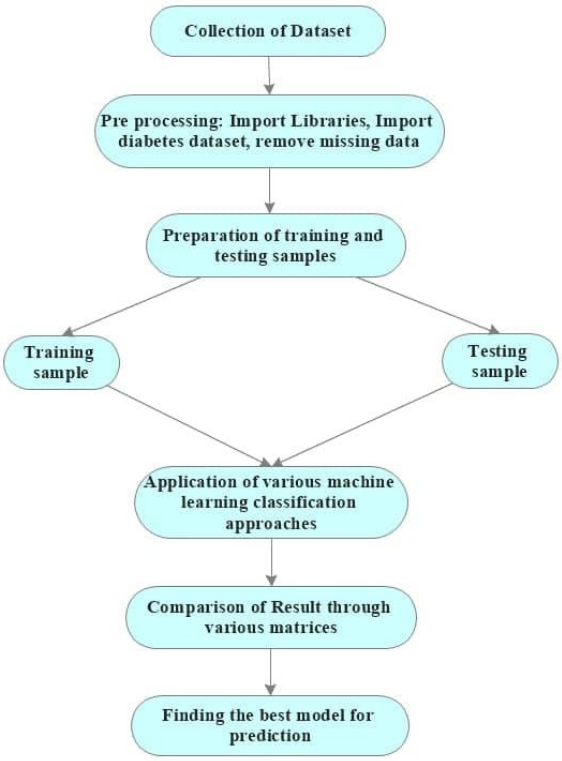

Fig.4. Flow graph for the proposed work

Table 1. Finding missing values in dataset

Properties	Missing Values
Pregnancies	0
Glucose	0
BloodPressure	0
SkinThickness	0
Insulin	0
BMI	0
DiabetesPedigreeFunction	0
Age	0
Outcome	0

Table 2. Matrix of Confusion for different classification methods

	Logistic Regression	K Nearest Neighbour	Support Vector Machine	Random Forest
Pima Dataset	[[149 11] [31 40]]	[[141 19] [28 43]]	[[142 8] [46 35]]	[[131 1] [2 97]]

The measure provided in equation 2-8 may be computed using the obtained confusion matrices. True Negative (TN), False Negative (FN), True Positive (TP), and False Positive (FP) were the results of these matrices (TP). Because there are more non-diabetic cases than diabetic cases in both datasets, the TN is greater than the TP. As a consequence, all of the techniques provide positive results. The following measurements have been calculated using the following formulae in order to determine the precise accuracy of each method:

$$\text{Precision} = \frac{TP}{TP+FP} \quad (2)$$

$$\text{Sensitivity} = \frac{TP}{TP+FN} \quad (3)$$

$$\text{Specificity} = \frac{TN}{TP+FP} \quad (4)$$

$$\text{MCC} = \frac{(TP*TN)-(FP+FN)}{\sqrt{(TP+FP)(TP+FN)(TN+FP)(TN+FN)}} \quad (5)$$

$$\text{ErrorRate} = \frac{FN+FP}{TP+TN+FN+FP} \quad (6)$$

$$\text{F-Measure} = \frac{2*(Precision*Sensitivity)}{Precision+Sensitivity} \quad (7)$$

$$\text{Accuracy} = \frac{TN+TP}{TP+TN+FN+FP} \quad (8)$$

Table 3. Comparison of Statistical measurement for various classification techniques

	Logistic Regression	K Nearest Neighbour	Support Vector Machine	Random Forest
Accuracy	**0.872**	**0.739**	**0.888**	**0.984**
Error	0.127	0.261	0.112	0.016
Sensitivity	0.923	0.778	0.898	0.987
Specificity	0.764	0.702	0.816	0.916
Precision	0.885	0.816	0.933	0.991
F-Measure	0.903	0.797	0.915	0.989
MCC	0.732	0.503	0.764	0.963
Kappa	0.727	0.516	0.713	0.922
AUC	**0.908**	**0.916**	**0.893**	**1**

Another finding as per table 3 is that the accuracy level of all the techniques is higher on our collected dataset than on the used PIMA dataset, owing to the former's

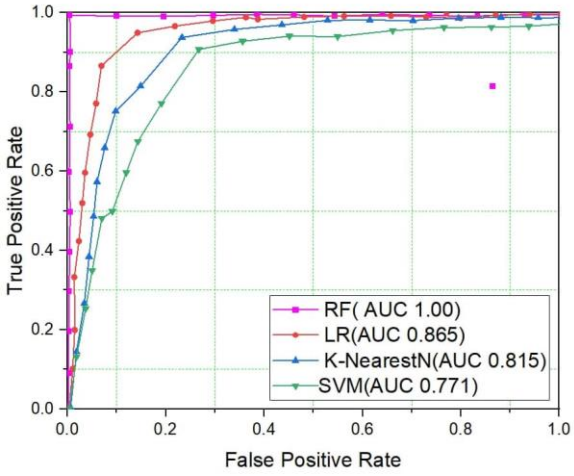

Fig.5. ROC Curve with AUC for PIMA dataset

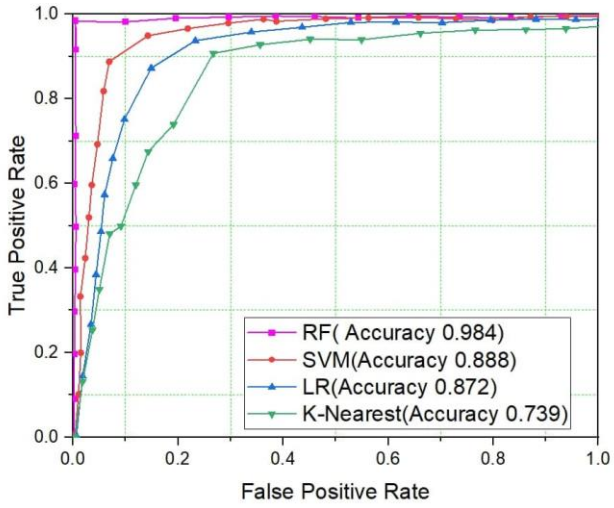

Fig.6. ROC Curve with AUC for PIMA dataset

greater number of variables relevant to assessing diabetes risk. The Random Forest classifier outperforms all others in terms of accuracy (98.4%), sensitivity, specificity, precision, and F-measure, proving that it is the best technique for our dataset. Furthermore, in the case of random forest, the AUC value is 1, indicating that this model performs exceptionally well in classification. Figure 5 Depicts the clear graph for the ROC curve and AUC the PIMA datasets and figure 6 depicts the Accuracy graph for the dataset. A comparison graph is presented in figure 7 that clearly compare all the available algorithms. Here it indicates that in the cases the RF classifier gives the highest result with value 1.

The cross validation process was also used to assess the efficacy of various models. A subset of the data is set aside for cross validation, and the remaining data is used to train it. And the procedure is repeated for each segment of data. The size of the pieces is determined by the value of k. Here for validation point of view 10-fold cross validation was used, which means the data was split into ten parts. Cross validation has the greatest accuracy for random forest. Random forest has a Kappa statistic of better than 0.9, indicating that it is outstanding.

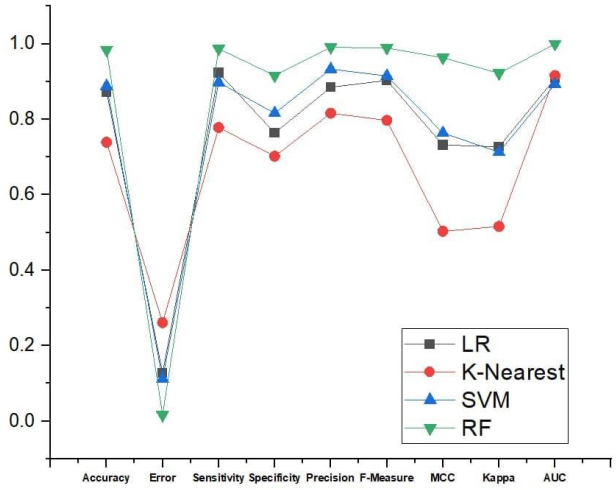

Fig.7. Comparison of different classification approaches

CONCLUSION

One of the most pressing worldwide health concerns is detecting diabetes risk at an early stage. Here in our research that aims to build up a system for predicting the risk of diabetes mellitus. Four machine learning techniques for classification algorithms were used in this work, and the results were compared to several statistical metrics. The above said four algorithms were used on the PIMA database. The accuracy level of RF classification in our dataset is 98.4 percent, which is the greatest among the others, according to the testing results. All of the models generated good results for various parameters like as accuracy, recall sensitivity, and so on, using four different machine learning methods. This result can be used to forecast any other illness in the future. This study is currently researching and improving on various machine learning approaches to forecast diabetes or any other condition.

REFERENCES

1. *Qin, Hailun, et al. "Triglyceride to high-density lipoprotein cholesterol ratio is associated with incident diabetes in men: A retrospective study of Chinese individuals." Journal of Diabetes Investigation 11.1 (2020): 192-198. [DOI:10.1111/jdi.13087]*

2. *Mujumdar, Aishwarya, and V. Vaidehi. "Diabetes prediction using machine learning algorithms." Procedia Computer Science 165 (2019): 292-299. [DOI:10.1016/j.procs.2020.01.047]*

3. *Dash S., Gantayat P.K., Das R.K. (2021) Blockchain Technology in Healthcare: Opportunities and Challenges. In: Panda S.K., Jena A.K., Swain S.K., Satapathy S.C. (eds) Blockchain Technology: Applications and Challenges. Intelligent Systems Reference Library, vol 203. Springer, Cham. https://doi.org/10.1007/978-3-030-69395-4_6*

4. *Swapna, G., Vinayakumar R., Soman K. P. (2018) "Diabetes detection using deep learning algorithms." ICT Express 4 (4): 243-246.*

5. *Md. Faisal Faruque, Asaduzzaman and I. H. Sarker, "Performance Analysis of Machine Learning Techniques to Predict Diabetes Mellitus," 2019 International Conference on Electrical, Computer and Communication Engineering (ECCE), 2019, pp. 1-4, doi: 10.1109/ECACE.2019.8679365.*

6. *Jyotismita Chaki, S. Thillai Ganesh, S.K Cidham, S. Ananda Theertan, Machine learning and artificial intelligence based Diabetes Mellitus detection and self-management: A systematic review, Journal of King Saud University - Computer and Information Sciences, 2020, ISSN 1319-1578, https://doi.org/10.1016/j.jksuci.2020.06.013*

7. *Choi, B.G., Rha, S. W., Kim, S. W., Kang, J. H., Park, J. Y., Noh, Y. K. (2019) "Machine Learning for the Prediction of New-Onset Diabetes Mellitus during 5-Year Follow-up in Non-Diabetic Patients with Cardiovascular Risks." Yonsei medical journal 60 (2): 191-9.*

8. *K. VijiyaKumar, B. Lavanya, I. Nirmala and S. S. Caroline, "Random Forest Algorithm for the Prediction of Diabetes," 2019 IEEE International Conference on System, Computation, Automation and Networking (ICSCAN), 2019, pp. 1-5, doi: 10.1109/ICSCAN.2019.8878802.*

9. *N. Nnamoko, A. Hussain and D. England, "Predicting Diabetes Onset: An Ensemble Supervised Learning Approach," 2018 IEEE Congress on Evolutionary Computation (CEC), 2018, pp. 1-7, doi: 10.1109/CEC.2018.8477663.*

10. *Tejas N. Joshi, Prof. Pramila M. Chawan, "Diabetes Prediction Using Machine Learning Techniques".Int. Journal of Engineering Research and Application, Vol. 8, Issue 1, (Part -II) January 2018, pp.-09-13, DOI: 10.9790/9622-0801020913*

11. *Sisodia, D., Sisodia, D. S. (2018) "Prediction of diabetes using classification algorithms." Procedia computer science 132: 1578-1585.*

12. *Sachikanta Dash, Pradosh Kumar Gantayat, 2020 "Liver Disease Prediction Using Machine Learning Algorithm" , Data Engineering and Intelligent Computing, Proceedings of ICICC 2020, https://link.springer.com/chapter, https://doi.org/10.1007/978-981-16-0171-2*

13. *Eswari, T., Sampath, P., Lavanya, S. (2015) "Predictive methodology for diabetic data analysis in big data." Procedia Computer Science 50: 203-208.*

14. *Perveen, S., Shahbaz, M., Keshavjee, K., Guergachi, A. (2019) "Metabolic Syndrome and Development of Diabetes Mellitus: Predictive Modeling Based on Machine Learning Techniques." IEEE Access 7: 1365-1375.*

15. *https://www.kaggle.com/uciml/pima-indians-diabetes-database*

BIOGRAPHICAL NOTES

Dr Sachikanta Dash is presently working as Associate Professor in the department of Computer Science and Engineering at DRIEMS Autonomous Engineering College. He received his B.Tech degree in Information Technology from Utkal University in 2004, M.Tech. degree Gandhi Institute of Engineering and Technology, Gunupur , BPUT, Orissa in 2009 and Ph.D. degree in Computer Science Berhampur University, India in 2019. He has published more than 8 journals in the field of Image processing, Blockchain, Healthcare sector, machine learning. He is a member of ISTE, CSI and IAENG.

Dr Pradosh Kumar Gantayat is presently working as AssociateProfessor in the Department of Computer Science and Engineering at DRIEMS Autonomous Engineering College.His Main research area are Delay Tolerant network,Wireless Network,Soft Computing.He has published many research papers in reputed Journal and Conferences.He has received “Best Paper “ award at NIT Meghalaya and Research Excellence Award from InSc Bangalore in the year 2021.

Raghunath Rout recei ved his B.E degree in the year 2002 in Computer Science and Engineering from Fakir Mohan University and Masters degree from Biju Pattnaik university of Technology in 2010. He subsequently undertook research in the area of wireless sensor networks in the year 2015 from the Biju Pattnaik University of Technology. His work is focused on studying ambient enviornment status in the Undeground mining using Gas sensors.

Performance Analysis of Wireless Sensor Network Node Localization using JAYA Optimization Algorithm

[1]Dr. J. Mehena , [2]Dr. R. K. Das

[1, 2] Department of Electronics & Telecommunication Engg.

DRIEMS (Autonomous), Cuttack, Odisha

ABSTRACT

The abstract Localization of node in wireless sensor network (WSN) plays a crucial role in establishing productive communication among varied devices connected within the field of communication and networking. The localization accuracy of wireless sensor network will be reduced because of the existence of the line of sight (LOS) in real environment. This analysis paper is targeted on the LOS node localization drawback for WSN. During this work, we tend to employ the PSO and JAYA optimization algorithm for estimating the overall location of the node that has been targeted. The experiment result's aimed to mitigate the localization drawback, wherever information concerning the node locations is inaccessible. With the assistance of the accessible signal strength indication (RSSI) received, the model can estimate placement of the sensor node. Here, the experimental result clearly shows that JAYA optimization algorithm has quicker convergence property than the PSO algorithm.

Keywords: *WSN, JAYA, PSO, LOS, RSSI, Localization*

1 INTRODUCTION

In the rapid technological advances enabled the event of low power, low priced sensing devices with multifunctional. Sensing devices nodes are autonomous with sensing integration, communication along with processing capabilities. Sensing node is associate degree device that does investigate environmental conditions like sound, chemicals, temperature, or the presence of objects. The pictured applications of those wireless sensor networks vary widely: ecological home ground watching, structure health watching, environmental watching, process management and object chase, among others. Wireless device networks are basically meant to supply data concerning the space-time characteristics of discovered world physically. Consequently, it's required to associate detected knowledge besides locations, creating geographically knowledge important. Variety of wide applications like object tracking, environmental condition monitoring, inherently place confidence in location data. Besides, location data additionally supports services of basic network layer, topology management, routing, and agglomeration. Consequently, localization is a mechanism for autonomously discovering and spatial relationships among sensors nodes establishing, is of nice importance in the evolution of wireless sensor networks [1, 2].

Here, we have a tendency to analysis the prevailing localization viewpoint from the two conditions: measurement physically and therefore the network wide localization. In general, all localization algorithms encompass alike two stages in an exceedingly method that first perform measurement physically to assemble knowledge, so do localization supported such knowledge. Here physical activity suggests that how for getting geometric relations physically in native plan, like investigation of nearest nodes and move the angle or segment distance [3, 4]. Aside from decisive the placement of one undetermined node given variety of near references, a wide drawback is the localization of network, wherever an oversized variety of unspecified nodes got localization in an exceedingly network along with number of relating nodes. The algorithms planning for network localization rely significantly on handiness of the resources and therefore the accuracy requirement. Variety of approaches for localization is planned supported various principles of positioning; constrains of environmental, accuracy necessities, and the like, creating them suitable or unsuitable for various utilization. We have a tendency to describe and compare the benefits and drawbacks of present approaches for localization problem. Generally, algorithms for localization rely extremely on a range of things like application wants and obtainable measurements physically. No particular algorithmic program may be a clear favorite across the spectrum [5, 6].

This analysis research work is arranged as follows. The planned algorithms and experimental results with comparison are represented in section II and Section III respectively. At last, Section IV contains conclusions with discussions.

2 PROPOSED ALGORITHM

2.1 Particle Swarm Optimization (PSO) Algorithm

PSO technique optimizes a problem by recurrently making an attempt to enhance a solution of candidate with relation to the standard measurement. The problem solution of having a population of candidate solutions, here dubbed particles are moving around inside the search space in line with straight forward over the particle's speed and position [7, 8]. Movements of every particle are influenced by the native greatest illustrious position. Additionally radio-controlled toward the most effective illustrious location within space provided in searching, that square measure upgrade as higher location square measure discovered by alternative particles. That is often anticipated to maneuver swarm towards most effective solutions. The optimization algorithm is metaheuristic because this makes hardly any or no assumptions regarding the matter remain optimized that might inspect terribly massive areas of solutions by the candidate. Though, metaheuristics like PSO don't surely associate degree best answer to be found ever [9, 10].This algorithm doesn't apply gradient of matter to be optimized, that suggests PSO doesn't need this problem of optimization being differentiable as it needed by classic improvement ways like gradient descent and quasi-newton techniques.

The PSO algorithm is given in the Table.1, where, the weight parameters w, r_p, r_g, c_1 and c_2 are within the scope 0 to 1. p and d are the population and dimension respectively.

2.2 Improved Particle Swarm Optimization Algorithm

Here, improvement is done by the range based localization distributed algorithmic rule for WSN. Variations in the middle of general PSO approach and improved approach are mirrored at intervals in subsequent four sub-sections.

2.2.1 Outline of Surrounding Box Methodology

The general algorithmic rule utilizes a group of possible answers inside the searching space, called the particles of swarm with initial locations randomly. Here, reduction is done initially in the search space utilizing a surrounding box methodology [11].The concept of surrounding box methodology is narrated in the Fig.1.

Table 1. General PSO Algorithm

Initialize : $w, c_1, c_2, Ub, Lb, p, d$	Size
Initialize : position $X \sim U[Ub, Lb]$	$[p \times d]$
Initialize : velocity $V \sim U([-\lvert Ub - Lb\rvert, \lvert Ub - Lb\rvert])$	$[p \times d]$
$P_{best} = min(f(X))$	$[1 \times 1]$
$P_{sol} = X(argmin(f(X)))$	$[1 \times d]$
$Gbest = Pbest$	$[1 \times 1]$
$G_{sol} = P_{sol}$	[1 × d]
while termination criteria not met **do**	
$V = w \times V + c_1 \times r_p \times (P_{sol} - X) + c_2 \times r_g \times (G_{sol} - X)$	$[p \times d]$
$X = X + V$	$[p \times d]$
$X = X\ [Ub, Lb]$	$[p \times d]$
$P_{best} = min(f(X))$	$[1 \times 1]$
$P_{sol} = X(argmin(f(X)))$	$[1 \times d]$
if $G_{best} > P_{best}$ **then**	
$Gbest = Pbest$	$[1 \times 1]$
$G_{sol} = P_{sol}$	[1 × d]
end if	
end while	
Final G_{sol} is that the best solution	
end procedure	

2.2.2 Flip Ambiguity Development

The flip ambiguity development is shown in Fig.2.The principles [12] are utilized together to forestall the prevalence of the flip ambiguity development. Once the node targeted is judged near collinear, the node targeted will not be localized throughout this repetition process [14]. During the repetition process, the node targeted will be a many more references and have localized till the recently references are to be judged and not near collinear.

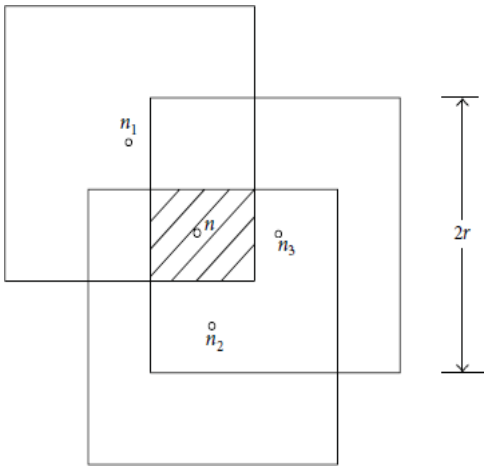

Fig. 1. Mapping of surrounding box methodology

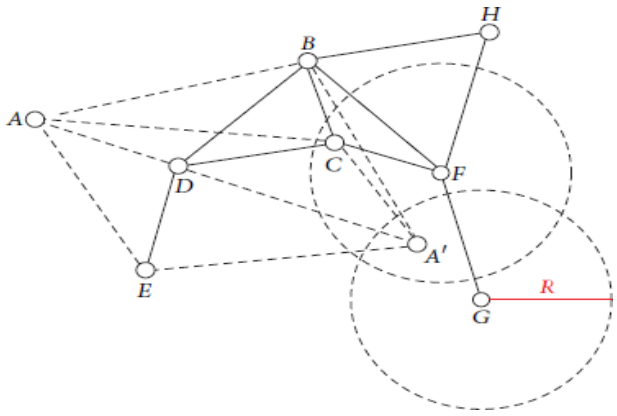

Fig. 2. Flip ambiguity Development

2.2.3 Refinement Part to Correct the Error

Refinement part is required to re-localize the nodes that have the problem of flip ambiguity. During refinement part, the localized nodes drops into the inexact neighborhood, additional term is join together along with the objective function so as to establish additional cost to replacement estimation [10].

2.2.4 Localize the Target Nodes

The nodes that have been targeted must full fill minimum three non near-collinear references and have two references or three near-collinear references [11].

2.3 Improved Particle Swarm Optimization Algorithm

A simple and powerful technique, that gaining attention because of its simplicity and robustness is that the Jaya algorithm. During this algorithm, this solution continuously tries to maneuver towards the best solution with no further recursive hyper- parameters. By assuming, $f(x)$ to the function targeted that has to be minimized or maximized at every iteration i. So, this algorithm continuously tries to to success nearly i.e. moving towards best solution. So, this algorithm represent as Jaya.

The JAYA Algorithm is given within the Table.2, where, *Ub* and *Lb* are represents the upper and lower bounds respectively. Population *P* designates the solutions amounts calculated at every recursion. P_{best} is the present best solution *and Gbest* is the globally best solution. *Pbest* and *Pworst* are the present best and worst sequence respectively. $r1$ and $r2$ are two distributed uniformly variables varied between 0 and 1.

3 EXPERIMENTAL RESULTS

The performance analysis of the algorithms proposed is conducted using MATLAB software. The target node, N = 100 randomly positioned in the sensor field within 100 X 100 square units. The PSO and JAYA algorithm parameters are randomly chosen to ; population = 50, iterations = 50 and 100, acceleration constants; $c_i = c_2 = 2.0$; $w_{max} = 0.8$, $w_{min} = 0.1$. The error is calculated and repeated for every node in the WSN system for a single node. The computational error is calculated as a mean of all the errors. For 50 and 100 iterations both the PSO and JAYA is simulated and their computational times are reported. For an arbitrary run, the mean of the Pbest and Gbest over 50 iteration are also presented as an proof of reduction in the objective function.

Table-2. JAYA Optimization Algorithm

Initialize : Ub, Lb, P, O	Size
Initialize : particles $B \sim U[Ub, Lb]$	$[P \times O]$
$P_{best} = max(f(B))$	$[1 \times 1]$
$P^{best} = B(argmax(f(B)))_{sol}$	$[1 \times O]$
$P^{worst} = B(argmin(f(B)))_{sol}$	$[1 \times O]$
$G_{best} = P_{best}$	$[1 \times 1]$
$G_{Sol} = P_{best}$	
while termination criteria not met **do**	
$B = B + r1 \times (P^{best} - B) - r2 \times (P^{worst} - B)$	$[1 \times O]$
$B = B \in [Ub, Lb]$	$[P \times O]$
$P_{best} = max(f(B))$	$[1 \times 1]$
$P^{best} = B(argmax(f(B)))_{sol}$	$[1 \times O]$
$P^{worst} = B(argmin(f(B)))_{sol}$	$[1 \times O]$
if $P_{best} > G_{best}$ **then**	
$G_{best} = P_{best}$	$[1 \times 1]$
$G_{sol} = P^{best}$	$[1 \times O]$
end if	
end while	
end procedure	

The objective function for a 100 X 100 area is presented in the Fig.3. By both the PSO and JAYA approach the objective is evaluated for 50 run and further results are analysed. The Fig.4 and 5 represents the Gbest and mean-Pbest outcomes respectively. These figures are obtained from an arbitrary run for 50 iteration one for PSO and other for JAYA algorithm. From the figure it is clear that the minimum objective is reached by both of the approaches, but the JAYA is much faster in convergence. Also the randomness of the Pbest results are alsominimized in case of JAYA optimization approach.

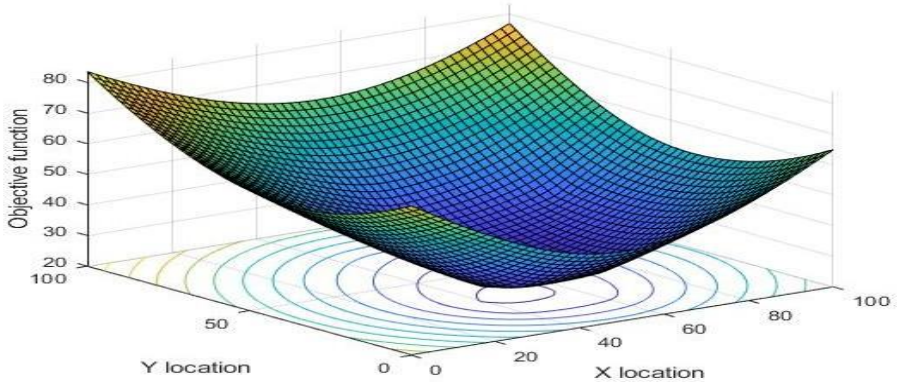

Fig.3. Objective function

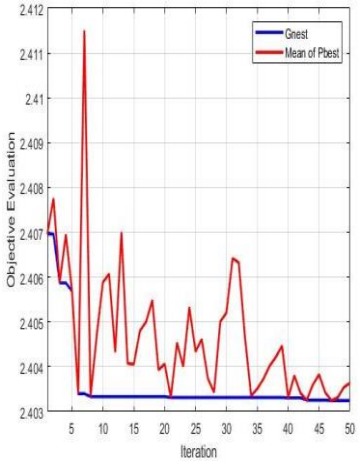

Fig.4.Gbest and mean-Pbest outcomes of PSO

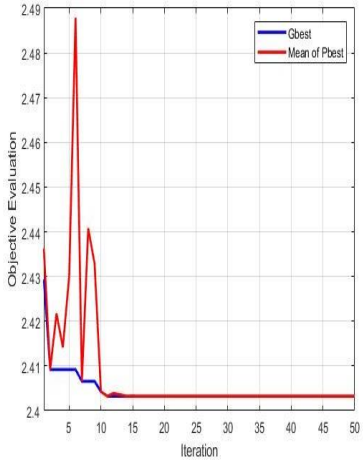

Fig.5.Gbest and mean-Pbest outcomes of JAYA

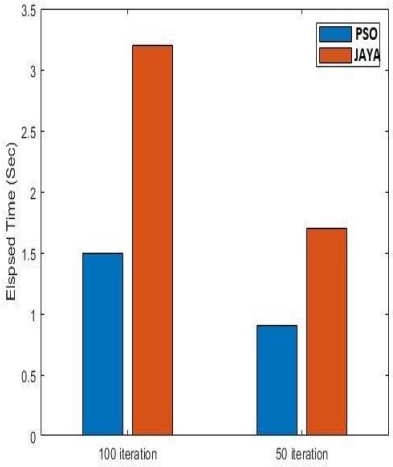

Fig.6. Elapsed time Comparison

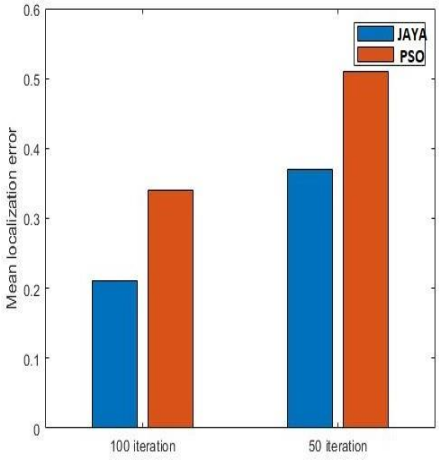

Fig.7. Mean Estimated localization error

The above process is repeated for 50 and 100 unknown nodes and the total elapsed time is shown in the Fig.5 for both the PSO and JAYA approach. It is clear that for 50 iteration both the approaches have minimal time as compared to 100 iteration. While, the JAYA consumes highertime as compared to the PSO approach in both the cases.

For 50 and 100 unknown nodes, the mean estimated localization error comparison is shown in the Fig.7. The error minimization takes place for 100 iteration, as compared to 50 iteration. While, the JAYA have minimal error as compared to the PSO approach.

CONCLUSION

Node localization for wireless sensor network is a highly nonlinear optimization problem. So, this requiresthe heuristic optimization approaches to solve the above said problem. In thepresent context the PSO and JAYA algorithm are fully exploited and the results are presented. The experiment result's aimed to mitigate the localization drawback, wherever information concerning the node locations is inaccessible. With the assistance of the accessible RSSI, developed model can estimate placement of sensor node. Here, the experimental results clearly show that JAYA has quicker convergence property than the PSO algorithm.

REFERENCES

1. *Ribeiro, A., Georgios B. Giannakis.: Bandwidth- constrained distributed estimation for wireless sensor Networks-part I: Gaussian case. IEEE Trans. On Sig. Proc., (2006) 512-516.*
2. *Luo, Z.: Universal decentralized estimation in a bandwidth constrained sensor network. IEEE Trans. Inf. Theory., (2005) 1020-1025.*
3. *Poli, R., An analysis of publications on particle swarm optimization applications. Technical Report CSM-469. Department of Computer Science, University of Essex, UK, (2007)*
4. *Xiao, J., Zhi-Quan L.: Universal decentralized detection in a bandwidth-constrained sensor network. IEEE Trans. On Sig. Proc., (2005) 1234-1239.*
5. *Mao, G., Fidan, B., Anderson, B.: Wireless sensor network localization techniques, Computer Network, (2007).*
6. *Kannan, A., Mao,G., Vucetic, B.: Simulated annealing based localization in wireless sensor network, Proceedings of the IEEE Conference on Local Computer Networks,Sydney, Australia,(2005)*
7. *Gopakumar, A., L. Jacob L.: Localization in wireless sensor networks using particle swarm optimization, Proceedings of the IET Conference on Wireless, Mobile and Multimedia Networks,(2008)*
8. *P. H. Namin P., Tinati, M.: Node localization using particle swarmoptimization,in Proceedings of the 7th International Conference on Intelligent Sensors, Sensor Networks and Information Processing,IEEE,(2011)*
9. *Kulkarni R .,Venayagamoorthy G.:Bioinspired algorithms forautonomous deployment and localization of sensor nodes,,IEEE Tranactions on Systems, Man and Cybernetics, Part C: Applications and Reviews,*

(2010)

10. *Kumar, A., Khosla, J., Saini, S, Singh, S.: Computational intelligence based algorithm for node localization in Wireless Sensor Networks, Proceedings of the 6th IEEE International Conference Intelligent Systems,(2012)*
11. *Lv, J., H. Cui, H.,Yang, M.:Distribute localization for wireless sensor networks using particle swarm optimization,Proceedings of the IEEE 3rd International Conference on Software Engineering and Service Science, (2012)*
12. *Dong, E., Chai, Y.,Liu, X.: A novel three-dimensional localization algorithm for wireless sensor networks based on particle swarm optimization,Proceedings of the 18th IEEE International Conference on Telecommunications, (2011)*

BIOGRAPHICAL NOTES

Dr. Jibanananda Mehena is presently working as Professor & Head in the Department of Electronics & Telecommunication Engineering and Dean (Academic) of DRIEMS Autonomous Engg. College,Cuttack. He has twenty years of teaching and research experience. He has published more than twenty five research papers in national and international journals and published eight books to his credit. His area of research includes VLSI Design, Wireless Sensor Networks, Microprocessor & Microcontroller, Signal and Image Processing.

Dr. Rajendra Kumar Das is an eminent scholar and administrator of repute with thirty years of experience in academics and industry. He has a large number of research publications in national and international journals to his credit. His research area includes Information & Communication Technology,Digital Design & Image Processing. He has been felicitated with awards of eminence like Mother Teresa Award, Rajib Gandhi Professional Award and Best Principal Award from ISTE, New Delhi.

Free and Forced Vibration Investigation of a Fractured Simply Supported Timoshenko Beam

[1]Alok Ranjan Biswal, [1]Poonam Prusty, [1]Rasmi Ranjan Senapati

[1] Mechanical engineering Department, DRIEMS Tangi Cuttack-754022

alokranjanbiswal@driems.ac.in, poonamprusty@driems.ac.in, rashmisenapati@driems.ac.in

ABSTRACT

The present paper deals with the vibration study of a fractured simply supported beam using Finite Element Method (FEM). The existence of structural defects has a great deal of attention towards analysis and necessary steps needed to take in order to avoid the catastrophic failure. The present article put forth the mathematical modelling of such beams with s and corresponding analysis. The finite element procedures have been incorporated to find out the responses. Two nodes per element with four degrees of freedom have been considered to carry out the analysis. The Hamilton's principle has been used to find out the mass and stiffness matrices. Timoshenko beam formulation has been used so as to ensure the detailed analysis with the inclusion of rotary inertia and shear deformation of the beam. Structural damping is also used in the formulation for the vibration analysis. The detailed mathematical formulation has been carried out in MATLAB environment and the responses have been found by proper validation of the developed code.

Keywords*: Timoshenko beam, Transverse fracture, Amplitude Variation, MATLAB*

1 INTRODUCTION

It has been observed from the last few decades, widespread research carried out to examine the faults in assemblies. It has been a well observation that most assembled members undergoes failure due to the existence of fractures. The performance and conclusion of fracture on the structural elements has been the key attention for many researchers. The development of local flexibility due to occurrence of fracture in a structural member whose orientation depends on the no of degrees of freedom [1].In order to solve the differential equation by analytical method, the local flexibility term is appropriate for the investigation of fractured beam [2]. Further it has a great deal of importance for semi-analytical method when both Fourier and mechanical impedance method used [3]. Using direct pertubative procedures, the natural frequencies can be obtained for a fractured Timoshenko beams[4]. The free and forced response measurements due to Fracture localization and sizing in a beam has been discussed [5].The Presence of fracture and its analysis using both beam formulation has been studied[6]. In their work the modelling of beamin both formulations have been studied to estimate the influence of fracture size and location on vibrational frequencies of fractured beam. The first four natural frequency of the fractured structure have been studied [7]. Armon's Rank-ordering method have been used for approximate the fracture location and finding out the above four natural frequencies. The experimental investigation have been carried out for fractures and damages on the

structures[8]. The fractured cantilever beam has been analysed by finite element procedure. The relationship between the modal vibration frequencies with fracture depth and fracture location has been studied [9].The fracture with different location and orientation has been studied. The analysis reveals a relationship between fracture depth and modal vibration frequency. Instead of local flexibility, Overall flexibility matrix has been studied for the transverse fractured beam [10].It has been concluded that the overall additional flexibility matrix shows very good result in comparison with the local flexibility matrix. Even though several works have been commenced still some research need to focus on this fractured beam. The paper deals with the finite element formulation of the transverse fracture in a simply supported beam. The mathematical formulation has been carried out in the subsequent section.

2 NUMERICAL FORMULATION

The mathematical formulation consists of modelling of unfractured and fractured beam with different fracture location using finite element method.

2.1 Modelling of unfractured beam

The prismatic simply supported beam element is shown in Fig 1. The beam element has uniform modulus of elasticity, mass moment of inertia and mass density.

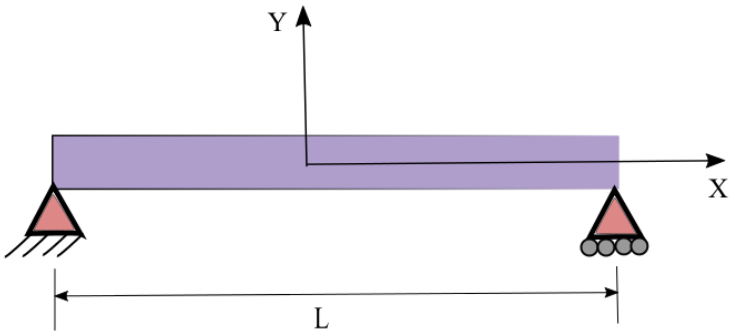

Fig 1 A simply supported homogeneous unfractured beam.

The displacement in the x, y and z directions taking into consideration of finite element formulation as

$$\begin{aligned} m(u,v,w,t) &= w\theta(u,t) = z\left(\frac{\partial o}{\partial u} - \beta(u)\right) \\ n(u,v,w,t) &= 0 \\ o(u,v,w,t) &= o(u,t) \end{aligned} \tag{1}$$

Where the longitudinal displacement *i*sm,the lateral displacement is*n*and transverse displacement is*o*. The rotation of the desired cross-section isθ. Theshear *is* β which has no contribution during finding out the axial displacement at a point at a distance w from the centre line. The governing equation of motion can be obtained by using Hamilton's principle.The principle is based on the concept of strain energy where the total strain energy is obtained by considering both kinetic energy and the work done of the systemas

$$\delta II = \int_{t_1}^{t_2} (\delta E_T - \delta E_K - \delta W_{external}) dt = 0 \quad (2)$$

Here E_T,E_K and $W_{external}$ is the total strain energy, kinetic energy and external work done of the given system and t is the time dependent parameter. After putting the values of the said time bound parameter the governing beam equation can be found. Let q be the displacement which is approximated by a cubic polynomial as

$$q = c_1 + c_2 u + c_3 u^2 + c_4 u^3 \quad (3)$$

Where x is the distance from the fixed end of the beam and c_1,c_2,c_3,$c_4$are the constant terms. These terms can be found by considering the boundary conditions of the beam. After solving the equation the mass matrix of the regular beam element has been found as

$$[M_b] = \int_0^{L_e} \begin{bmatrix} [N_q] \\ [N_\theta] \end{bmatrix}^T \begin{bmatrix} \rho A & 0 \\ 0 & \rho I \end{bmatrix} \begin{bmatrix} [N_q] \\ [N_\theta] \end{bmatrix} du \quad (4)$$

The mass matrix is obtained by considering both translational mass and the rotational mass.Similarly, the stiffness matrix of the beam element is found by considering bending stiffness and the shear stiffness that obtained as

$$[K_b] = \int_0^{L_e} \begin{bmatrix} \frac{\partial [N_\theta]}{\partial u} \\ [N_\theta] + \frac{\partial [N_q]}{\partial u} \end{bmatrix}^T \begin{bmatrix} EI & 0 \\ 0 & kGA \end{bmatrix} \begin{bmatrix} \frac{\partial [N_\theta]}{\partial u} \\ [N_\theta] + \frac{\partial [N_q]}{\partial u} \end{bmatrix} du \quad (5)$$

Where $[N_q]$ & $[N_\theta]$ are the terms used for shape functions for displacement and rotation taking into consideration of the shear deformation (ϕ) of the beam. The shear deformation is presented as

$$\phi = \frac{12EIK}{AGL^2}$$
$$\frac{1}{k} = k_y \quad (6)$$

Substituting the shape function values $[N_q]$ & $[N_\theta]$, the stiffness matrix of the proposed beam element can be found.

2.2 Modelling of a transverse fractured beam

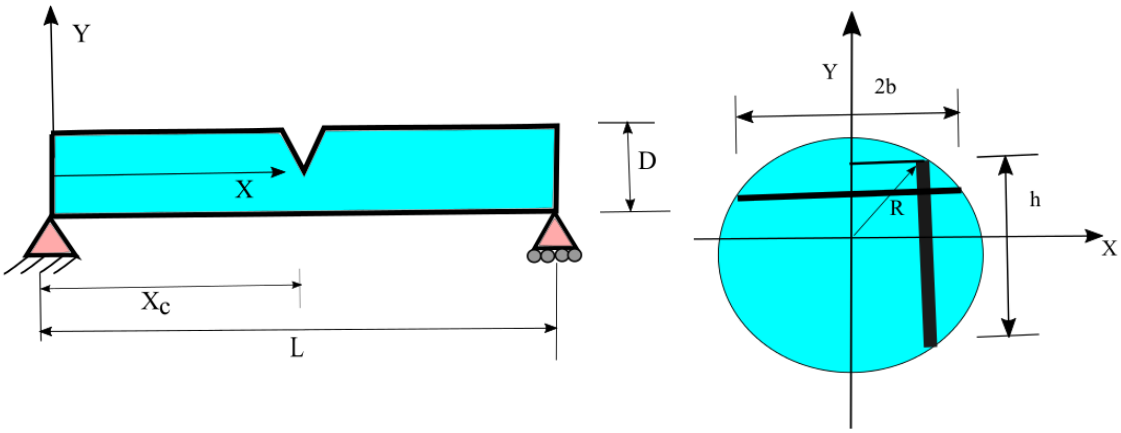

Fig 2 Modelling of Simply Supported beam with transverse fracture at any position along the beam length.

The modelling of Simply **S**upported beam with circular cross-section has been put forth in this section. The diameter of the circular section is *D* with a single transverse fracturehaving constant depth *a*as shown in Fig 2.The fracture is assumed to be at a distance of $X_c$from one end of the beam. The beam is divided into elements with length 'Le'.

$$b = \sqrt{2Ra - a^2}$$

$$h = \sqrt{4R^2 - 4x^2} \tag{7}$$

$$\alpha = \frac{1}{2}\left[\sqrt{4R^2 - 4x^2} - (2R - 2a)\right]$$

The fractured beam element has been modelled by assuming both force and moment applied at each node of the element. The consequent displacements are denoted as *v* and *θ*. Let *Lc* denote the distance offracture locationand other end of the proposed beam. The term *a* denotes the relative fracture depth. The beam element has flexural rigidity *EI*.By considering the finite element co-ordinate system, the correlation between the displacement and the forces can be expressed as

$$\begin{Bmatrix} v_j - v_i - \theta_i \\ \theta_j - \theta_i \end{Bmatrix} = Y_{ovl} \begin{Bmatrix} V_j \\ M_j \end{Bmatrix} \tag{8}$$

The unfractured Timoshenko beam element with flexibility matrix as

$$\begin{Bmatrix} v_j - v_i - \theta_i \\ \theta_j - \theta_i \end{Bmatrix} = Y_{\text{int}\,act} \begin{Bmatrix} V_j \\ M_j \end{Bmatrix} \tag{9}$$

The total flexibility matrix of the fractured Timoshenko beam element can be obtained as

$$Y_{total} = Y_{ovl} + Y_{\text{int}\,act} \tag{10}$$

Considering the total flexibility matrix along with transformation matrix, the stiffness matrix of the fractured element can be obtained as

$$K_c = T Y_{total}^{-1} T^T \tag{11}$$

Where transformation matrix is represented as *T*

3 RESULT OF THE MATHEMATICAL FORMULATION

The Timoshenko Simply Supported beam with a transverse open fracture has been considered for numerical analysis. The geometric and physical parameters of the beam are L=0.985m, D=1.8cm, E=206Gpa, ρ=7850Kg/m^3&μ=0.3.The beam length is divided into y no of finite elements. From the convergence report it has been found if the beam will be divided into 27 no of elements it predict a very good result. Hence for further analysis 27 no of elements has been considered. The natural frequencies for the unfractured and fractured Timoshenko beam with different relative fracture depths have been compared and presented.

The analysis has been conducted in MATLAB environment. The developed code has been validated with the existing result shown in Table 2. From the table it has been observed that the results so obtained from the developed code well suited to the existing one. The variation of first three natural frequencies with relative fracture depths of 0.1, 0.2, 0.3 and 0.4 and relative position of 0.2, 0.5, 0.6 and 0.8 of the proposed Timoshenko simply supported beam has been presented in

Table 3.

Table 6.From the table it has been found that for a given relative fracture position, as the relative fracture depth increases the frequency decreases for all modes of vibration.

Table 2 Validation of vibrational frequencies for unfractured Timoshenko beam.

ω (rad/sec)	Present result using MATLAB code	Existing available result Calculation
1st frequency	237.528	237.459
2nd frequency	986.396	985.995
3rd frequency	2187.856	2186.742

Similarly, as the relative position changes the frequency decreases for all modes of vibration.

Table 3Vibration Frequencies of fractured Timoshenko beam with relative fracture location 0.20.

ω (rad/sec)	Fracture position	Relative fracture depth =0.1	Relative fracture depth =0.2	Relative fracture depth =0.3	Relative fracture depth =0.4
1st frequency	0.2	237.32	236.12	235.87	234.67
2nd frequency	0.2	985.29	984.78	983.46	982.91
3rd frequency	0.2	2187.23	2186.58	2185.79	2184.37

Table 4Vibration Frequencies of fractured Timoshenko beam with relative fracture location 0.50.

ω (rad/sec)	Fracture position	Relative fracture depth =0.1	Relative fracture depth =0.2	Relative fracture depth =0.3	Relative fracture depth =0.4
ω_1	0.5	236.45	235.65	234.73	233.58
ω_2	0.5	985.12	984.49	983.16	981.67
ω_3	0.5	2187.11	2186.09	2185.65	2183.49

Table 5Vibration Frequencies of fractured Timoshenko beam with relative fracture location0.60.

ω (rad/sec)	Fracture position	Relative fracture depth =0.1	Relative fracture depth =0.2	Relative fracture depth =0.3	Relative fracture depth =0.4
ω_1	0.6	235.87	233.77	232.76	230.46
ω_2	0.6	984.76	983.56	981.58	979.67
ω_3	0.6	2186.86	2184.25	2182.36	2178.06

Table 6Vibration Frequencies of fractured Timoshenko beam with relative fracture location 0.80.

ω (rad/sec)	Fracture position	Relative fracture depth =0.1	Relative fracture depth =0.2	Relative fracture depth =0.3	Relative fracture depth =0.4
ω_1	0.8	234.45	232.79	230.98	230.135
ω_2	0.8	983.16	981.49	980.08	979.16
ω_3	0.8	2185.74	2184.59	2182.27	2180.73

The first mode shape of unfractured and fractured beam with relative fracture depths of 0.1, 0.2, 0.3 and 0.4 at relative position of 0.5 has been plotted in Fig. 3. It has been observed from the figure that the relative amplitude has been decreased to 36% (average) for the assumed relative fracture depths. An abrupt change in the pattern of the mode shape has been visualized at the location of presence of fracture. It has been also observed that as the relative fracture depth increases, the abrupt nature shows a considerable amount. It is due to the fact that as the fracture depth increases the strain of the beam decreases.

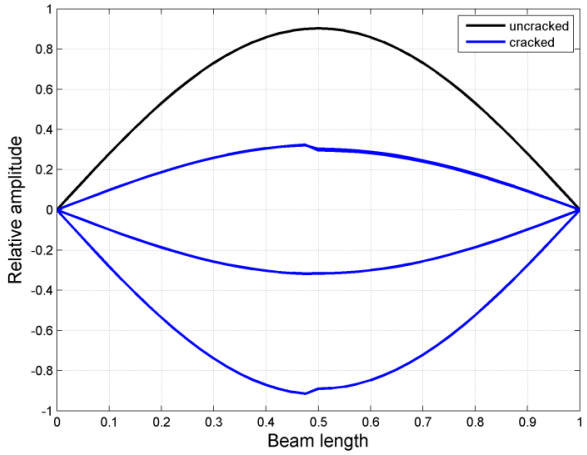

Fig. 3 1st mode variation of unfractured and fractured beam with relative fracture depths of 0.1, 0.2, 0.3and 0.4 respectively.

The second mode shape of unfractured and fractured beam with relative fracture depths of 0.1, 0.2, 0.3 and 0.4 at relative position of 0.5 has been plotted in Fig. 4. It has been observed from the figure that the relative amplitude has been decreased to 49% (average) for the assumed relative fracture depths. An abrupt change in the pattern of the mode shape has been visualized at the location of presence of fracture for higher value of relative fracture depths. The amplitude of the mode shape decreases as the fracture depth increases.

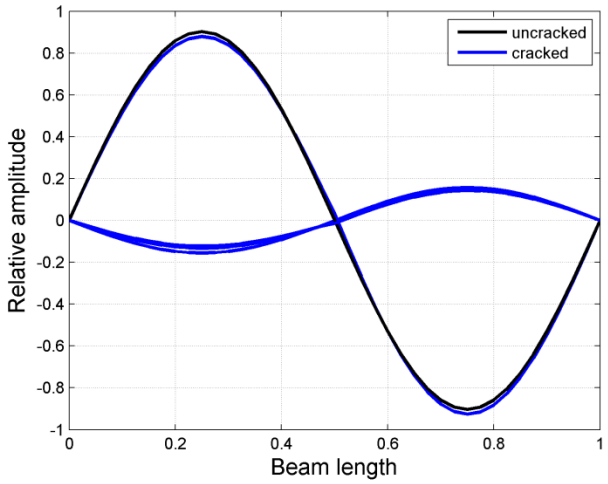

Fig. 4 2nd mode variation of unfractured and fractured beam with relative fracture depths of 0.1, 0.2, 0.3and 0.4 respectively

The Third mode shape of unfractured and fractured beam with relative fracture depths of 0.1, 0.2, 0.3 and 0.4 at relative position of 0.5 has been plotted in Fig 5. It has been observed from the figure that the relative amplitude has been decreased to 62% (average) for the assumed relative fracture depths. A sudden change in the amplitude in the pattern of the mode shape has been clearly visualized at the location of presence of fracture for higher value of

relative fracture depths. The amplitude of the mode shape decreases as the fracture depth increases due to the decrease in strain in the beam.

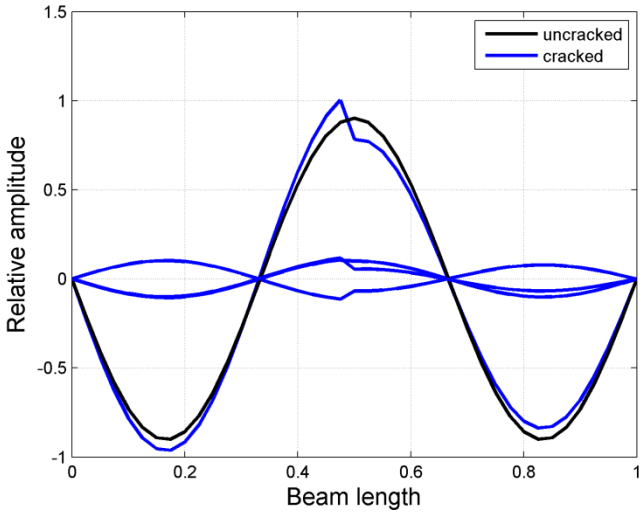

Fig 5 3rd mode variation of unfractured and fractured beam with relative fracture depths of 0.1, 0.2, 0.3and 0.4 respectively

Similarly the forth mode shape of unfractured and fractured beam with relative fracture depths of 0.1, 0.2, 0.3 and 0.4 at relative position of 0.5 has been plotted in Fig 6. It has been observed from the figure that the relative amplitude has been decreased to 73% (average) for the assumed relative fracture depths. A sudden change in the amplitude in the pattern of the mode shape has been clearly visualized at the location of presence of fracture for higher value of relative fracture depths. Due the presence of antinodes in forth mode shapes the abrupt change is slightly visible but considerable reduction in amplitude has been found.

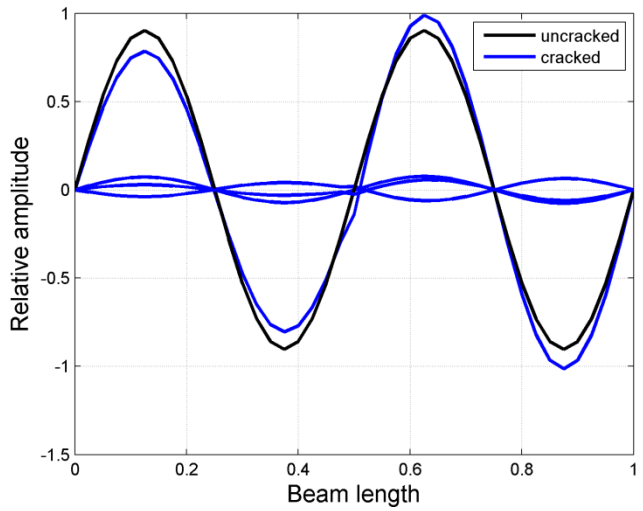

Fig 6 4th mode variation of unfractured and fractured beam with relative fracture depths of 0.1, 0.2, 0.3and 0.4 respectively

Similarly the fifth mode shape of unfractured and fractured beam with relative fracture depths of 0.1, 0.2, 0.3 and 0.4 at relative position of 0.5 has been plotted in Fig 7. It has been observed from the figure that the relative amplitude has been decreased to 83% (average) for the assumed relative fracture depths. A sudden change in the amplitude in the pattern of the mode shape has been clearly visualized at the location of presence of fracture for

higher value of relative fracture depths. At relative fracture depth of 0.4 a considerable amount of reduction in amplitude has been found. Taking into consideration of all the mode shapes and relative fracture depths it has been found due to the presence of fracture in the beam the frequency of the beam decreasing so as the mode shapes. The abrupt or sudden change in amplitude of the beam indicates the presence of transverse fracture with certain amount of relative fracture depths.

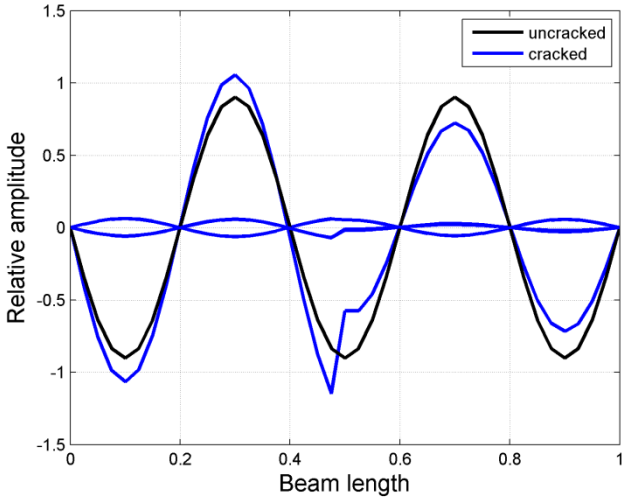

Fig 7 5th mode variation of unfractured and fractured beam with relative fracture depths of 0.1, 0.2, 0.3and 0.4 respectively

The dynamic response of unfractured and fractured beam with relative fracture depths of 0.1, 0.2, 0.3 and 0.4 at relative position of 0.5 has been plotted in Fig 8. From the Figure it has been observed that the peak amplitude at resonant frequency has been decreased as the driving frequency increased. Presence of fracture with relative fracture depths in a beam shows shifting of resonant frequency. From the figure it has been observed that the peak amplitude reduces to 21% in unfractured beam whereas for fractured beam it has been reduced to 27% (Average) for relative fracture depths of 0.1, 0.2, 0.3 and 0.4. Furthermore, there has been a decrease in amplitude to 34% from second to third resonant frequency. For unfractured beam whereas decrease in 39% (average) incase of fractured beam.

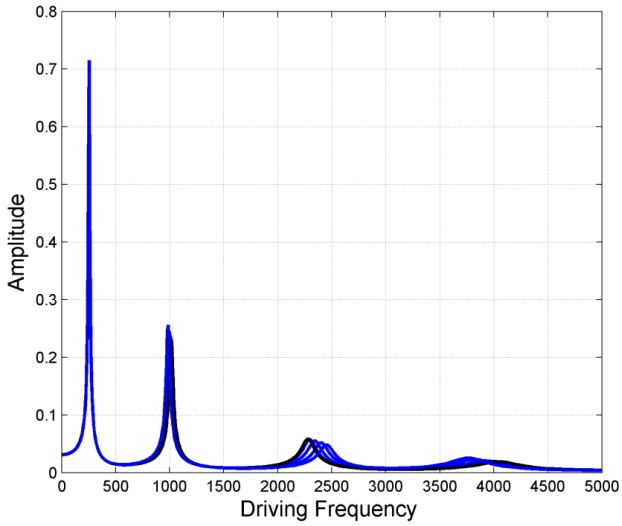

Fig 8 Frequency response of the unfractured and fractured beam with relative fracture depths of 0.1, 0.2, 0.3and 0.4 respectively subjected to an impulse load 50 N.

The extended figure for the variation in fundamental frequency response for unfractured and fractured beam with relative fracture depths of 0.1, 0.2, 0.3 and 0.4 at relative fracture location of 0.5 has been presented in the figure. The proportional damping has been taken into consideration for the analysis. Due to the proportional damping the peak amplitude of resonant frequency decreased. The driving frequency has been varies within the range of 0-500 Rad/sec. with an impulse load of 50N.

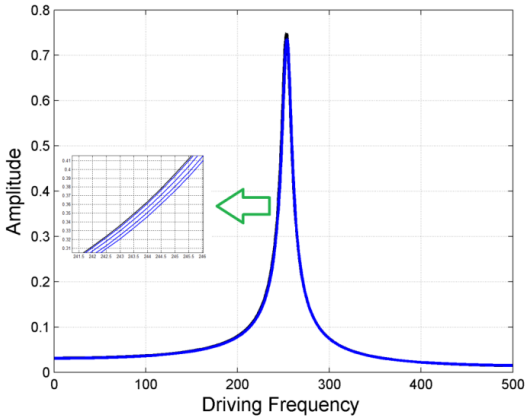

Fig. 9 Frequency response of the unfractured and fractured beam with relative fracture depths of 0.1, 0.2, 0.3and 0.4 respectively subjected to an impulse load 50 N within the range of 0-500 Rad/sec.

The extended figure for the variation in 2nd natural frequency response for unfractured and fractured beam with relative fracture depths of 0.1, 0.2, 0.3 and 0.4 at relative fracture location of 0.5 has been presented in Fig. 10. The driving frequency has been varies within the range of 700-1200 Rad/sec. with an impulse load of 50N.A shifting of resonant frequency has been visualized for different relative fracture depths of 0.1, 0.2, 0.3 and 0.4. It has been observed that the second resonant frequency decreases to 6% (average) as the relative fracture depth increases from 0.0 to 0.4. The peaks in the frequency response are due to the presence of proportional damping which renders the amplitude to a considerable amount.

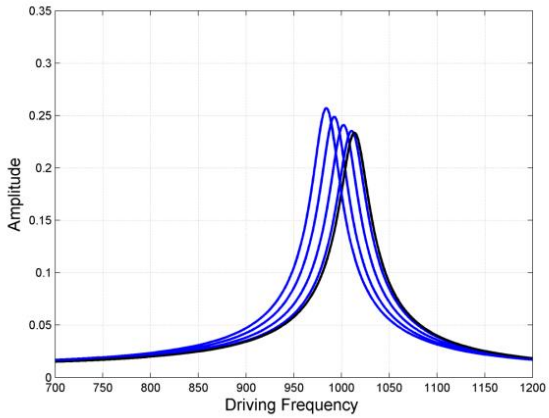

Fig. 10 Frequency response of the unfractured and fractured beam with relative fracture depths of 0.1, 0.2, 0.3 and 0.4 respectively subjected to an impulse load 50 N within the range of 700-1200 Rad/sec

Similarly the extended figure for the variation in 3rd natural frequency response for unfractured and fractured beam with relative fracture depths of 0.1, 0.2, 0.3 and 0.4 at relative fracture location of 0.5 has been presented in Fig.11. The driving frequency has been varies within the range of 1500-3000 Rad/sec. with an impulse load of 50N.A shifting of resonant frequency has been visualized for different relative fracture depths of 0.1, 0.2, 0.3 and 0.4. It has been observed that the third resonant frequency decreases to 10% (average) as the relative fracture depth increases

from 0.0 to 0.4. The peaks in the frequency response are due to the presence of proportional damping which renders the amplitude to a considerable amount.

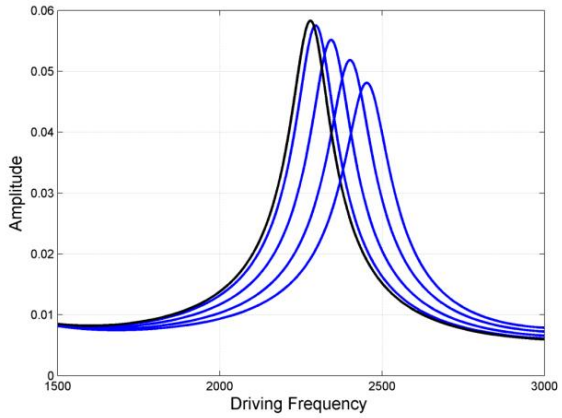

Fig. 11 Frequency response of the unfractured and fractured beam with relative fracture depths of 0.1, 0.2, 0.3and 0.4 respectively subjected to an impulse load 50 N within the range of 1500-3000 Rad/sec

CONCLUSION

The present paperfocus on vibration investigation of a Timoshenko beam with transverse open fracture.The overall additional flexibility matrix has been obtained for evaluating the natural frequencies of the beam with fracture. From the investigation it has been observed that presence of fracture decreases the natural frequencies for all cases of position and relative fracture depths. The change of natural frequencies not only depends on the change of relative fracture depth but also location of the fracture in the beam. It is concludedthat with increase in relative fracture depth the natural frequency decreases and there is an unexpected change in mode shape due to presence of fracture.

REFERENCE

1. *Papadopoulos, C.A., Dimarogonas, A.D.: Coupled longitudinal and bending vibrations of a rotating shaft with an open crack. J. Sound Vib. 117, 81–93 (1987). Https://doi.org/10.1016/0022-460X(87)90437-8.*
2. *Shifrin, E.I., Ruotolo, R.: NATURAL FREQUENCIES OF A BEAM WITH AN ARBITRARY NUMBER OF CRACKS. J. Sound Vib. 222, 409–423 (1999). Https://doi.org/10.1006/jsvi.1998.2083.*
3. *Bamnios, Y., Douka, E., Trochidis, A.: CRACK IDENTIFICATION IN BEAM STRUCTURES USING MECHANICAL IMPEDANCE. J. Sound Vib. 256, 287–297 (2002). Https://doi.org/10.1006/jsvi.2001.4209.*
4. *Loya, J.A., Rubio, L., Fernández-Sáez, J.: Natural frequencies for bending vibrations of Timoshenko cracked beams. J. Sound Vib. 290, 640–653 (2006). Https://doi.org/10.1016/j.jsv.2005.04.005.*
5. *Karthikeyan, M., Tiwari, R., Talukdar, S.: Crack localisation and sizing in a beam based on the free and forced response measurements. Mech. Syst. Signal Process. 21, 1362–1385 (2007). Https://doi.org/10.1016/j.ymssp.2006.06.002.*
6. *Identification of Cracking in Beam Structures Using Timoshenko and Euler Formulations | Journal of Engineering Mechanics | Vol 130, No 11, https://ascelibrary.org/doi/abs/10.1061/(ASCE)0733-9399(2004)130:11(1297), last accessed 2021/08/28.*

7. *Lee, Y.-S., Chung, M.-J.: A study on crack detection using eigenfrequency test data. Comput. Struct. 77, 327–342 (2000). Https://doi.org/10.1016/S0045-7949(99)00194-7.*
8. *Crack localization in non-rotating shafts coupled to elastic foundation using sensitivity analysis techniques | Emerald Insight, https://www.emerald.com/insight/content/doi/10.1108/13552510310482415/full/html, last accessed 2021/08/28.*
9. *Biswal, A.R., Roy, T., Behera, R.K., Pradhan, S.K., Parida, P.K.: Finite Element Based Vibration Analysis of a Nonprismatic Timoshenko Beam with Transverse Open Crack. Procedia Eng. 144, 226–233 (2016). Https://doi.org/10.1016/j.proeng.2016.05.028.*
10. *Zheng, D.Y., Kessissoglou, N.J.: Free vibration analysis of a cracked beam by finite element method. J. Sound Vib. 273, 457–475 (2004). Https://doi.org/10.1016/S0022-460X(03)00504-2.*

BIOGRAPHICAL NOTES

Dr. Alok Ranjan Biswal is an Associate Professor in ME Department cum Vice Principal (A&R) of DRIEMS (Autonomous) has more than fifteen years of Teaching and Research experience in the field of Mechanical Vibration based Energy Harvesting, Nonlinearity in vibration, Functionally Graded Materials, Optimization, Smart Structure, Fracture Mechanics and so on. He has many National and International publications in Journals with high Impact Factors which have been indexed in Science Citations (SCI), Scopus, Web of Science etc. and Conferences organized by Central Universities, Research Centres, NITs and IITs. During his tenure of teaching he has been Awarded **Best Teacher Award** (2007, 2009 and 2010) in JIET, Cuttack, Odisha for his significant contribution towards excellence in teaching. Based on the Academic innovation, integrity & ethics, process management and service quality he has been awarded with **Quality Education Leadership Award** by Golden AIM Awards for Excellence and Leadership in Education in 2020. He is also a life time member of Indian Society for Technical Education(ISTE),Society of Failure Analysis(SFA) and Federation of Quality Education Council.

Er. Poonam Prusty is an Assistant Professor in Mechanical Engineering Department of DRIEMS (Autonomous), Cuttack, Odisha. She has done her B.Tech in Mechanical Engineering from Orissa Engineering College (OEC), Bhubaneswar, Odisha and obtained Master of Technology in Thermal Engineering from College of Engineering and Technology (CET), Bhubaneswar, Odisha. She has 4 years of teaching experience in both Govt. and private institutes. She has significant number of publications and attended many National and International conferences, seminars and webinars.

Er. Rasmi Ranjan Senapati is an Assistant Professor in Mechanical Engineering Department in DRIEMS, Cuttack, Odisha. He has done his Bachelor of Technology (Mechanical Engineering) under Biju Patnaik University of Technology, Rourkela, Odisha with first class and obtained Master of Technology in Mechanical system Design from IGIT, Sarang under BPUT, Odisha. He has more than 10 yrs. Of teaching experiences in Private Institutes. He has a publication in international journal. He has guided many of his students in various in-house projects. He has significant number of publications and attended many National and International conferences, seminars and webinars. He is a life time member of Indian Society for Technical Education(ISTE).

Vibration Investigation of a Damped Axially Functionally Graded Beam

[1]Deepak Ranjan Biswal, [1]Shibabrata Mohapatra, [1]Abinash Bibek Dash

[1] Mechanical engineering Department, DRIEMS Tangi Cuttack-754022

deepakrbiswal@gmail.com, shibabratamohapatra@gmail.com, abinashdash@driems.ac.in

ABSTRACT

The current article deal with the damped vibration investigation of a rectangular beam with nonuniform material properties in longitudinal direction. The investigation has been carried out by finite element method (FEM) with consideration of structural damping parameters. Each element of the beam assumed to have nodes and each node with two degrees of freedom for the investigation in finite element procedure. Polynomial variation of material properties such as density and Young's modulus have been used in the analysis. The static and dynamic analysis for the process has been found out using the finite element procedure. Hamilton's rule has been incorporated to find out the mass and stiffness matrices. For time domain analysis Newmark-B Method has been incorporated in the analysis.

Keywords: *Finite Element Analysis; Hamilton's principle, Dynamic analysis*

1 INTRODUCTION

Functionally gradient materials (FGMs) are the most versatile material which is prepared by changing the microstructure with a precise gradient. It can be deliberated for explicit function and applications. FGMs are generally prepared in the form of several structures, such as beams[1], plates [2] and shells [3]. In this context, the properties may be oriented in thickness direction or/and length direction. For graded beams with properties variation in thickness direction, several research works have been commenced out of which few are described. To analyze the free vibration characteristics of FGM beams a transfer matrix method has been established whose material properties vary in thickness of the beam through power law variation[4]. Further, to investigate the free vibration behavior of FGM beams the dynamic stiffness method has been formulated [5]. A completely new method has been introduced by using Timoshenko beam theory to investigate beams without application of load [6].Beam with exponentially varying width and material properties has been investigated for free vibration [7].The analysis has been carried out analytically through first-order shear deformation assumption[8].The functionally graded piezoelectric material beam, which the material properties are assumed to have a power law or sigmoid law variation across the depth has been investigated [9]. A high-order shear deformation assumption has been proposed for free vibration of FGM beams with continuously varying material properties under different boundary conditions [10]. The free vibration of a simply supported FGM beams in which the material properties change arbitrarily in the thickness direction has been discussed [11].The free vibration with nonlinear behavior of a sandwiched porous beam has been studied [12]. The investigation carried out by considering the Von Karman geometric nonlinearity. The free bending vibrations of straight beams with inconsistent cross section has been studied using Bessel's functions [13].In this

paper, the transfer matrix method has been incorporated to determine the frequencies of a conical and cylindrical beam. Even though several research works have been performed on beams with varying material properties still there is some directions upon which attention need to be focused. The variation of properties in longitudinal direction has put the attention in a great way. The present article deal with the variation of properties in the axial direction and its effect due to vibration. Both the static and dynamic analysis of the beam has been carried out with the application of impulse load.

2 Numerical Formulation of the Proposed Beam

The numerical formulations and investigation involve the modelling of the beam using finite element procedures. The mathematical formulation is presented in the following subsections. A cantilever beam is shown Fig. 12 for dynamic analysis when subjected to an impulse force.

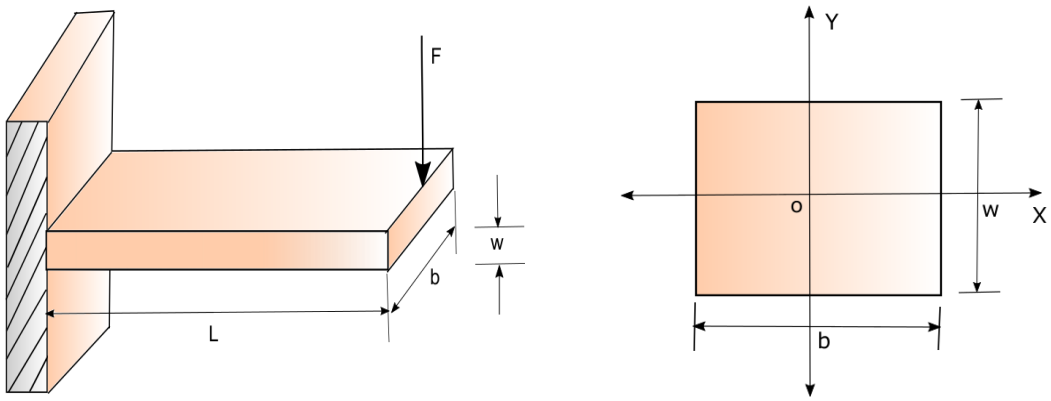

Fig. 12 Proposed Cantilever beam having variation of properties in longitudinal direction.

The length of the proposed beam has been taken to be L .The width and thickness of the beam has been carried out as b and w. An impulse load of F is applied at the free end of the cantilever beam. Euler-Bernoulli formulation has been considered for free and forced vibration analysis of the beam. All mathematical formulation has been coded in Matlab environment. The beam element with degrees of freedom at each node is shown in Fig. 13. In Finite Element modeling, each nodal point assumed to experience 2 degrees of freedom i.e. transverse displacement (v) and rotation (θ) which are supposed to act due to the shear force and bending moment.

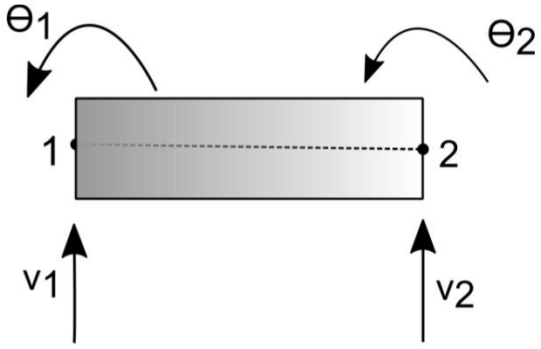

Fig. 13 Nodal degrees of freedom at each node of the element.

The displacement field of the beam element using finite element formulation in Cartesian coordinate system can be written as

$$\begin{aligned} m(x,y,z,t) &= z\theta(x,t) = z\left(\frac{\partial w}{\partial x}\right) \\ n(x,y,z,t) &= 0 \\ o(x,y,z,t) &= o(x,t) \end{aligned} \tag{1}$$

Where *u, v, w* are the time-dependent axial, lateral and transverse displacements along *x, y, z*-axes respectively. The transverse displacement is represented by the term *w(x, t)*. θ is the term denoted for rotation of the midplane whereas t denotes the time. The axial displacement at any point is neglected in the midplane as its effect is negligible compared to transverse displacement. The material property i.e. Young's modulus and density of the proposed beam has been changed continuously in axial direction and the order of variation is considered in polynomial function. The proposed variation has been considered as follows

$$E(x) = d_0 + d_1\left(\frac{x}{L}\right) + d_2\left(\frac{x}{L}\right)^2 + d_3\left(\frac{x}{L}\right)^3 + d_4\left(\frac{x}{L}\right)^4 + d_5\left(\frac{x}{L}\right)^5 + d_6\left(\frac{x}{L}\right)^6$$

where

$$d_0 = \frac{587}{5}; d_1 = \frac{203}{5}; d_2 = 45; d_3 = \frac{44}{5}; d_4 = \frac{3}{5}; d_5 = -2; d_6 = 1$$

and (2)

$$\rho(x) = z_0 + z_1\left(\frac{x}{L}\right) + z_2\left(\frac{x}{L}\right)^2$$

where

$$z_0 = 1; z_1 = 1; z_2 = 1$$

The field of displacement can be represented as

$$\{r\} = [N_w]\{\delta\} \tag{3}$$

Here *r* and N_w denotes the nodal degrees of freedom and the shape functions respectively.

$$\{\delta\} = \begin{Bmatrix} w_1 \\ \theta_1 \\ w_2 \\ \theta_2 \end{Bmatrix} where\ \theta_1 = \frac{\partial w_1}{\partial x} \text{ and } \theta_2 = \frac{\partial w_2}{\partial x} \tag{4}$$

Since there are four degrees of freedom with four nodal values, the polynomial function with four constants has been considered for the analysis.

$$r = c_1 + c_2 x + c_3 x^2 + c_4 x^3 \tag{5}$$

The above equation satisfies compatibility and completeness requirement. Now

$$\theta = \frac{\partial w}{\partial x} = a_2 + 2a_3 x + 3a_4 x^2 \tag{6}$$

For convenience we select local coordinate system

$$\begin{aligned} &x_1 = 0; x_2 = L \\ &\therefore\ w_1 = c_1; \theta_1 = c_2; \\ &w_2 = c_1 + c_2 L + c_3 L^2 + c_4 L^3 \\ &\theta_2 = c_2 + 2c_3 L + 3c_4 L^2 \end{aligned} \tag{7}$$

$$\{\delta\}=\begin{Bmatrix} w_1 \\ \theta_1 \\ w_2 \\ \theta_2 \end{Bmatrix}=\begin{bmatrix} 1 & 0 & 0 & 0 \\ 0 & 1 & 0 & 0 \\ 1 & L & L^2 & L^3 \\ 0 & 1 & 2L & 3L^2 \end{bmatrix}\begin{Bmatrix} c_1 \\ c_2 \\ c_3 \\ c_4 \end{Bmatrix} \tag{8}$$

$$\{\delta\}=\begin{Bmatrix} w_1 \\ \theta_1 \\ w_2 \\ \theta_2 \end{Bmatrix}=\begin{bmatrix} 1 & 0 & 0 & 0 \\ 0 & 1 & 0 & 0 \\ 1 & L & L^2 & L^3 \\ 0 & 1 & 2L & 3L^2 \end{bmatrix}^{1}\begin{Bmatrix} w_1 \\ \theta_1 \\ w_2 \\ \theta_2 \end{Bmatrix}=\frac{1}{3L^4\ \ 2L^3}\begin{bmatrix} L^4 & 0 & 3L^2 & 2L \\ 0 & L^4 & 2L^3 & L^2 \\ 0 & 0 & 3L^2 & 2L \\ 0 & 0 & L^3 & L^2 \end{bmatrix}\begin{Bmatrix} w_1 \\ \theta_1 \\ w_2 \\ \theta_2 \end{Bmatrix}$$

$$=\begin{bmatrix} 1 & 0 & 0 & 0 \\ 0 & 1 & 0 & 0 \\ \frac{3}{L^2} & \frac{2}{L} & \frac{3}{L^2} & \frac{1}{L} \\ \frac{2}{L^3} & \frac{1}{L^2} & \frac{2}{L^3} & \frac{1}{L^2} \end{bmatrix}\begin{Bmatrix} w_1 \\ \theta_1 \\ w_2 \\ \theta_2 \end{Bmatrix} \tag{9}$$

$$\therefore\ w=c_1+c_2x+c_3x^2+c_4x^3 \tag{10}$$

$$=\begin{bmatrix} 1 & x & x^2 & x^3 \end{bmatrix}\begin{Bmatrix} c_1 \\ c_2 \\ c_3 \\ c_4 \end{Bmatrix}=\begin{bmatrix} 1 & x & x^2 & x^3 \end{bmatrix}\begin{bmatrix} 1 & 0 & 0 & 0 \\ 0 & 1 & 0 & 0 \\ \frac{3}{L^2} & \frac{2}{L} & \frac{3}{L^2} & \frac{1}{L} \\ \frac{2}{L^3} & \frac{1}{L^2} & \frac{2}{L^3} & \frac{1}{L^2} \end{bmatrix}\begin{Bmatrix} w_1 \\ \theta_1 \\ w_2 \\ \theta_2 \end{Bmatrix} \tag{11}$$

$$=\begin{bmatrix} 1-\frac{3x^2}{L^2}+\frac{2x^3}{L^3} & x-\frac{2x^2}{L}+\frac{x^3}{L^2} & \frac{3x^2}{L^2}-\frac{2x^3}{L^3} & \frac{x^2}{L}+\frac{x^3}{L^2} \end{bmatrix}\begin{Bmatrix} w_1 \\ \theta_1 \\ w_2 \\ \theta_2 \end{Bmatrix} \tag{12}$$

$$\begin{bmatrix} N_1 & N_2 & N_3 & N_4 \end{bmatrix}\{\delta\}_e=[N]\{\delta\}_e \tag{13}$$

$$[N]=\begin{bmatrix} N_1 & N_2 & N_3 & N_4 \end{bmatrix} \tag{14}$$

$$\begin{aligned} N_1 &= 1-\frac{3x^2}{L^2}+\frac{2x^3}{L^3} \\ N_2 &= x-\frac{2x^2}{L}+\frac{x^3}{L^2} \\ N_3 &= \frac{3x^2}{L^2}-\frac{2x^3}{L^3} \\ N_4 &= \frac{x^2}{L}+\frac{x^3}{L^2} \end{aligned} \tag{15}$$

The mass and stiffness matrix of the beam element can be found by using Hamilton's rule. The Hamilton's rule uses the strain energy principle with time dependent parameters of kinetic energy, potential energy and work done as

$$\partial \Pi = \int_{t_1}^{t_2} [\partial (E_K - E_P + W)] dt = 0 \tag{16}$$

Where E_K, E_P and W is the kinetic energy, total electromechanical enthalpy and total work done by the external mechanical force respectively.t_1 and t_2 represent the initial and final time. The expressions for the above energies can be written as

$$E_k = \frac{1}{2} \int_V \rho_b \dot{r}^T \dot{r} dV \tag{17}$$

$$E_p = \frac{1}{2} \int_V \varepsilon_1^T \sigma_1 dV \tag{18}$$

$$W = \sum_{i=1}^{nf} r(x_i) Q(x_i) \tag{19}$$

Using the equation, the elemental mass matrix and stiffness matrices for the beam can be obtained as

$$[M_b^e] = \int_0^{L_b} [N_w]^T \rho_b A_b [N_w] dx \tag{20}$$

$$[K_b^e] = \int_0^{L_b} \left[\frac{\partial [N_\theta]}{\partial x} \right]^T E_b I_b \left[\frac{\partial [N_\theta]}{\partial x} \right] dx \tag{21}$$

Where $[N_\theta] = \partial [N_w.] / \partial x$ .The dynamic equation of the structure is obtained by using the equation The length of entire beam is separated into 20 finite elements. The mass and stiffness matrices are grouped together and the global matrices are obtained. The equation of motion of the structure be represented as

$$\left[M_b^e\right]\{\ddot{r}\} + \left[K_b^e\right]\{r\} = \{Q^e\} \tag{22}$$

The global stiffness matrices, mass matrices have been evaluated by numerical integration. The damping ratio is predicted from the computed fundamental frequency as

$$C^e = \alpha \left(M_b^e\right) + \beta \left(K_b^e\right) \tag{23}$$

Where α and β are found out from

$$\zeta_i = \frac{\alpha}{2\omega_i} + \frac{\beta \omega_i}{2}, \quad i=1, 2, \ldots n \tag{24}$$

Where ζ_i is the damping ratio of the structure. The equation of motion considering the damping parameter for the proposed beam can be found as

$$\left[M_b^e\right]\{\ddot{r}\} + \left[C^e\right]\{\dot{r}\} + \left[K_b^e\right]\{r\} = \{Q^e\} \tag{25}$$

The global equation can be obtained after assembling the elemental equation as

$$[M_B]\{\ddot{r}\} + [C]\{\dot{r}\} + [K_B]\{r\} = \{Q^e\} \tag{26}$$

Where the global mass matrices of beam be represented as M_B, the global stiffness matrices of the beam be represented as K_B is and the global damping matrix be represented as C respectively.

3 OUTCOME OF THE PRESENT FORMULATION

Based on the mathematical formulations a MATLAB code has been prepared for the investigation of the proposed beam. The MATLAB code has been validated and results are presented in the following sub sections. The developed code has been validated for the proposed cantilever beam. The physical dimensions of the beam are (875×68×3.9) mm. As per the analysis the variation of Young's modulus and density of the beam has been taken as polynomial variation. In static analysis the frequency and mode shapes of the beam have been analyzed. For free vibration

analysis an initial displacement has been given to the beam at the free end. The first four natural frequencies have been calculated using the MATLAB environment. The convergence result has been presented in the table .From the table it has been found that for 16numbers of elements the first four natural frequencies are converged properly. Further, four mode shapes are analyzed to find out the lateral displacement of the proposed beam. The Proposed beam with variation in material properties is considered for the analysis and different loads are applied at the free end. The frequency and mode shapes are found out for free vibration. The present code is validated by considering a cantilever beam of rectangular cross section. Material properties of the beam are considered as per the mathematical expression discussed.

Table 7 Convergence of natural frequencies of the proposed beam

frequency	No of elements =4	No of elements =8	No of elements =12	No of elements =16	No of elements =17
ω_1	0.1314	0.1398	0.1415	0.1423	0.1424
ω_2	0.8776	0.8817	0.8905	0.8919	0.8919
ω_3	2.4769	2.4815	2.4964	2.4977	2.4978
ω_4	4.8750	4.8835	4.8947	4.8950	4.8951

From the Table it has been observed that the convergence will take place at number of beam elements are16. Hence for further calculation same amount of beam element numbers are taken into consideration. The validation of the results so obtained using the MATLAB code has been shown in Table 8.From the Table it has been found that the frequencies using the developed MATLAB code for the proposed beam has less than 15% of error for all the cases. Further The percentage of error decreases as the mode of the frequency increases.

Table 8 Validation of frequencies with existing results.

Frequency	Available Result	Result developed through MATLAB code	% of error
ω_1	0.1623	0.1424	12.26
ω_2	0.9215	0.8919	3.9
ω_3	2.5362	2.4978	1.5
ω_4	4.9325	4.8951	0.7

The amplitude variation of 1stmode for the proposed beam has been presented in Fig. 14. From the figure it has been observed that the shape of the beam is equivalent to the beam with prismatic and homogeneous condition. From the Figure it has been observed that the maximum amplitude is 0.38 mm and it has no antinode. In first mode of vibration the bema vibrate rapidly hence its natural frequency is very less compared to other natural frequencies. Due to this the 1st natural frequency is otherwise known as fundamental frequency.

The amplitude variation of 2nd mode for the proposed beam has been presented in Fig 15. From the figure it has been observed that the shape of the beam is equivalent to the beam with prismatic and homogeneous condition. From the figure it has been observed that it has only one antinode at a distance of 0.34mm. The maximum amplitude in the 2nd mode variation is 0.1mm.

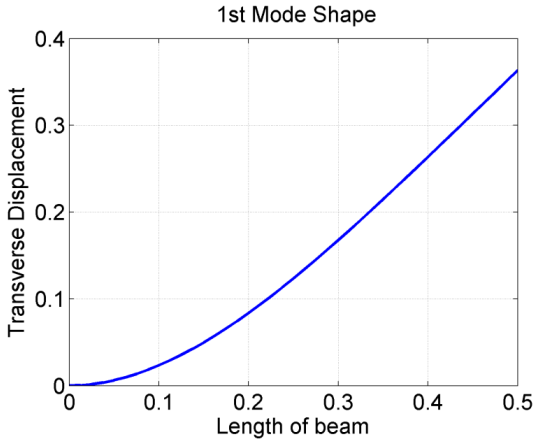

Fig. 14 Variation in amplitude for 1st mode vibration of the cantilever beam

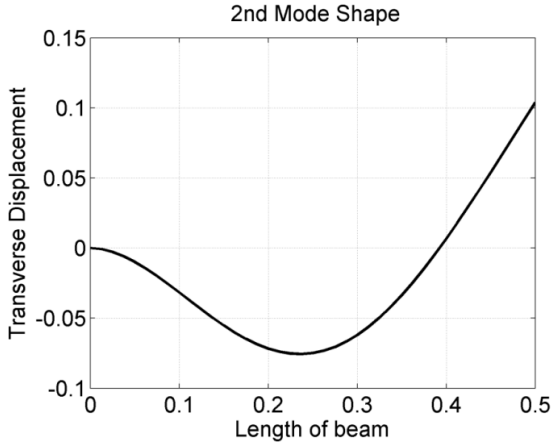

Fig 15. Variation in amplitude for 2nd mode vibration of the cantilever beam

The amplitude variation in 3rd mode for the proposed beam has been presented in Fig. 16. From the figure it has been observed that the shape of the beam is equivalent to the beam with prismatic and homogeneous condition.

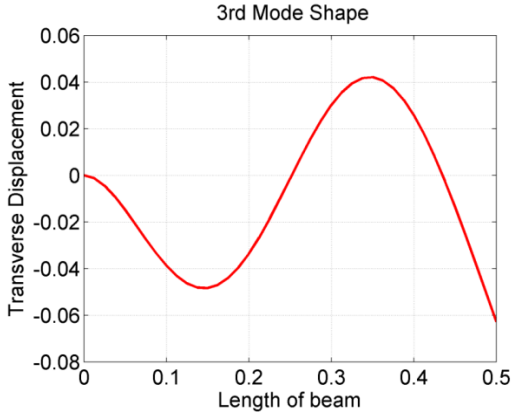

Fig. 16 Variation in amplitude for 3rdmode vibration of the cantilever beam

From the figure it has been observed that it has two antinodes at a distance of 0.25mmand 0.43mm respectively. The maximum amplitude of the 3rd mode shape is 0.061mm.

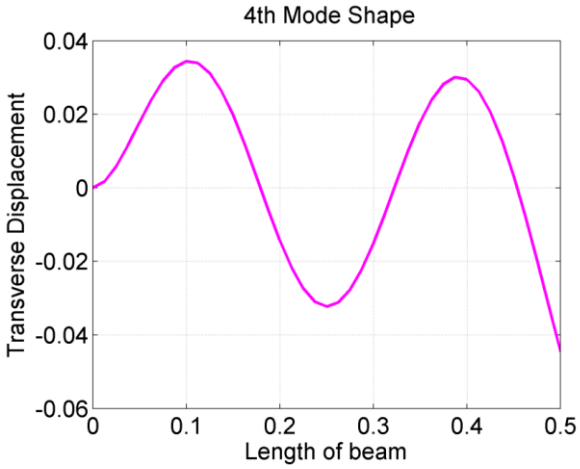

Fig. 17 Variation in amplitude for 4th mode vibration of the cantilever beam

The amplitude variation in 4th mode for the proposed beam has been presented in Fig. 17.From the figure it has been observed that the shape of the beam is equivalent to the beam with prismatic and homogeneous condition. From the figure it has been observed that it has three antinodes at a distance of 0.14mm, 0.32mm and 0.43mm respectively. The maximum amplitude of the 4thmode shape is 0.023mm.The dynamic analysis of the beam is carried out for different loading conditions. As from static analysis it has been observed that the proposed beam with polynomial variation of material properties shows good result in accordance with the homogeneous beam. For dynamic analysis four different loading (8N, 12N, 16N & 20N) magnitudes are considered and the corresponding frequency analysis result has been incorporated. Firstly the beam is subjected to a load of 8 N at the fee end of the beam. The vibration response has been presented with the help of Matlab environment. Fig. 18 shows the frequency response of the proposed cantilever beam when it is subjected to 8N of force at the free end. The frequency response is plotted between the amplitude of the vibration and the driving frequency. The driving frequency is varying from 0-2 rad/sec. The amplitude of 1st natural frequency is higher than the second natural frequency. Hence the peak response in 1st natural frequency is higher than 2nd natural frequency. The peak response for 1st natural frequency is 0.24mm and that for 2nd natural frequency is 0.045mm.

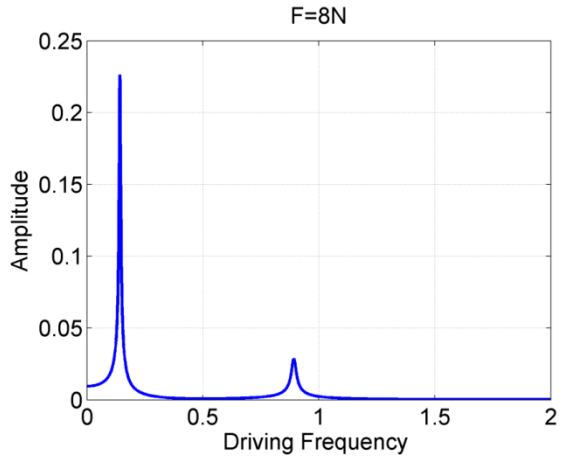

Fig. 18 Frequency response due to the impulse load of 8N at free end of the proposed beam.

Fig. 19. Shows the frequency response of the proposed cantilever beam when it is subjected to 12N of force at the free end. The frequency response is plotted between the amplitude of the vibration and the driving frequency.

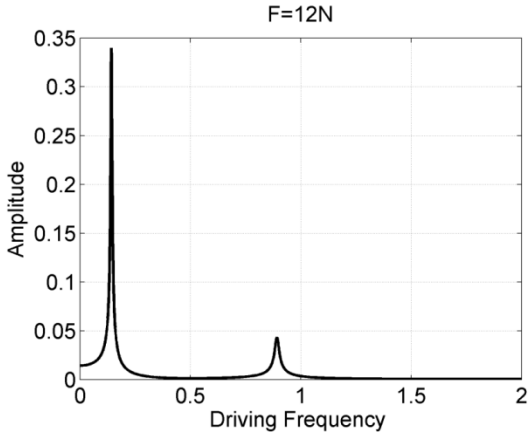

Fig. 19 Frequency response due to the impulse load of 12N at free end of the proposed beam.

The driving frequency is varying from 0-2 rad/sec. From the figure it has been observed that the amplitude of 1st natural frequency is higher than the second natural frequency. Hence the peak response in 1st natural frequency is higher than 2nd natural frequency. The peak response for 1st natural frequency is 0.34mm and that for 2nd natural frequency is 0.031mm.The higher frequencies responses are not shown as the amplitude decreases with increase in frequency.

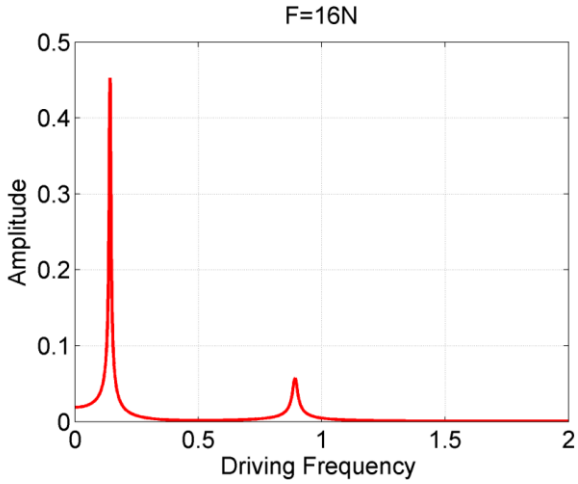

Fig. 20 Frequency response due to the impulse load of 16N at free end of the proposed beam.

Fig. 20 shows the frequency response of the proposed cantilever beam when it is subjected to 16N of force at the free end. The frequency response is plotted between the amplitude of the vibration and the driving frequency. The driving frequency is varying from 0-2 rad/sec. From the figure it has been observed that the amplitude of 1st natural frequency is higher than the second natural frequency. Hence the peak response in 1st natural frequency is higher than 2nd natural frequency. The peak response for 1st natural frequency is 0.45mm and that for 2nd natural frequency is 0.076mm.The higher frequencies responses are not shown as the amplitude decreases with increase in frequency.

Fig 21 shows the frequency response of the proposed cantilever beam when it is subjected to 16N of force at the free end. The frequency response is plotted between the amplitude of the vibration and the driving frequency. The driving frequency is varying from 0-2 rad/sec. From the figure it has been observed that the amplitude of 1st natural frequency is higher than the second natural frequency. Hence the peak response in 1st natural frequency is higher than 2nd natural frequency. The peak response for 1st natural frequency is 0.57mm and that for 2nd natural frequency is 0.86mm.

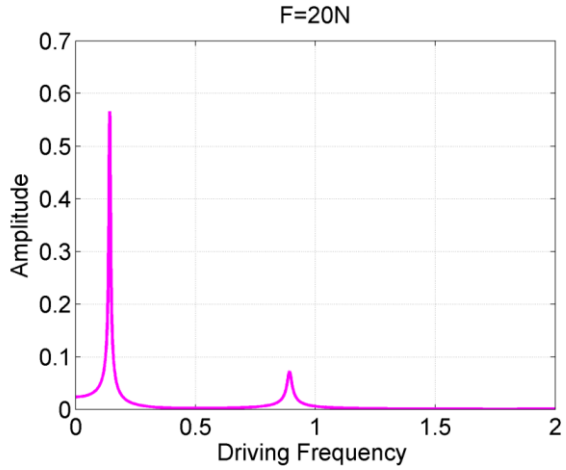

Fig 21 Frequency response due to the impulse load of 20N at free end of the proposed beam.

The higher frequencies responses are not shown as the amplitude decreases with increase in frequency. The time domain analysis has been carried out in Matlab environment with 16N of impulse load at the free end of the cantilever beam. The responses are carried out in time plot curve where 600 sec has been taken and corresponding responses are presented. Fig. 22 shows the displacement time plot of the proposed cantilever beam when the free end has been applied with 16 N of force. From the figure it has been observed that the peak response is 0.018 mm and the amplitude goes on decreasing as time lapse increasing. This is due to the fact that presence of proportional damping reduces the amplitude of the proposed beam and the value diminishes after certain time period.

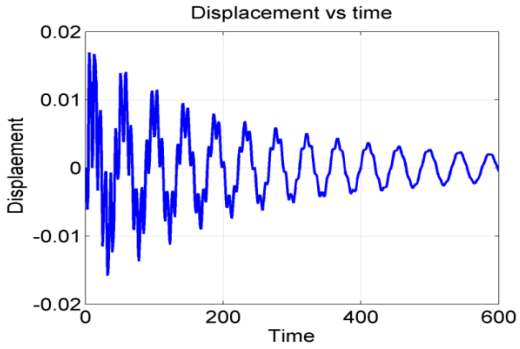

Fig. 22Time domain displacement response at the free end due to the application of 16N force at free end

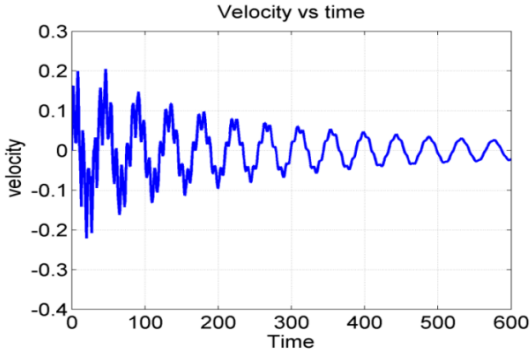

Fig 23 Time domain velocity response at the free end due to the application of 16N force at free end

Similarly Fig 23 shows the velocity time plot of the proposed cantilever beam when the free end has been applied with 16 N of force. From the figure it has been observed that the peak velocity response is 0.21 mm/sec and the amplitude of velocity goes on decreasing as time period increasing. This is due to the presence of proportional

damping or structural damping in the beam which has been consider in this proposed .The value of velocity will diminishes further as the time period increasing.

Further Fig 24 shows the acceleration time plot of the proposed cantilever beam when the free end has been applied with 16 N of force.

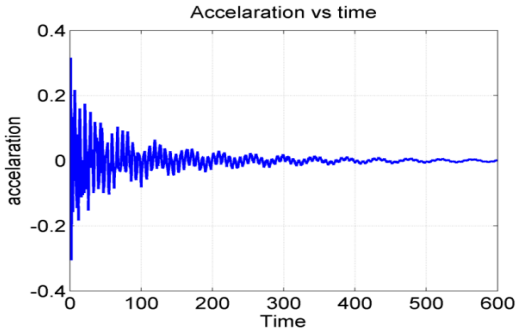

Fig 24 Time domain acceleration response at the free end due to the application of 16N force at free end

From the figure it has been observed that the peak acceleration response is 0.23 mm/sec^2 and the amplitude of acceleration goes on decreasing as time period increasing. This is due to the proportional damping or structural damping in the beam which has been considered in this proposed beam. The value of acceleration will diminish further as the time period increasing.

CONCLUSION

The present research encompasses the finite element procedure for vibration investigation of a cantilever beam with variation of properties in longitudinal direction. Hamilton's rule has been incorporated to find out the global mass and stiffness matrices. From the analysis it has been found that the changing of properties such as Young's modulus and density in longitudinal direction has impact in different modes of vibration. The developed code has been validated with the existing results. The proposed beam developed the similar pattern of variation of frequencies as that of regular beam. The static and dynamic analysis has been carried out with the proportional damping and it has been found the responses diminish with time due to the application of impulse load.

REFERENCE

1. *Analytical solution for a functionally graded beam with arbitrary graded material properties - ScienceDirect, https://www.sciencedirect.com/science/article/abs/pii/S1359836812003551, last accessed 2021/08/16.*
2. *Hao, Y.X., Chen, L.H., Zhang, W., Lei, J.G.: Nonlinear oscillations, bifurcations and chaos of functionally graded materials plate. J. Sound Vib. 312, 862–892 (2008). https://doi.org/10.1016/j.jsv.2007.11.033.*
3. *Hao, Y.X., Zhang, W., Yang, J.: Nonlinear Dynamics of Cantilever FGM Cylindrical Shell under 1:2 Internal Resonance Relations. Mech. Adv. Mater. Struct. 20, 819–833 (2013). https://doi.org/10.1080/15376494.2012.676717.*
4. *Lee, J.W., Lee, J.Y.: Free vibration analysis of functionally graded Bernoulli-Euler beams using an exact transfer matrix expression. Int. J. Mech. Sci. 122, 1–17 (2017). https://doi.org/10.1016/j.ijmecsci.2017.01.011.*
5. *Su, H., Banerjee, J.R., Cheung, C.W.: Dynamic stiffness formulation and free vibration analysis of functionally graded beams. Compos. Struct. 106, 854–862 (2013). https://doi.org/10.1016/j.compstruct.2013.06.029.*
6. *Static and free vibration analysis of functionally graded beams by combination Timoshenko theory and finite volume method - Science Direct, https://www.sciencedirect.com/science/article/abs/pii/S0263822315010302, last accessed 2021/08/16.*
7. *Ait Atmane, H., Tounsi, A., Meftah, S.A., Belhadj, H.A.: Free Vibration Behavior of Exponential Functionally Graded Beams with Varying Cross-section. J. Vib. Control. 17, 311–318 (2011). https://doi.org/10.1177/1077546310370691.*

8. *Sina, S.A., Navazi, H.M., Haddadpour, H.: An analytical method for free vibration analysis of functionally graded beams. Mater. Des. 30, 741–747 (2009). https://doi.org/10.1016/j.matdes.2008.05.015.*
9. *Sharma, P.: Efficacy of Harmonic Differential Quadrature method to vibration analysis of FGPM beam. Compos. Struct. 189, 107–116 (2018). https://doi.org/10.1016/j.compstruct.2018.01.059.*
10. *Li, X.-F., Wang, B.-L., Han, J.-C.: A higher-order theory for static and dynamic analyses of functionally graded beams. Arch. Appl. Mech. 80, 1197–1212 (2010). https://doi.org/10.1007/s00419-010-0435-6.*
11. *Celebi, K., Yarimpabuc, D., Tutuncu, N.: Free vibration analysis of functionally graded beams using complementary functions method. Arch. Appl. Mech. 88, 729–739 (2018). https://doi.org/10.1007/s00419-017-1338-6.*
12. *Nonlinear free vibration of shear deformable sandwich beam with a functionally graded porous core - ScienceDirect, https://www.sciencedirect.com/science/article/abs/pii/S0263823116303056, last accessed 2021/08/16.*
13. *Boiangiu, M., Ceausu, V., Untaroiu, C.D.: A transfer matrix method for free vibration analysis of Euler-Bernoulli beams with variable cross section. J. Vib. Control. 22, 2591–2602 (2016). https://doi.org/10.1177/1077546314550699.*

BIOGRAPHICAL NOTES

Er. Deepak Ranjan Biswal is an Associate Professor and Head in the Department of Mechanical Engineering in DRIEMS, Cuttack, Odisha. He has done his B.E.(Mechanical Engineering) under Utkal University with first class (Hons.) and obtained Master of Technology in CAD/CAM from GIET, Gunpur under BPUT, Odisha. He is currently pursuing his Ph.D. in Robotics and Automation in CET, Bhubaneswar under BPUT, Odisha. He has more than 17 yrs. of teaching experiences in both Govt. and Private Institution of Odisha. He has significant no. of publications in National and International Journals and Conferences so far and also authored a book Hydraulics and Fluid Mechanics. Many students have been nominated excellence awards in various Universities and National label Project Exhibitions under his guidance. He has been awarded as best performer in WIPRO Mission 10X Faculty development programme. He is a life time member of Indian Society for Technical Education(ISTE) and Society of Failure Analysis (SFA).

Er. Shibabrata Mohapatra is working as Asst.Prof.in the Department of Mechanical Engineering, DRIEMS Autonomous, Cuttack. He has 8years of teaching experience. His area of interest includes Mechanical System Design, Composite Materials, Mechanical properties characterization etc. He has significant number of publications and attended many National and International conferences, seminars and webinars.. He is a life time member of Indian Society for Technical Education(ISTE) and International Association of Engineers (IAENG).

Er. Abinash Bibek Dash is an Assistant Professor in Mechanical Engineering Department in DRIEMS, Cuttack, Odisha. He has done his B.TECH (Mechanical Engineering) under BPUT with first class and obtained Master of Technology in Production Engineering from REC, Bhubaneswar under BPUT, Odisha. He has 8 years of teaching experiences. He has significant number of publications and attended many National and International conferences, seminars and webinars. He is a life time member of Indian Society for Technical Education (ISTE)

Pre-eminence of fuzzy logic controller on PI in alleviating the frequency deviation of a non-linear power system for different operating conditions

Anurekha Nayak [1], Nayan Ranjan Samal[2]

[1] Department of Electrical Engineering, Assistant Professor, DRIEMS Autonomous, Tangi, Cuttack, Odisha

[2] Department of Electrical Engineering, Professor, DRIEMS Autonomous, Tangi, Cuttack, Odisha *

anurekha2611@gmail.com, nayan15_samal@yahoo.co.in

ABSTRACT:

Any instantaneous change in the connected load of an electrical energy system, could interrupt the stable operation of the system. This leads to a discrepancy in operating values of system's frequency and interchange power through tie line. Load frequency control performs a significant role in restoring these deviation to their nominal values. In this paper, a two area thermal power system with GRC nonlinearity has been integrated to study the issues associated with LFC in a nonlinear power system. The power system with difference in saturation limits of GRC are contemplated for various loading conditions. The functioning of a fuzzy logic controller in reducing the frequency and tie line power deviations in the system model has been compared with the performance of a PI controller.

Keywords: *Two area nonlinear power system, Load Frequency Control (LFC), Generation rate constraint (GRC), proportional and integral controller, Fuzzy Logic Controller (FLC).*

1 INTRODUCTION

The continuous advancement of science, technology and changing lifestyles these days, have made the load utilisation more intense and severe. With an aim to satisfy the load requirement of the consumers, various neighbouring power system units are unified through tie-lines. Though, it makes the power system efficient, but multifaceted the systematic operation and control of it. As the power system exposed to discrepancy in load, the power system frequency and prescheduled tie-line power, deviate from their standard operating values, making the power system vulnerable [1]. To preserve consistency in power system operation, it is essential to retain the system frequency and tie line power error at zero. Hence, load frequency control was implemented as a regulatory control to offset the plants' generation with erratically varying load and to uphold the frequency with tie-line power variation at their pre-intended values [2, 3].

In last four decades, a lot of research emphasizing various challenges in LFC have been incorporated and significant contributions are being made. The power system stability and dynamics are greatly affected by the physical constraints of the power plant model. So the analysis of LFC includes both linear and non-linear model of generating units in the system.

In [4], Kothari et al. initially had investigated the implication of generation rate constraint in LFC analysis. E.Cheers in his paper considered a non-linear model of a thermal power plant highlighting the appropriate location of

generation rate constraint in it [5]. In [6], Wang et al. have contemplated a robust adaptive controller to analyse LFC issues associated with a reheat thermal generating unit comprising various physical constraints. But the robustness of the controller was not examined for a multi area system which left its superiority in doubt.

At the present time, a multisource multi area system need to be designed to meet with changing loads. Therefore, to meet with the purpose of employing LFC in a multi-source multi area power system, a number of approaches have also been recommended [7-10]. Furthermore, the issues associated with frequency control of a multi-source power system, combining various physical constraints were deeply analysed earlier [11-13]. A detailed study of load frequency control of generating units with GRC nonlinearity is incorporated in [14]. Moreover, the study includes a variation in saturation limits of GRC and various loading conditions. This motivated the authors to consider this multi area power system model incorporating GRC nonlinearity. It can be seen from the literature survey that, various algorithms and optimization techniques are used to optimize the conventional controller parameters for load frequency control in a power system with nonlinearity and the researchers have aimed to prove the primacy of their suggested techniques [15-18]. To deal with the limitations associated with various optimization techniques used for conventional controller, researchers were motivated to take on an intelligent and economical controller which can substitute the conventional controller [19-21]. As the parameter values of a conventional controller are fixed and cannot be changed with the dynamic response of a power system, an intelligent fuzzy logic controller is implied as the supplementary controller in this paper.

In view of the previous research carried out and to discern more about the issues associated with LFC of generating units with nonlinearity, a two area non-reheat thermal power with GRC is incorporated in this paper. Initially a relative analysis among PI and FLC in alleviating the frequency and scheduled tie line power discrepancy are presented. In addition to the variation in the saturation limit of GRC non linearity, system's dynamic performance is also examined under various step loading conditions. A detailed comparative analysis is done among PI and FLC.

2 SYSTEM MODEL DESCRIPTION

The transfer function representation of a two area thermal power unit is illustrated in fig. 1. Two identical thermal power plants are being unified through a tie line and each plant incorporates a speed governor, a non-reheat steam turbine with GRC non-linearity, and a rotating inertia along with a load to investigate the issues related to LFC.

In the transfer function model, ΔP_{Ref} is the incremental power output due to change in speed, ΔP_{Gov} is the output power of speed governor, ΔP_{mech} is the mechanical power output of turbine, ΔF is the difference in the area frequency, ΔP_d is the load change. The power equation of the speed governing system ΔP_G for an incremental increase in governor control can be furnished as

$$\Delta P_G(s) = \Delta P_{Ref}(s) - \left(\frac{1}{R}\right)\Delta F(s) \qquad (1)$$

where ΔP_G is the incremental change in governor control

ΔP_{Ref} is the incremental regulation in reference power adjustment

R is the factor of speed regulation and is calculated in Hz/per unit Megawatt

The value of R can be calculated for corresponding change in position of the valve setting. The hydraulic amplifier adapts the valve movement from low power to high power, to assist the opening and closing of steam or water valve inlet against high pressure steam or water and eventually control the mechanical power output of the turbine. The transfer function for a speed governing system of a non-reheat steam turbine with hydraulic amplifier can be given as

$$\Delta P_{Gov}(s) = \frac{1}{1+sT_g}\Delta P_G(s) \quad (2)$$

where T_g is the coefficient of time associated with governor.

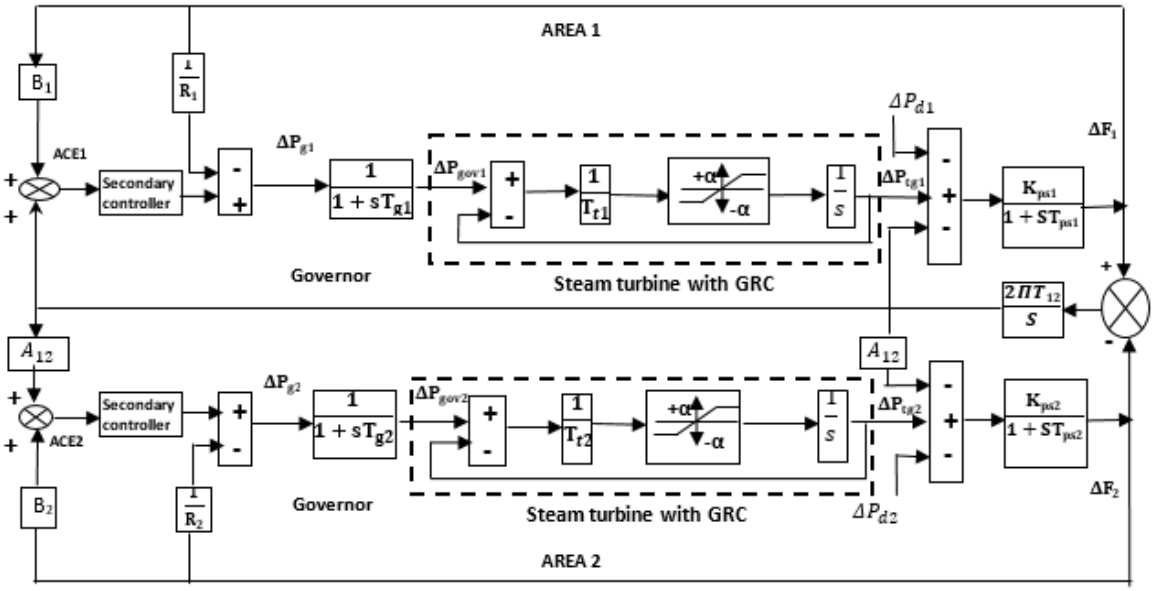

Fig.1 Two area non-reheat thermal power plant reflecting GRC non linearity

The electrical power developed in the synchronous generator changes accordingly with the difference in the mechanical power output of the turbine, to keep in with the power output of generator load model. The incremental turbine output power (ΔP_{Tg}) of the non-reheat steam turbine is represented by the equation

$$\Delta P_{Tg}(s) = \left(\frac{1}{1+sT_t}\right)\Delta P_{Gov}(s) \quad (3)$$

The performance of the turbine is governed by the turbine time constant T_t .

In a non-reheat thermal power, the rate of change of generated power in the steam turbine is relatively low. The generation rate is hence considered between 5 to 10 % p.u. MW per minute. The governor model includes GRC saturation limiters to restrict opening and closing of the control valve. Kothari et al. chose the value of GRC in a reheat thermal plant as 3% p. u. MW per minute [4]. But a detailed literature study on GRC shows that, most of them prefer limiter value between ± 3% to ± 10 % p. u. MW per minute for a realistic non reheat thermal plant [9, 10, 11, 15, 17]. So, in this paper, the limiter values of α, are chosen as 5% and 2.5% p.u. MW per minute to investigate the LFC problem. The misalliance between the generation and turbine power ensues change in turbine speed followed by the system frequency. This can be established as

$$G_{ps}(s) = \frac{K_{ps}}{1+sT_{ps}} \quad (4)$$

Each control area maintains its power flow with its neighboring area, by raising and lowering its generations according to the load changes in the electrical system. The incremental change in tie line power depends on load variation in the corresponding areas. This can be represented in equation as

$$\Delta P_{tie\ 12}(s) = \frac{2\pi T_{12}}{s}[\Delta F_1(s) - \Delta F_2(s)] \quad (5)$$

3 CONTROL ACTION

The stable operation of power system under different loading conditions, can be restored by adding up supplementary controller to the generating units. So a controller is employed to achieve the improved output response of the systems under consideration. The simple and robust design of a conventional PI controller influence its extensive use over other controllers in industries.

The PI control parameters which work effectively in a linear power system, may not be able to perform in a similar way for a power system with a degree of non-linearity. Hence it is utmost necessary for a system to implement an intelligent controller which could manage the dynamic response of the system to preserve its stability. Therefore, proposed system implicated a fuzzy logic controller as its supplementary control action.

4 FUZZY LOGIC CONTROLLER

In a fuzzy logic controller, the fuzzy rules and its membership functions can be outlined by extracting human experiences and behaviour. The membership functions can be designed in distinctive shapes with the designer's choice and preferences. This designed fuzzy logic controller with its linguistic control technique, makes an attempt to minimize the deviations in the system dynamic response. The operating states of a fuzzy logic controller explained as fig.2.

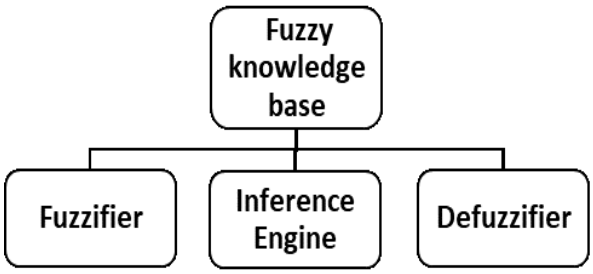

Fig.2. Block Diagram of FLC

In present work, the triangular membership function is exercised to define the linguistic variables. With the increasing number of fuzzy logic membership functions, the output response attains to be more

accurate. Based on this, 7 membership functions are deliberated for this work and they are utmost negative (UN), intermediate negative (IN), least negative (LN), zero (ZO), utmost positive (UP), intermediate positive (IP), least positive (LP), respectively. Mamdani inference system is used with the linguistic variables attained from expert's experience. The arrangement of fuzzy rules of the fuzzy inference system are displayed in table 1.

Table.1 fuzzy rule viewer

	d(ACE)						
ACE	**UN**	**IN**	**LN**	**ZO**	**LP**	**IP**	**UP**
UN	**UN**	**UN**	**UN**	**UN**	**IN**	**LN**	**ZO**
IN	**UN**	**UN**	**IN**	**IN**	**LN**	**ZO**	**LP**
LN	**UN**	**IN**	**IN**	**LN**	**ZO**	**LP**	**IP**
ZO	**IN**	**IN**	**LN**	**ZO**	**LP**	**IP**	**UP**
LP	**IN**	**LN**	**ZO**	**LP**	**IP**	**IP**	**UP**
IP	**LN**	**ZO**	**LP**	**IP**	**IP**	**UP**	**UP**
UP	**ZO**	**LP**	**IP**	**UP**	**UP**	**UP**	**UP**

5 COMPARATIVE ANLYSIS OF SIMULATION RESULTS

The MATLAB/SIMULINK environment is used to develop the proposed non reheat model of the thermal power plants [9, 15, and 17] and the FLC and PI controller are applied to evidence the optimum effectiveness of a fuzzy logic controller. To organize a detailed relative analysis, the system under study has been investigated in view of variation in saturation limits of GRC and system parameter values at once. For more insight of LFC issues, different loading conditions are included in the analysis.

Hence different possible combinations of operating conditions are summarized as case I to IV.

Case I: GRC saturation limit = ±0.05 and step load increase in area-1 =5%

The control area-1 with an inclusion of GRC considering $\alpha = \pm 0.05$ is applied with a 5% step increase in the prescheduled load demand at time t=0.

A relative comparison of the dynamic responses established for differences in frequency ΔF_1 and ΔF_2 and change in exchange power through tie line (ΔP_{tie}) for PI and FLC are shown in fig.3. The damping oscillations and response settling time are effectively reduced with fuzzy logic controller.

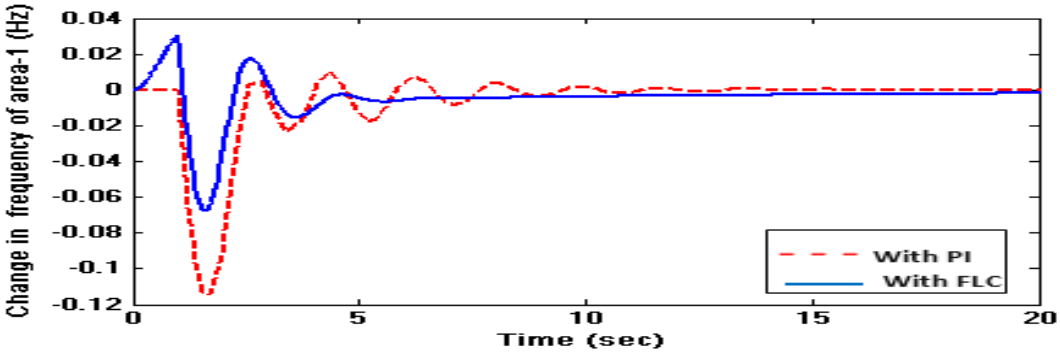

(a)

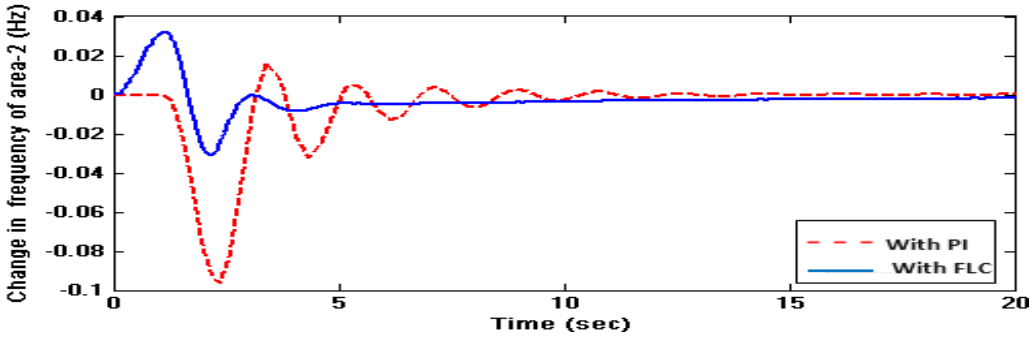

(b)

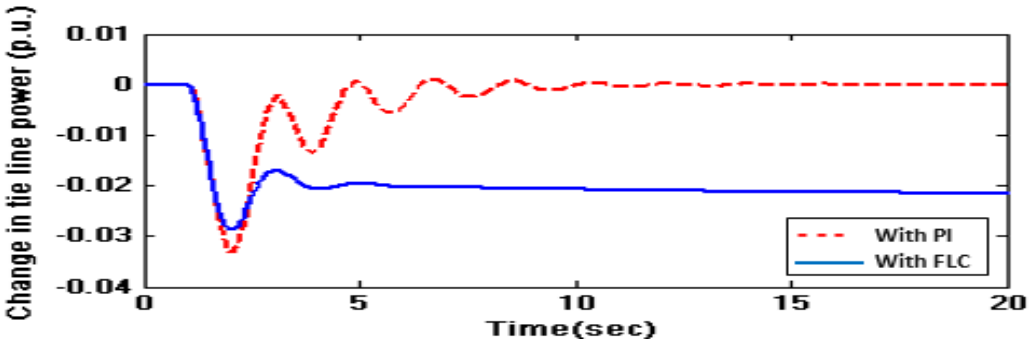

(c)

Fig.3. Dynamic responses of two area power generating unit including GRC having α = ±0.05 and a 5% step load increase at area-1(a)Change in frequency of control area -1(ΔF_1) (b) Change in frequency of control area -2(ΔF_2) (c) Change in tie line power (ΔP_{tie})

Case II: GRC saturation limit = ±0.05, a simultaneous step increase in load (area-1 = 5% and area-2 = 2%)

At time t=0, an instantaneous step increase of 5% in load demand for the area-1 and 2% in load demand of area-2 with a GRC saturation limit of α = ±0.05 are applied in the system. The differences found in frequency and interchange tie line power are shown in fig.4. It can be noticed that the settling time and undershoots obtained with PI are effectively reduced with FLC. Hence FLC outperforms PI in steadying the dynamic response.

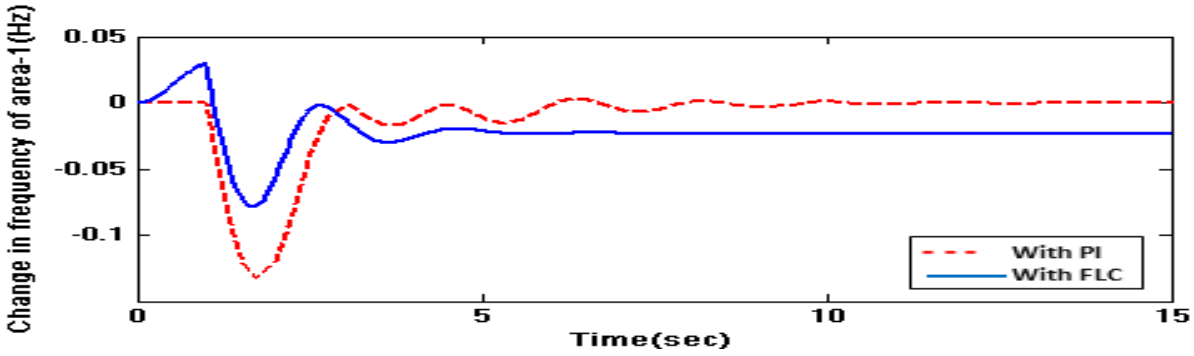

(a)

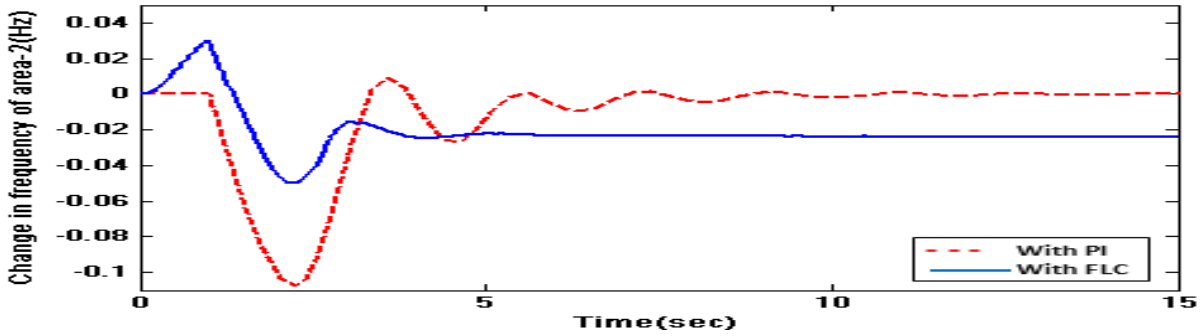

(b)

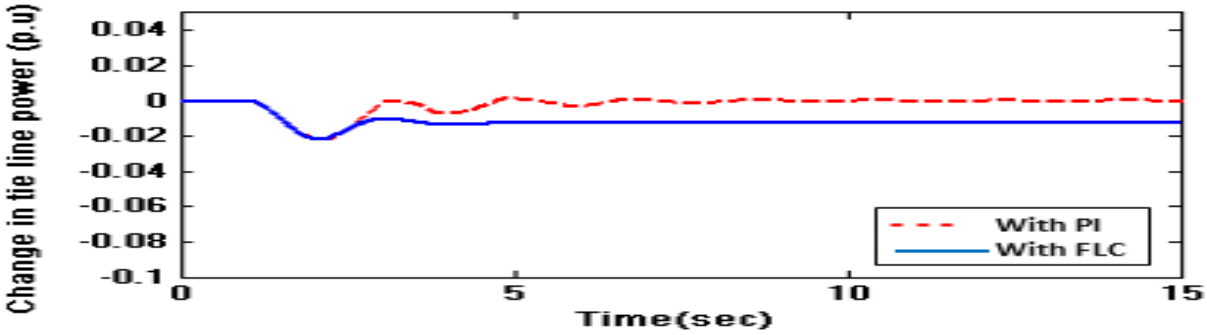

(c)

Fig.4. Dynamic responses of two area power generating unit including GRC having α = ±0.05 and a 5% step load increase at area-1 and 2% increase in load at area-2 simultaneously

(a)Change in frequency of control area -1(ΔF_1) (b) Change in frequency of control area -2(ΔF_2) (c) Change in tie line power (ΔP_{tie})

Case III: GRC saturation limit = ±0.025 and step load increase in area-1 = 5%

In this case, the proposed system model is investigated with a variation in the saturation limit of GRC. The proposed nonlinear power system with a variation in GRC saturation limit α = ±0.025 and 5% step increase in prescheduled load at area-1 is examined at time t=0.The frequency deviations in area-1and area-2 and exchange of power through tie line are exhibited in fig.5. The response with PI controller characterized the impact of a different limiter value.

Hence, the response with PI controller became more oscillatory and required a larger settling time. However, with FLC, the damped oscillations are significantly alleviated and the system attains stability faster than PI controller.

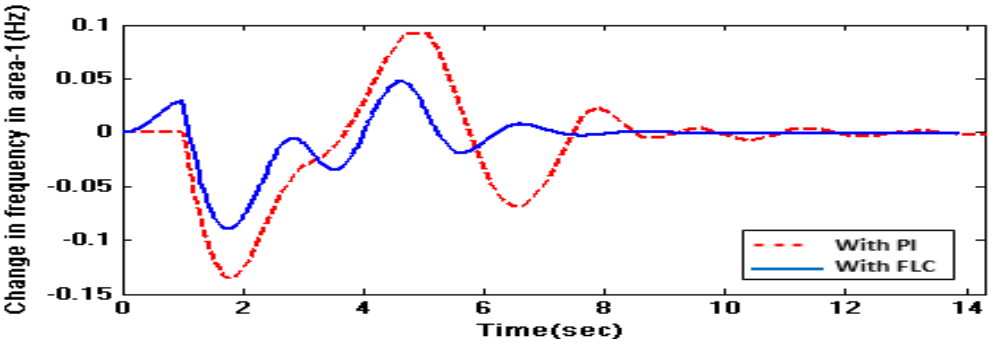

(a)

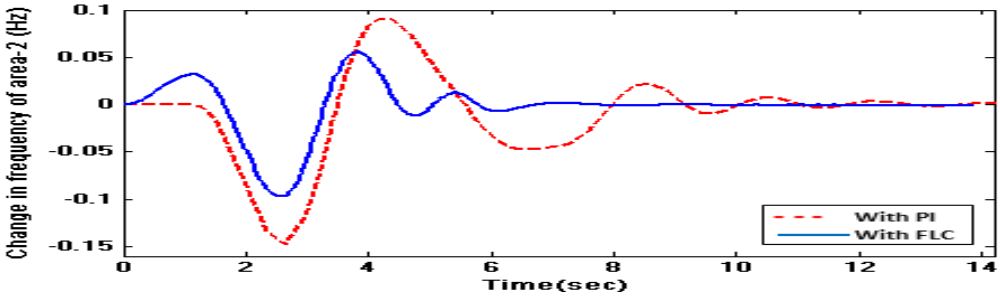

(b)

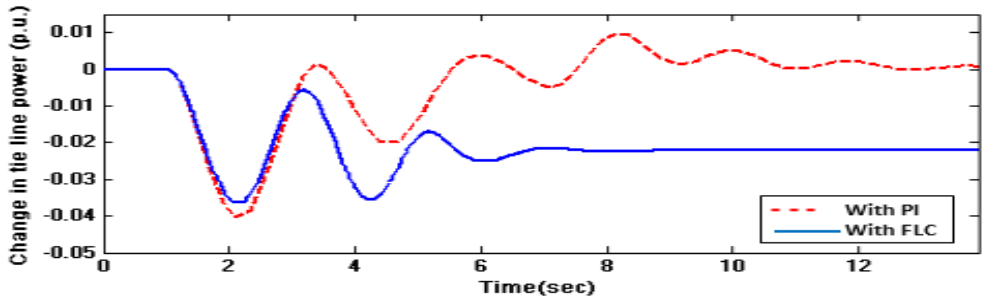

(c)

Fig.5. Dynamic responses of two area power generating unit including GRC having α = ±0.025 and a 5% step load increase at area-(a)Change in frequency of control area -1(ΔF_1) (b) Change in frequency of control area -2(ΔF_2) (c) Change in tie line power (ΔP_{tie})

Case IV: GRC saturation limit = ±0.025, a simultaneous step increase in load (area-1 = 5% and area-2=2%)

In this case, the saturation limit of GRC is considered as α = ±0.025. In addition to this, an instantaneous step load increase of 5% in prescheduled load demand of area-1 and 2% at area-2 at t=0sec are examined for the system model. The system dynamic response for above operating conditions are exhibited in fig.6. It can be analysed from the figures that, FLC outperforms PI in diminishing the unsteadiness and settling time of the system dynamic responses.

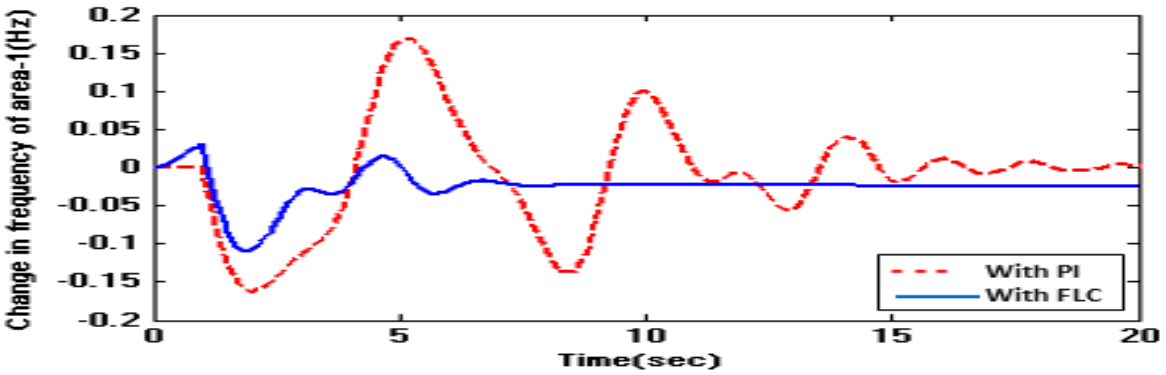

(a)

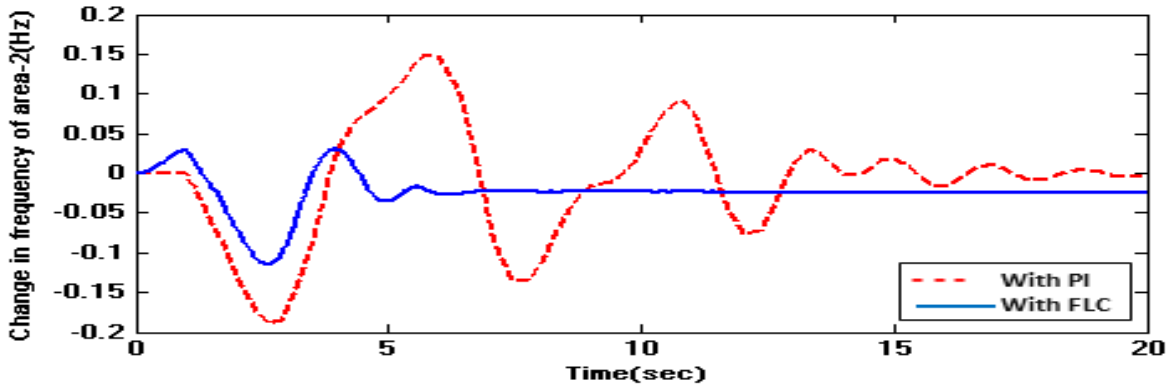

(b)

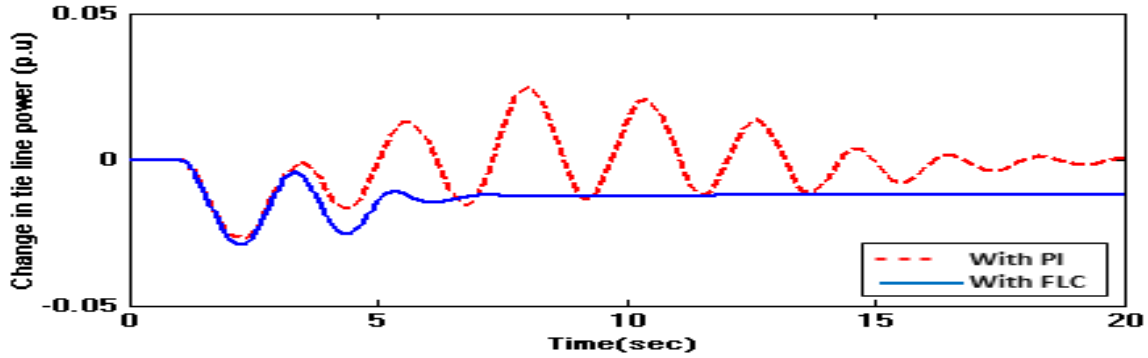

(c)

Fig.6. Dynamic responses of two area power generating unit including GRC having α = ±0.025 and a 5% step load increase at area-1 and 2% increase in load at area-2 simultaneously. (a)Change in frequency of control area -1(ΔF_1) (b) Change in frequency of control area -2(ΔF_2) (c) Change in tie line power (ΔP_{tie})

To represent a comprehensible assessment of the proposed controller's efficacy, the derived results of all the above four cases have been summarised in table 2. The comparison of the results clearly illustrates the effectiveness of FLC upon PI in reducing undershoots and settling times of the system's dynamic responses. A graphical representation of these results has been furnished in fig.7

Table.2 Comparative analysis of dynamic responses for proposed conditions of the system with PI and FLC

	Case-I (α = ± 0.05, 5% SLP at area-1)				Case-II (α = ± 0.05, 5% SLP at area-1, 2% SLP at area-2)				Case-III (α = ± 0.025,5% SLP at area-1)				Case-IV (α = ± 0.025, 5% SLP at area-1, 2% SLP at area-2)			
	Undershoot		T_s		Undershoot		T_s		Undershoot		T_s		Undershoot		T_s	
	PI	FLC	PI	FLC	PI	FLC	PI	FLC	PI	FLC	PI	FLC	PI	FLC	PI	FLC
ΔF_1	0.11	0.067	13.8	5.73	0.13	0.08	9.71	4.9	0.13	0.09	13.3	6.92	0.16	0.11	20.1	6.2
ΔF_2	0.09	0.031	13.2	5.12	0.11	0.05	10.2	4.8	0.14	0.09	14.8	7.09	0.19	0.10	20.7	5.82
ΔP_{tie}	0.03	0.028	14.1	5.8	0.01	0.01	7.9	3.8	0.04	0.03	14.8	6.7	0.02	0.02	22.3	6.1

Comparative analysis of settling time T_s (sec)

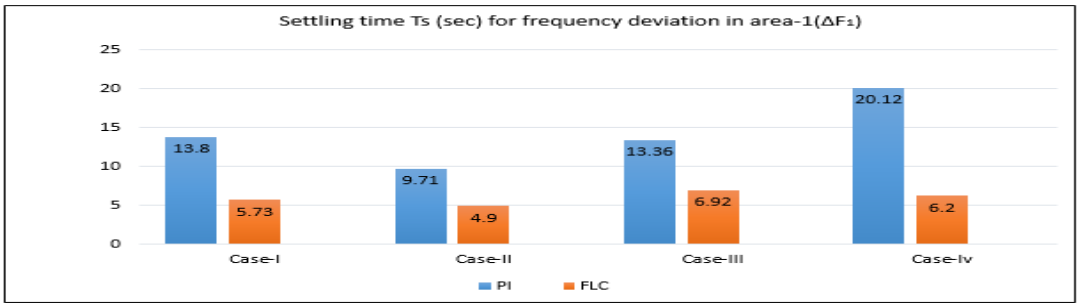

(a)

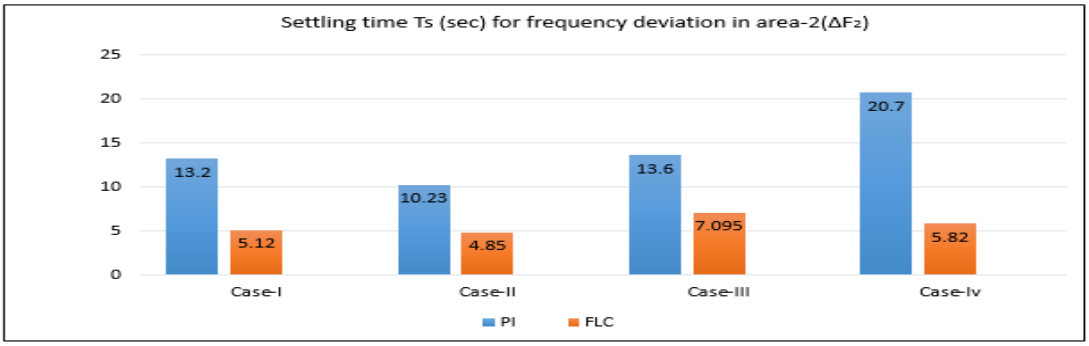

(b)

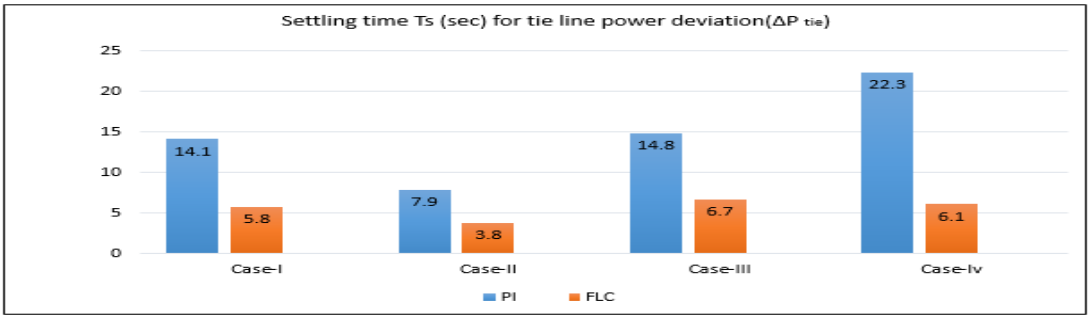

(c)

Fig.7.Bar graph comparison of settling time for ΔF_1, ΔF_2 and ΔP_{tie} for case I to case-IV

CONCLUSION

Since the frequency control models and data are mostly non-linear and exposed to various sources of error, to find a solution is bit difficult task in power system operation. So the issues and challenges associated with LFC in restoring the differences found in area frequency and scheduled tie line power are investigated with various realistic conditions. A two area nonlinear thermal power plant with a variation in scheduled load demand of the control areas are kept under investigation. The irregularities emerged in the dynamic responses of frequency and interchange tie line power for variation in saturation limits of GRC are examined. The ascendancy of fuzzy logic controller upon PI in alleviating the frequency and tie line power variation of the nonlinear system for different system conditions are verified. The detailed analysis of simulation results witnessed the superiority of fuzzy logic controller on PI controller. Hence, this paper proved the robustness of its proposed fuzzy logic controller over other controllers as incorporated in literature, while considering different possible combinations of operating conditions.

REFERENCES

1. *P.Kundur, Power System Stability and Control, 1st ed.,Tata McGraw-Hill, 1994, pp.601-617.*
2. *H. Bevrani, Robust Power System Frequency Control, New York: Springer-Switzerland, 2014, ch. 2.*
3. *O.I. Elgerd, C.E. Fosha, "Optimal megawatt frequency control of multi area electric energy system", IEEE Transaction, Vol. 89, No.4, pp.556-563, April 1970.*
4. *Kothari, M., Satsangi, P., Nanda, J. "Sampled-data automatic generation control of interconnected reheat thermal systems considering generation rate constraints", IEEE Trans. Power Apparatus System, 1981, PAS-100, pp. 2334–2342.*
5. *E. Cheres, "The Application of Generation Rate Constraint in the Modelling of a Thermal Power System", Taylor & Francis, Electric Power Components and Systems, 2001, 29:83–87.*
6. *Wang Y, Zhou R, Wen C, "New robust adaptive load frequency control with system parameter uncertainties, IEEE proceedings-Generation Transmission and Distribution 1994; 141(3).*
7. *K.Parmar, S. Majhi and D. P. Kothari, "Load Frequency Control of A Realistic Power System With Multi-Source Power Generation", International Journal of Electrical Power and Energy Systems, 2012, Vol. 42, No. 1, pp. 426-433.*
8. *B. Mohanty, P. Hota, "Load Frequency Control of Nonlinear Interconnected Hydro-Thermal System Using Differential Evolution Technique", International Journal of Electrical and Computer Engineering, 2014, Vol:8, No:2, pp.453-460.*
9. *E.S.Ali,S.M.Abd-Elazim, "BFOA based design of PID controller for two area Load Fre nquency Control with nonlinearities", International Journal of Electrical Power and Energy Systems, 2013, Vol. 51, No. 1, pp. 224-231.*
10. *K.Jagatheesan ,B.Anand, "Load frequency control of an interconnected three area reheat thermal power systems considering non linearity and boiler dynamics with conventional controller", Advances in Natural and Applied Sciences, 8(20) , 2014, pp. 16-24 .*
11. *W.Tan , S.Chang, R. Zhou, "Load frequency control of power systems with non-linearities", IET Generation, Transmission & Distribution, 2017, Vol. 11 Iss. 17, pp. 4307-4313.*
12. *R.K.Sahu,S.Panda,S.Pradhan, "Optimal gravitational search algorithm for automatic generation control of interconnected power system", Elsevier Ain Shams Engineering Journal ,2014.*
13. *M. Elsisi, M. Soliman, M. A. S. Aboelela, W. Mansour, "GSA-Based Design of Dual Proportional Integral Load Frequency Controllers for Nonlinear Hydrothermal Power System", World Academy of Science, Engineering and Technology Vol:9 2015-08-01,pp.1142-1148.*

14. *R.K.Sahu,S.Panda,S.Pradhan, "A hybrid firefly algorithm and pattern search technique for automatic generation control of multi area power system" International Journal of Electrical Power and Energy Systems, 2015, Vol. 64, pp. 9-23.*
15. *J. Morsali, K. Zare, M.T.Ragh, "Appropriate Generation Rate Constraint (GRC) Modelling Method for Reheat Thermal Units to Obtain Optimal Load Frequency Controller (LFC)"IEEE Conference on Thermal Power Plant,2014, pp.29-34.*
16. *B.Mohanty, S.panda,P.K.Hota, "Differential evolution algorithm based automatic generation control for power systems with non-linearity" Elsevier Alexandria Engineering Journal,2014, Vol.53,pp.537-552.*
17. *R.K.Sahu,T.S.Gorripotu,S.Panda,"Automatic generation control of multi-area power systems with diverse energy sources using teaching Learning Based Optimization Algorithm" Engineering Science and Technology, an International Journal 19(2016)113-134.*
18. *T.S.Tsay, " Load frequency control of interconnected power system with governor backlash non-lineraities",Electrical Power and Energy System,2011,Vol 33,pp.1542-1549.*
19. *A. Annamraju, S. Nandiraju , "Robust frequency control in a renewable penetrated power system: an adaptive fractional order-fuzzy approach", Protection and Control of Modern Power Systems (2019) 4:16.*
20. *R.K.Sahu, S.Panda,U.K.Rout, "DE optimized parallel 2-DOF PID controller for load frequency control of power system with governor dead-band non linearity," International Journal of Electrical Power and Energy Systems, 2013, Vol. 49, pp. 19-33.*
21. *G. Panda, S. Panda and C. Ardil , "Automatic Generation Control of Interconnected Power System with Generation Rate Constraints by Hybrid Neuro Fuzzy Approach", International Journal of Electrical, Computer, Energetic, Electronic and Communication Engineering, 2012, Vol:6, No:4,pp.31-36.*
22. *K. R. M. V. Chandrakala, S. Balamurugan and K. Sankaranarayanan, "Variable structure fuzzy gain scheduling based load frequency controller for multi source multi area hydro thermal system", Electrical Power and Energy Systems, Vol.53, 2013, pp. 375–381.*

BIOGRAPHICAL NOTES

Anurekha Nayak, is currently serving as Assistant Professor in Department of Electrical Engineering, DRIEMS (Autonomous), Cuttack, Odisha, India. She did her B.Tech. from Utkal University, Odisha, M.Tech in Power System from BPUT, Odisha. She has 15+ years of teaching and research experience, and guided many M.Tech students. She has published several papers in international and national journal and attained several national and international conferences. Her areas of interests are frequency control in power system, Energy management system.

Dr. N.R.Samal is currently serving as Professor in the Department of Electrical Engineering, DRIEMS (Autonomous), Cuttack, Odisha, India. He received his Ph.D in Control System Engineering from Jadavpur University, Kolkata, M. Tech in power system from VSSUT Burla, Odisha and bachelor degree from Utkal University, Odisha. He has 21+ years of teaching and research experience, and guided many M.Tech and PhD Students. He published several papers in international and national journal and attained several national and international conferences. His areas of research interest are soft computing, optimization techniques.

Constraining nuclear matter parameters and neutron star observables using PREX-2 and NICER data

[1]S. K. Biswal, [2,3] H. C. Das, [2,3]Ankit Kumar, [2,3]S. K. Patra

[1]Department of Engineering Physics, DRIEMS Autonomous Engineering College, 754022, India

[2]Institute of Physics, Sachivalaya Marg, Bhubaneswar 751005, India and

[3]Homi Bhabha National Institute, Training School Complex, Anushakti Nagar, Mumbai 400094, India

ABSTRACT

We try to constraints some of the nuclear matter parameters such as symmetry energy (J) and its slope (L) from the recent inferred data of the PREX-2. Other nuclear matter parameters are adopted from ***[Phys. Rev. C 85 035201 (2012), Phys. Rev. C 90 055203 (2014)]*** *papers and the linear correlation among them are checked by using Pearson's formula. We find the correlation between $J - L$, $K_\tau - J$ and $K_\tau - L$ with coefficients 0.85, 0.81 and 0.76 respectively. The neutron star properties such as mass and radius are calculated with 50 unified equations of states. The results are consistent with recently observed pulsars and NICER data except few exceptions. From the radii constraints, we find that the new NICER data allows a narrow radius range contrary to a large range of PREX-2 and the old NICER data leaving us an inconclusive determination of the neutron star radius.*

Keywords: *Neutron star, Relativistic Mean Field formalism, Symmetry energy*

1 INTRODUCTION

The neutron star (NS), a highly dense and asymmetric nuclear system having a central density 5–6 times the nuclear saturation density [1]. It has a unique internal structure, where all the four fundamental forces play an essential role. Study of the NS reveals that the internal structure is more complicated because new degrees of freedom like hyperons [2–9] and quarks are in the core [10–12]. To explore its properties, such as mass, radius and tidal deformability, etc., one has to consider the interaction between nucleons in the form of interaction Lagrangian. This provides the equation of state (EOS), the main ingredient for the calculation of the NS properties.

Different formalisms have been developed to calculate the EOSs of the NS. The relativistic mean-field (RMF) [13–19], Skyrme-Hartree-Fock (SHF) [20–27], density-dependent RMF (DD-RMF) [28], and point couplings [29] formalism are quite successful. First, we focus on the nuclear matter (NM) system, where the Coulomb and surface interactions are neglected. The binding energy per particle of the NM system is ≈ -16 MeV at the saturation density $\rho_0 \sim 0.148\ fm^{-3}$ [30]. The characteristics EOS of the NM is calculated by using different force interactions [26]. There are few empirical/experimental data to constraint the NM EOSs as given in Refs. [19, 31]. Different NM quantities such as incompressibility, symmetry energy and its slope parameter etc. play important

roles in exploring the NS properties [26,32–37]. In this study, our motivation is to constraint these NM parameters using recent experimental data [38–40].

Recently, the updated Lead Radius Experiment (PREX) has given the neutron skin thickness of ^{208}Pb as $R_{skin} = 0.283 \pm 0.071$fm [38]. Based on this data Patnaik $etal.$ [41] tuned the G3 and IOPB-I parameter sets. The impacts of PREX-2 data on the NM and NS properties have been explicitly studied in the Ref. [39]. The inferred values of NM quantities such as symmetry energy (J), its slope parameter (L) are 38.1 ± 4.7 MeV and 106 ± 37 MeV, respectively. The inferred limits are systematically larger as compared with either theoretical or experimental values [35,42–52]. Reed $etal.$ has also been calculated the NS properties by combining old NICER and PREX-2 constraints. The predicted radius range is $13.25 < R_{1.4} < 14.26$ km. Recently, NICER also put a revised limit, which is inferred by combining the old NICER data, ~ $2M_{\odot}$ pulsars, and the tidal deformability constraints form GWs data, and different EOSs modelling. The new NICER radius range for the canonical star is 12.45 ± 0.65 km. In this study, we want to constraint the radius of the canonical NS using both NICER and Reed et.al. data.

The paper is organized as follows: The formalism for the calculation of different NM quantities is given in Sec. II. The results and discussions on the NM and NS properties are provided in Sec. III. A summary of our work is enumerated in the Sec. IV.

2 FORMALISM

The energy density $E(\rho, \alpha)$ of the NM system can be expanded in a Taylor series in terms of asymmetry factor $\alpha\left(=\frac{\rho_n - \rho_p}{\rho_n + \rho_p}\right)$ [19, 47]:

$$E(\rho, \alpha) = E(\rho) + S(\rho)\xi^2 + O(\xi^4), \quad (1)$$

where ρ, ρ_n and ρ_p are the total baryon, neutron, and proton densities, respectively, The $E(\rho)$ is the energy density of the symmetric NM. The density dependence symmetry energy $S(\rho)$ can be written as

$$S(\rho) = \frac{1}{2}\left(\frac{\partial^2 E}{\partial \alpha^2}\right)_{\alpha=0}. \quad (2)$$

The value of $S(\rho)$ is the most uncertain property of the NM, and it has a large diversion at a high-density limit [53]. Many progresses have been made to constrain the $S(\rho)$ starting from heavy-ion collision to NS [31, 54]. Here, we can expand the $S(\rho)$ in a leptodermous expansion near the saturation density as follow [19, 55–58]:

$$S(\rho) = J + L\xi + \frac{1}{2}K_{sym}\xi^2 + \frac{1}{6}Q_{sym}\xi^3 + O(\xi^4), \quad (3)$$

where $\xi = \frac{\rho - \rho_0}{3\rho_0}$, J is the symmetry energy at saturation density ρ_0 and the other parameters like slope (L), curvature (K_{sym}) and skewness (Q_{sym}) are given as follow:

$$L = 3\rho \frac{\partial S(\rho)}{\partial \rho}|_{\rho=\rho_0}, \quad (4)$$

$$K_{sym} = 9\rho^2 \frac{\partial^2 S(\rho)}{\partial \rho^2}|_{\rho=\rho_0}, \quad (5)$$

$$Q_{sym} = 27\rho^3 \frac{\partial^3 S(\rho)}{\partial \rho^3}|_{\rho=\rho_0}. \quad (6)$$

Similarly, one can expand the asymmetric NM incompressibility $K(\alpha)$ as

$$K(\alpha) = K + K_\tau \alpha^2 + O(\alpha^4), \quad (7)$$

where K is the incompressibility of the NM at the saturation density and

$$K_\tau = K_{sym.} - 6L - \frac{Q_0 L}{K}, \quad (8)$$

with $Q_0 = 27\rho^3 \frac{\partial^3 E}{\partial \rho^3}$ in symmetric NM at saturation density. We use another quantity $K' = -Q_0$.

3 RESULTS AND DISCUSSIONS

3.1. *Nuclear Matter Properties*

In this section, we constrain the values of J and . Moreover, with the addition of NM properties, we also want to constraint the mass and radius of the NS with the help of recent NICER data. To calculate NM properties, we take 224 RMF, 240 SHF, 7 DD-RMF, 18 PC parameter sets from the Dutra $etal.$ [26, 29], which span a large parameter space. For the calculation of NS properties, we take 50 well-known EOSs from the Refs. [59, 60].

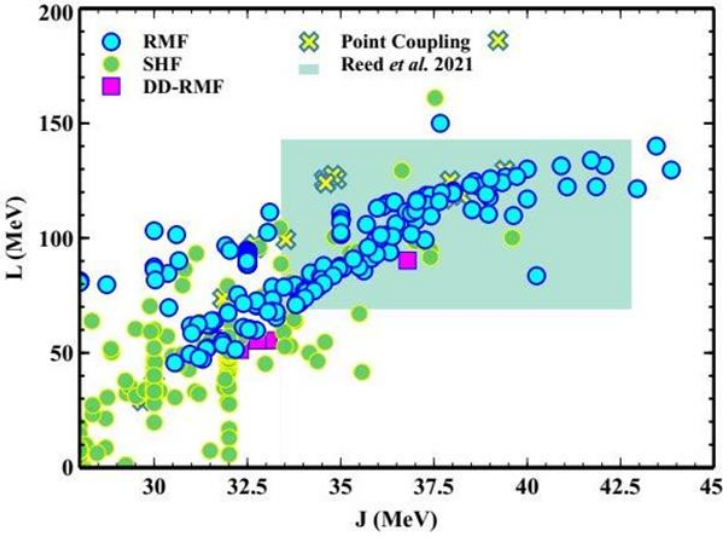

Figure 1: The value of slope parameters for 224 RMF, 240 SHF, 7 DD-RMF and 18 PC parameter sets are shown. The light green box represents the values of MeV and MeV taken from the Ref. [39].

In Fig. 1, we plot the symmetry energy (J) as a function of the slope parameter (L) for the considered parameter sets. Recently, the PREX-2 experiments put a limit on the skin thickness of ^{208}Pb is $R_{skin} = 0.283 \pm$

0.071 fm [38]. There is strong correlation have been observed between $R_{skin}$and Lat saturation density [39, 61]. Reed $etal.$[39] inferred the values of J and L as 38.1 ± 4.7MeV and 106 ± 37 MeV respectively. We put a light green box in Fig. 1 to constraint the values of J and L. Most of the RMF and PC parameter sets satisfy the constraints well as compare to SHF and DDRMF parameter sets. Hence, we conclude that the parameter sets which predict higher values of J and L are consistent with Reed $etal.$ data.

To check the correlation between different NM parameters as calculated in Sub-Sec. II, we plot the correlation matrix as shown in Fig. 2. To check the linear correlation between pairs of quantities, we calculate the correlation coefficient using Pearson's formula as used in Ref. [60]. We find that the correlation coefficient between J and L is found to be 0.85. Slightly weaker correlations are found between $K_\tau - Jand\ K_\tau - L$ with coefficients 0.81 and 0.76, respectively.

3.2. *Neutron Star Properties*

The NS is composed of neutrons, protons, and leptons. Inside the NS, the neutron decays to proton, electron, and antineutrino. This process is called β-decay. Both

βequilibrium and charge neutrality processes are required for the stability of the NS [30]. Therefore, the total EOS of the NS is the addition of baryons and leptons as given as [19, 62]

$$E_{NS} = E + E_l, P_{NS} = P + P_l, \tag{9}$$

where $E(E_l)$ is the energy density of the NM (leptons) as given in Refs. [62–64]. The l correspond to both electron (e^-) and muon (μ^-).

In Fig. 3, we plot 50 selected unified EOS taken from the Refs. [59,60] for comparison. The mass and radius of the NS are calculated by solving Tolman-Oppenheimer-Volkoff equations [65, 66] with boundary conditions $P(0) = P_c$ and $P(R) = 0$ for a fixed central density. Each EOS gives a different maximum mass and radius. We calculate the mass-radius ($M - R$) profile of the NS for considered EOSs as shown in Fig. 4 . The massive pulsars data such as PSR J1614-2230 [67], PSR JO348+0432 [68] and PSR J0740+6620 [69] are shown with different colour bars. Recently, the secondary component of the GW190814 event is observed in the mass range $2.50 - 2.67M_\odot$. A lot of debates are in progress, whether the secondary component is the lightest black hole or heaviest NS [70, 71]. The old NICER data depicted with two violet boxes from two different analyses [72, 73]. New NICER data [40] is shown with a double-headed dark red line. Recently, Reed $et\ al.$ [39] have given radius constraints for canonical stars inferred from the PREX-2, and old NICER data is also shown with double-headed black line. From the Fig. 4, it is clear that all EOSs reproduces $\sim 2M_\odot$ except for a few RMF EOSs. None of the EOSs reproduce the GW190814 data. Almost all EOSs satisfy old NICER data, as clearly visible in the figure. The old NICER radius range is 11.52–14.26 km which provides a wider limit. But the new NICER radius range is 11.8–13.1 km, which is a narrow band compared to old NICER data. Reed $etal.$ radius range is 13.25–14.26 km which satisfy by some RMF and few SHF EOSs. If one carefully observes three radius limits, there is a large uncertainty to constraint the radius of the NS. Future observation may put a tight constraint on the radius of the NS.

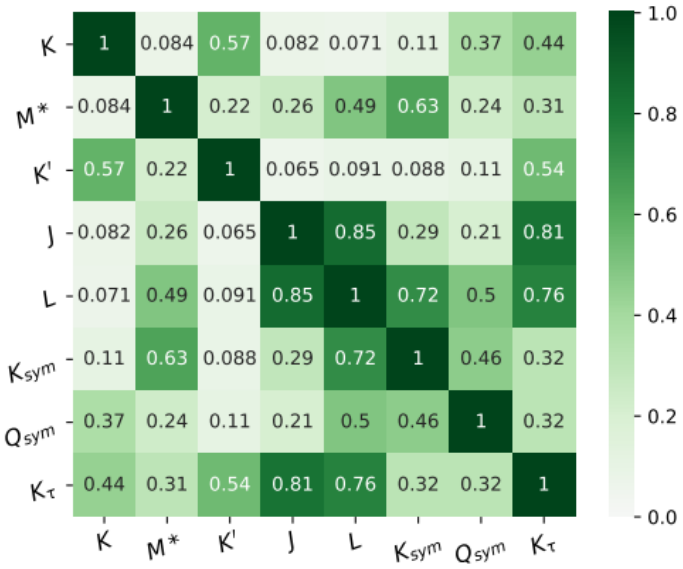

Figure 2: Correlations matrix represent the correlation between different NM parameters. The number inside the box represents the correlation coefficient between corresponding parameters.

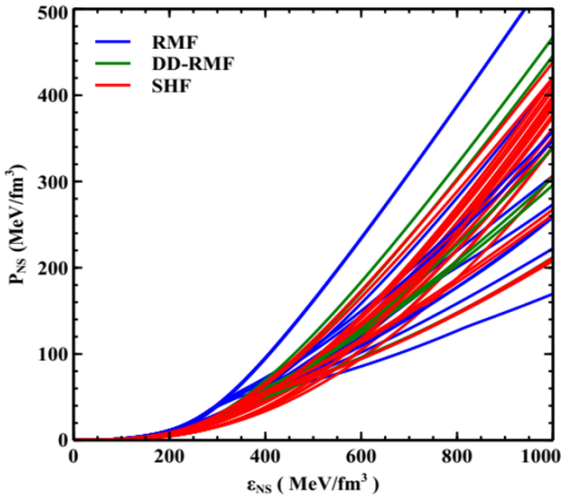

Figure 3: EOSs are shown for RMF, SHF and DD-RMF sets with blue, red and green lines respectively

4 SUMMARY

In this manuscript, we calculate the NM properties with different formalisms such as RMF, SHF, DD-RMF, and PC. The symmetry energy and its slope are constrained by the recently inferred data from the PREX-2 experiment. We find that a numbers of RMF parameter sets, almost all PC parameter sets, and few SHF and DDRMF parameter sets satisfy the constraints given by Reed $etal.$ data. We also obtain the correlations between $-L$, $K_\tau - J$ and $K_\tau - L$ with correlation coefficients 0.85, 0.81 and 0.76 respectively.

For the NS case, we take 50 unified EOSs and calculate the mass and radius. Almost all EOSs satisfy $2M_\odot$ constraints. None of the considered parameter sets satisfy the GW190814 data. The old NICER radius range is reproduced by almost all considered EOSs as it spans over a broader radius region. But the new NICER data can reproduced by almost all SHF and DD-RMF with few of the RMF sets. From the PREX-2 and old NICER data,

Reed $etal.$ inferred the radius of the canonical star, which is shown with a double-headed black line. Only stiff EOSs satisfy the Reed $etal.$ data because the radius range is a little bit higher as compare to new NICER data.

In conclusion, the PREX-2 data supports the EOSs, which are stiffer. Therefore, all the NM and NS properties inferred from PREX-2 data provide large value symmetry energy coefficient as compare to other theoretical/experimental data. In the case of the NS, the implied radius range is also push towards a higher value, which can only be supported by stiffer EOSs. But new NICER data provides the radius range, which supports by the softer EOSs. Therefore, a possible uncertainty has been developed to constraints the radius of the NS. We hope future experiments/observations may answer this question.

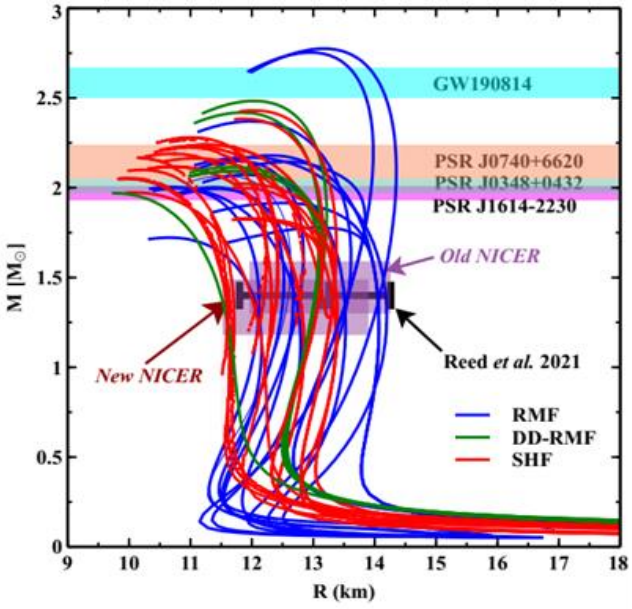

Figure 4: $M - R$ are shown for RMF, SHF and DD-RMF sets with different observational constraints. Both old NICER data shown with two violet boxes [72, 73] and new NICER data with dark red doubled head lines are also depicted [40] for canonical star. Recently radius constraint given by Reed *et al.* [39] is also shown with black headed line.

REFERENCES

1. *J. M. Lattimer and M. Prakash, Science **304**, 536 (2004).*
2. *V. A. Ambartsumyan and G. S. Saakyan, sovast **4**, 187 (1960).*
3. *N. K. Glendenning, APJ **293**, 470 (1985).*
4. *J. Schaffner and I. N. Mishustin, Phys. Rev. C **53**, 1416 (1996).*
5. *S. K. Biswal, B. Kumar, and S. K. Patra, (2016), **arXiv:1602.08888** [nucl-th].*
6. *M. Fortin, S. S. Avancini, C. Providˆencia, and I. Vidaˆna, Phys. Rev. C **95**, 065803 (2017).*
7. *M. Bhuyan, B. V. Carlson, S. K. Patra, and S.-G. Zhou, IJMP E **26**, 1750052 (2017).*
8. *S. K. Biswal, AIP Conf. Proceedings **2127**, 020031 (2019).*
9. *S. K. Biswal, S. K. Patra, and S.-G. Zhou, APJ **885**, 25 (2019).*
10. *J. C. Collins and M. J. Perry, Phys. Rev. Lett. **34**, 1353 (1975).*
11. *M. Orsaria, H. Rodrigues, F. Weber, and G. A. Contrera, Phys. Rev. C **89**, 015806 (2014).*
12. *R. Mellinger, F. Weber, W. Spinella, G. Contrera, and M. Orsaria, Universe **3**, 5 (2017).*
13. *L. D. Miller and A. E. S. Green, Phys. Rev. C **5**, 241 (1972).*
14. *B. D. Serot and J. D. Walecka, Adv. Nucl. Phys. **16**, 1 (1986).*
15. *R. J. Furnstahl, C. E. Price, and G. E. Walker, Phys. Rev. C **36**, 2590 (1987).*

16. *P. G. Reinhard, Z. Phys. A Atomic Nuclei **329**, 257 (1988).*
17. *R. J. Furnstahl, B. D. Serot, and H.-B. Tang, Nucl. Phys. A **615**, 441 (1997).*
18. *B. Kumar, S. Singh, B. Agrawal, and S. Patra, Nuclear Physics A **966**, 197 (2017).*
19. *B. Kumar, S. K. Patra, and B. K. Agrawal, Phys. Rev. C **97**, 045806 (2018).*
20. *T. H. R. Skyrme, The Philosophical Magazine: A Journal of Theoretical Experimental and Applied Physics **1**, 1043 (1956).*
21. *T. Skyrme, Nuclear Physics **9**, 615 (1958).*
22. *D. Vautherin and D. M. Brink, Phys. Rev. C **5**, 626 (1972).*
23. *E. Chabanat, P. Bonche, P. Haensel, J. Meyer, and R. Schaeffer", Nucl. Phys. A **635**, 231 (1998).*
24. *B. Alex Brown, Phys. Rev. C **58**, 220 (1998).*
25. *J. Stone and P.-G. Reinhard, Progress in Particle and Nuclear Physics **58**, 587–657 (2007).*
26. *M. Dutra, O. Lourenc¸o, J. S. S´a Martins, et al., Phys. Rev. C **85**, 035201 (2012).*
27. *J. Decharg´e and D. Gogny, Phys. Rev. C **21**, 1568 (1980).*
28. *S. Typel, Phys. Rev. C **71**, 064301 (2005).*
29. *M. Dutra, O. Lourenc¸o, S. S. Avancini, et al., Phys. Rev. C **90**, 055203 (2014).*
30. *N. K. Glendenning, Compact stars: Nuclear physics, particle physics, and general relativity (Springer-Verlag New York, 1997).*
31. *P. Danielewicz, R. Lacey, and W. G. Lynch, Science **298**, 1592 (2002).*
32. *M. Centelles, X. Roca-Maza, X. Vi˜nas, and M. Warda, Phys. Rev. Lett. **102**, 122502 (2009).*
33. *C. Xu, B.-A. Li, and L.-W. Chen, Phys. Rev. C **82**, 054607 (2010).*
34. *F. J. Fattoyev, W. G. Newton, J. Xu, and B.-A. Li, Phys. Rev. C **86**, 025804 (2012).*
35. *A. W. Steiner and S. Gandolfi, Phys. Rev. Lett. **108**, 081102 (2012).*
36. *W. G. Newton, M. Gearheart, and B.-A. Li, APJ Suppl. Series **204**, 9 (2012).*
37. *S. K. Singh, M. Bhuyan, P. K. Panda, and S. K. Patra, JPG: Nuclear and Particle Physics **40**, 085104 (2013).*
38. *D. Adhikari, H. Albataineh, D. Androic, et al. (PREX Collaboration), Phys. Rev. Lett. **126**, 172502 (2021).*
39. *B. T. Reed, F. J. Fattoyev, C. J. Horowitz, and J. Piekarewicz, Phys. Rev. Lett. **126**, 172503 (2021).*
40. *M. C. Miller, F. K. Lamb, A. J. Dittmann, et al., (2021), **arXiv:2105.06979** [astro-ph.HE].*
41. *J. A. Pattnaik, R. N. Panda, M. Bhuyan, and S. K. Patra, (2021), **arXiv:2105.14479** [nucl-th].*
42. *Z. Zhang and L.-W. Chen, Physics Letters B **726**, 234 (2013).*
43. *C. J. Horowitz and J. Piekarewicz, Phys. Rev. Lett. **86**, 5647 (2001).*
44. *C. Ducoin, J. Margueron, and C. Provid˙encia, EPL **91**, 32001 (2010).*
45. *C. Ducoin, J. Margueron, C. m. c. Provid˙encia, and I. Vida˜na, Phys. Rev. C **83**, 045810 (2011).*
46. *K. Hebeler, J. M. Lattimer, C. J. Pethick, and A. Schwenk, The Astrophysical Journal **773**, 11 (2013).*
47. *C. J. Horowitz, E. F. Brown, Y. Kim, et al., JPG: Nuclear and Particle Physics **41**, 093001 (2014).*
48. *C. Drischler, R. J. Furnstahl, J. A. Melendez, and D. R. Phillips, Phys. Rev. Lett. **125**, 202702 (2020).*
49. *G. Hagen, A. Ekstr¨om, C. Forss´en, et al., Nature Physics **12**, 186 (2016).*
50. *L.-W. Chen, C. M. Ko, B.-A. Li, and J. Xu, Phys. Rev. C **82**, 024321 (2010).*
51. *S. Gandolfi, J. Carlson, S. Reddy, A. W. Steiner, and R. B. Wiringa, The EPJ A **50**, 10 (2014).*
52. *X. Roca-Maza, X. Vinas, M. Centelles et al. , Phys. Rev. C **92**, 064304 (2015).*
53. *B.-A. Li, P. G. Krastev, D.-H. Wen, and N.-B. Zhang, EPJ A **55** (2019).*
54. *B.-A. Li and X. Han, Physics Letters B **727**, 276 (2013).*
55. *T. Matsui, Nucl. Phys. A **370**, 365 (1981).*
56. *S. Kubis and M. Kutschera, Phys. Lett. B **399**, 191–195 (1997).*
57. *M. Del Estal, M. Centelles, X. Vi˜nas, and S. K. Patra, Phys. Rev. C **63**, 024314 (2001).*
58. *W.-C. Chen and J. Piekarewicz, Phys. Rev. C **90**, 044305 (2014).*
59. *M. Fortin, C. Provid˙encia, A. R. Raduta, et al., Phys. Rev. C **94**, 035804 (2016).*
60. *S. K. Biswal, H. C. Das, A. Kumar, B. Kumar, and S. K. Patra, **arXiv:2012.13673** [astroph.HE] (2020)*
61. *X. Roca-Maza, M. Centelles, X. Vi˜nas, and M. Warda, Phys. Rev. Lett. **106**, 252501 (2011).*

62. *H. C. Das, A. Kumar, B. Kumar, et al., MNRAS **495**, 4893 (2020).*
63. *H. C. Das, A. Kumar, B. Kumar, S. K. Biswal, and S. K. Patra, JCAP **2021**, 007 (2021).*
64. *H. C. Das, A. Kumar, and S. K. Patra, (2021), arXiv:2104.01815 [astro-ph.HE].*
65. *R. C. Tolman, Phys. Rev. **55**, 364 (1939).*
66. *J. R. Oppenheimer and G. M. Volkoff, Phys. Rev. **55**, 374 (1939).*
67. *P. B. Demorest, T. Pennucci, S. M. Ransom, et al., Nature **467**, 1081 (2010).*
68. *J. Antoniadis, P. C. C. Freire, et al., Science **340** (2013) .*
69. *H. T. Cromartie, E. Fonseca, S. M. Ransom, P. B. Demorest, et al., Nature Astronomy **4**, 72 (2020).*
70. *R. Abbott, T. D. Abbott, S. Abraham, et al., The Astrophysical Journal **896**, L44 (2020),*
71. *H. C. Das, A. Kumar, and S. K. Patra, (2021), arXiv:2109.01853 [astro-ph.HE].*
72. *M. C. Miller, F. K. Lamb, A. J. Dittmann, et al., APJ **887**, L24 (2019).*
73. *T. E. Riley, A. L. Watts, S. Bogdanov, et al., APJ **887**, L21 (2019).*

BIOGRAPHICAL NOTES

Dr subrata Kumar Biswal, is now working as assistant professor in Physics, DRIEMS Autonomous Engineering college, Tangi, Cuttack. He did his PhD from Institute of Physics, Bhubaneswar, India in 2016. He has four years of postdoctoral experiences in various national and international institutions like NISER (India), Institute of Theoretical Physics (Beijing, China) and Xiamen University (Fujian, China). He has published more than 30 research papers in reputed international journal with high impact factor. His area of research includes structure of super heavy nucleus, Giant Monopole resonances, equation of state of the neutron star and gravitational waves. He is also working as a reviewer of many international journals.

Mr. Harish Chandra Das is now working as research scholar in Institute of Physics Bhubaneswar. His research area includes equation of state of the neutron star, gravitational waves and dark matter. He did his master degree from Ravenswa University, Cuttack, Odisha . He has published more than 10 research papers in various international journals.

Mr. Ankit Kumar, is now working as research scholar in institute of Physics Bhubaneswar. His research area includes equation of state of the neutron star, gravitational waves and dark matter. He has published more than 10 research papers in various international journals.

Prof. S. K. Patra, is now working as a professor in Institute of Physics, Bhubaneswar, Odisha. He did his Ph.D from institute of Physics Bhubaneswar. He has 8 years postdoc experiences in various international research institutes and universities. He has published more than 100 research paper in international journal. He is also working as an editorial member and reviewer of many international journals. He has already supervised more than 10 Ph.D. students. He had received many national and international fellowships like Alexander von Humboldt Research Fellow, Germany, (1995-97), Spain Education Ministry Fellowship, Spain (1999-2001) and National Science Council Fellow, Taiwan, (1997-99).

DRIEMS Autonomous Engineering College

Tangi, Odisha, India

www.ijicas@driems.ac.in